A COMPARATIVE STUDY OF THE EXISTING METHODS FOR THEIR SUITBILITY TO BEAM STABILIZATION IN STORAGE RING AT CANADIAN LIGHT SOURCE

A Thesis

Submitted to the College of Graduate Studies and Research

in Partial Fulfillment of the Requirements

for the Degree of

Master of Science

in the

Division of Biomedical Engineering

University of Saskatchewan

Saskatoon, Saskatchewan

Canada

By

Penghui Shi

PERMISSION TO USE

In presenting this thesis in partial fulfilment of the requirements for a Master of Science degree from the University of Saskatchewan, the author agrees that the Libraries of this University may make it freely available for inspection. The author further agrees that permission for copying of this thesis in any manner, in whole or in part, for scholarly purposes may be granted by the professor or professors who supervised the thesis work or, in their absence, by the Head of the Department or the Dean of the College in which the thesis work was done. It is understood that any copying or publication or use of this thesis or parts thereof for financial gain shall not be allowed without the author's written permission. It is also understood that due recognition shall be given to the author and to the University of Saskatchewan in any scholarly use which may be made of any material in this thesis.

Requests for permission to copy or to make other use of material in this thesis in whole or part should be addressed to:

Head of the Division of Biomedical Engineering

University of Saskatchewan

Saskatoon, Saskatchewan S7N 5A9 CANADA

ABSTRACT

The stabilization of electron beam in the Storage Ring (SR) is an important task in the 3rd generation synchrotron facility worldwide. Deviations in the position and angle of electron beam with respect to a desired orbit must be below 10% of the beam size. This requirement corresponds to about 3 μm deviations at the Canadian Light Source (CLS). Further, the higher the correction bandwidth, the better in the stabilization process. The correction bandwidth at CLS was expected to increase to be 45 Hz or higher from the current operating rate at 18 Hz. In addition, there is requirement to control the beam deviation at specific positions on the orbit. To meet these requirements, a comparative study of the existing methods for the stabilization of electron beam in the SR is thus necessary, which is the main motivation of this thesis study.

The overall objective of this thesis study was to find the most suitable method for CLS so that the correction bandwidth can be 45 Hz or higher. The study was primarily conducted by simulation due to the restriction in performing experiments on the whole beamline. The transfer functions of three important devices at the storage ring, which are Beam Position Monitor (BPM), Orbit Correction Magnets (OCM) and Vacuum Chamber (VC), were identified. Noises on the storage ring were also identified to improve the reliability of the simulation study. The existing methods for beam orbit correction, such as (1) Singular Value Decomposition (SVD), (2) Eigen Vector method with Constraints (EVC) and (3) SVD plus Proportional integral derivative (PID), were compared based on the simulation technique.

Several conclusions can be drawn from this study: (1) there is no significant difference between the EVC method and SVD method in terms of overall orbit correction performance, and they both can meet the correction bandwidth of 45 Hz. The EVC method is however much better than the SVD method in terms of the beam orbit correction performance at specific positions; (2) the SVD plus PID method is much better than the SVD method as well as EVC method in terms of

the overall orbit correction performance, and its performance for specific position orbit correction is comparable with the performance of EVC. Therefore, the SVD plus PID method is recommended for CLS.

This study has made the following contributions on the problem of beam stabilization the storage ring in the synchrotron technology: (1) provision of the models of BPM and OCM and the PID controller tailored to specific BPM and OCM devices, which is useful to other synchrotron facilities in the world; (2) generation of the knowledge regarding the performances of SVD, EVC and SVD plus PID methods on one synchrotron facility is valuable, and this knowledge is useful to other synchrotron facilities in selection of the best methods for electron orbit correction.

ACKNOWLEDGEMENTS

This thesis is the outcome of my MSc. Project at the Division of Biomedical Engineering at the University of Saskatchewan. I would like to thank my supervisor Professor Chris Zhang for giving me opportunity of working on this very interesting and promising topic. Moreover, I thank him for his high quality supervision, which is very instructive and practical.

I would also express my gratitude to my supervisor Elder Matias at the Canadian Light Source for his supportive and pleasant guidance.

The main part of my research work is performed on the facility of CLS. I would like to thank Song Hu, Bud Fogal, Johannes Vogt, Karen McKeith, Ward Wurtz, Jack Bergstrom, Mark de Jong, and Les Dallin for their generous and patient help with technical details of this research, which set me to the right direction in my moments of doubt.

Also, I would like to thank the members of advisory committee, Professor Daniel Chen and Professor (Emeritus) Madan M. Gupta, for their suggestions and comments in my project.

Last but not the least, I am truly thankful to my family (especially my parents and my wife) and friends that continuously support me in all ways during my study at the University of Saskatchewan.

CONTENTS

LIST OF FIGURES

LIST OF TABLES

LIST OF ABBREVIATIONS

BPM	Beam Position Monitor
BR	Booster Ring
CLS	Canadian Light Source
EPICS	Experimental Physics and Industrial Control System
EVC	Eigen Vector method with Constraints
IAE	Integral of Absolute value of the Error
LS	Least Square
MIMO	Multiple Input and Multiple Output
MSIT	Matlab System Identification Toolbox
OCM	Orbit Corrector Magnet
PID	Proportional Integral Derivative
PS	Power Supply
RF	Radio Frequency
RMS	Root Mean Square
SISO	Single Input and Single Output
SR	Storage Ring
SROC	Storage Ring Orbit Control system
SVD	Singular Value Decomposition
VC	Vacuum Chamber
VME	Versa Module Eurocard

CHAPTER 1 INTRODUCTION

1.1 Research Background

Canadian Light Source (CLS) is the only national synchrotron light source facility in Canada, which is located at the City of Saskatoon (52º08'N, 106º41'W) in the Middle of Canada. An important system of CLS is Storage Ring (SR) which provides high energy electron beams that are further introduced to different stations for different scientific research purposes.

1.1.1 Electron Beam Orbit

In physics, an orbit is the closed trajectory of a moving object around a point in space. The object moves under a field force such as the gravitational force. In synchrotron science, an orbit refers to charged particles or beams moving from a start position to a goal position in a magnetic field (**Error! Reference source not found.**). In **Error! Reference source not found.**, solid line is a design orbit (i.e., the orbit which is desired), and dashed lines are actual orbits. Orbit deviation refers to the error between the design orbit and actual orbit.

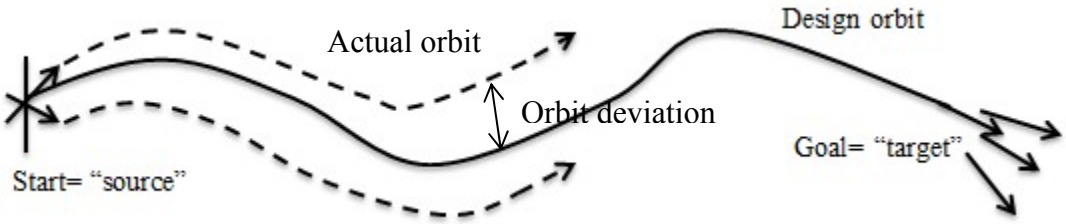

Figure 1.1 Definition of the orbit (adapted from Boge, 2008)

The SR is composed of several magnets which make the orbit be closed and guide the beam to run in the ring. The Dipole magnets determine a closed orbit (**Error! Reference source not found.**) on which a particle has a nominal value of energy, initial position, and angle (Hofmann,

2004). Particles with small deviations are gathered in the vicinity of the nominal orbit by the Quadrupole magnets which make the charged particles be attracted to the orbit. The longitudinal coordinate *s* represents the actual path of a particle moving along the orbit. The horizontal x-coordinate is perpendicular to the orbit, pointing from the center to the outside, the vertical y-coordinate is perpendicular to the orbit plane, and the z coordinate is along the tangent direction (Figure 1.2). The orbit deviation is corrected by the Sextupole magnets in the SR. The foregoing three types of magnets will be explained in the next chapter.

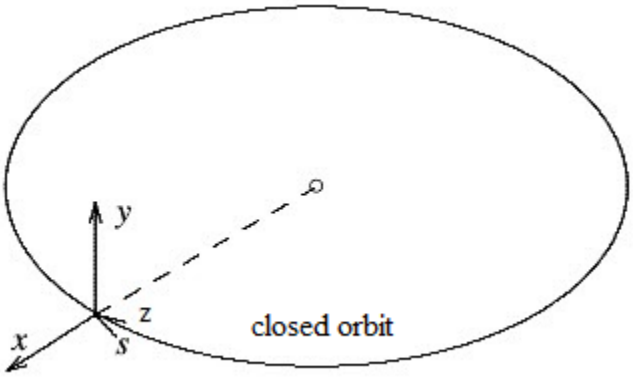

Figure 1.2 The coordinate of a particle on the orbit in the SR (adapted from Hofmann, 2004)

1.1.2 Beam Stabilization

Stabilization of the beam in the SR (orbit stabilization for short) is a very basic yet important task in the synchrotron radiation technology. The beam from the SR is guided to various stations around the SR. So, a stable beam in the SR lays a foundation for the beam at each station. Beam stabilization is also with the purpose of ensuring a proper protection of the equipment against miss-steered beams. Furthermore, for machines with a small aperture, unstable beams can reduce the life time and injection efficiency (Bocchetta et al., 1998). It is noted that injection efficiency refers to the ratio of the amount of electrons remaining in the orbit divided by the total amount of electrons injected into the orbit.

In SR of CLS, there are 48 sensors named Beam Position Monitor (BPM) and correctors named Orbit Correction Magnet (OCM) located around the SR. To a general control system, BPM acts

like a sensor, and OCM acts like an actuator. They are responsible for monitoring the position of the beam and correcting the deviation. The details of the two devices will be explained later in this thesis (in Chapter 3).

The beam stability is measured by the deviation of the actual beam position with respect to the desired orbit (Figure 1.1), which is the output from BPM, denoted by x_i (where i stands for the i-th BPM). The overall performance of the beam stability with respect to the whole orbit is measured by the Root Mean Square (RMS) over all the x_i, i=1, 2, …, n (n: the total number of BPMs), which is denoted by x_{rms}, and it is found by

$$x_{rms} = \sqrt{\frac{1}{n}(x_1^2 + x_2^2 + \cdots + x_n^2)} \tag{1.1}$$

There is another form of the RMS (Bissell and Chapman, 1992) – see below:

$$x_{rms} = \sqrt{\bar{x}^2 + \sigma_x^2} \tag{1.2}$$

where $\bar{x}$ is the mean value of x_i, i=1, 2, …, n, and σ_x is the standard deviation.

Requirements on beam stabilization are typically specified in terms of the tolerated bunch centroid movements as a fraction of the beam size. This is about 10% of the beam size, which is about 3 microns at CLS, at a particular BPM. This is further translated to the RMS, corresponding to 1 micron (RMS) at CLS. In 2005, the CLS achieved this requirement, as shown in Figure 1.3. In Figure 1.3, the red line is the trajectory of Golden orbit or reference orbit, and the blue line is the actual trajectory of the beam. The horizontal axis represents the BMP, where the number indicates a particular BPM. The vertical axis represents the deviation.

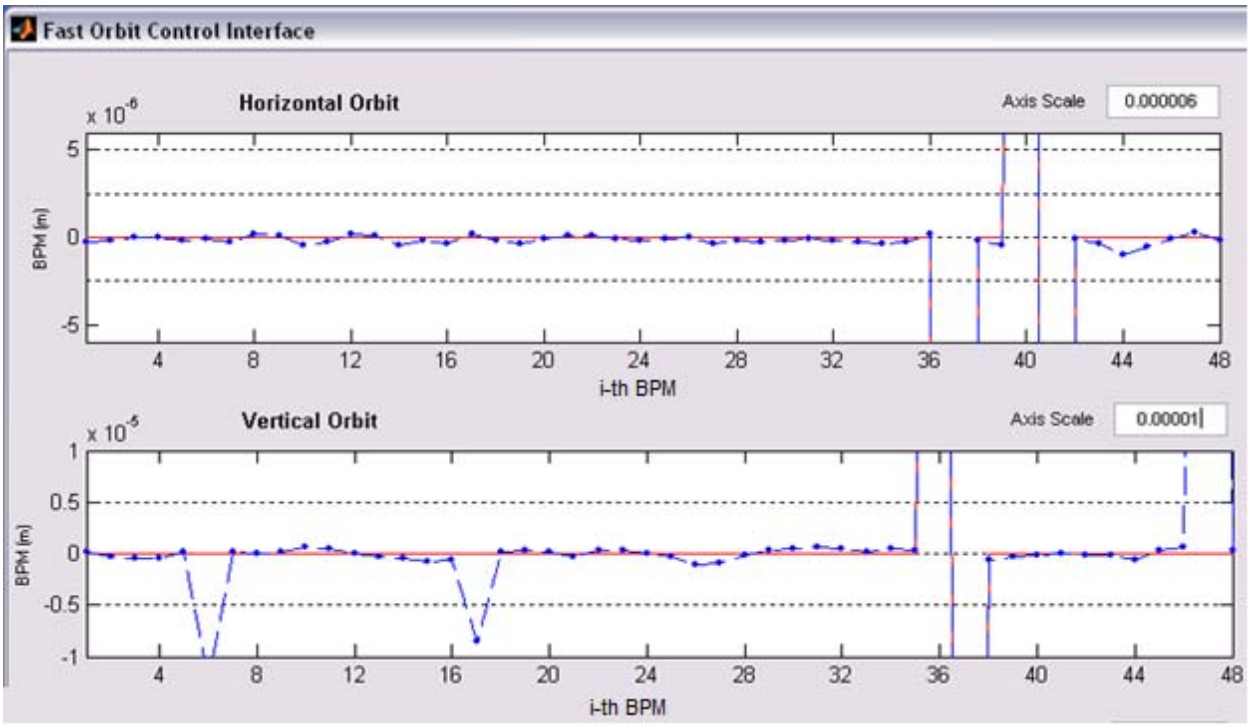

Figure 1.3 The current status of the orbit correction (Horizontal RMS: 0.29 micron; Vertical RMS: 0.41micron) (screen shot from the real-time control system interface)

1.1.3 Updating Rate

The updating rate is a parameter to represent the frequency of executing the correction in SR. The higher the rate, the more times the control system performs the correction and the better the performance of the beam stability. Currently, the operating updating rate at CLS is at 18 Hz. In order to achieve the next goal, 45 Hz, CLS updated its hardware systems including voltage stabilization for the SR power supplies and modification of the SR water system in 2011. CLS further updated its new control system to match the updated hardware in January 2012. However, the result is unsatisfactory, which means that the control system in 2012 did not work well to achieve the updating rate of 45 H.

1.1.4 Global Correction, Local Correction, Specific Positions Correction

Global correction means that the correction is based on the RMS of the whole storage ring. In this case, the control problem can be stated as: given the deviation information measured by

BPMs and the RMS and required tolerance on the RMS, to reduce the RMS by OCMs so that the actual RMS is within the tolerance. Local correction means that the correction is based on the deviation of beam at specific BPMs. The control problem can be stated as: given the deviation information at specific BMPs and required tolerance on the deviation, to reduce the deviation by OCMs so that the actual deviation is within the tolerance. Local correction may also be called specific positions correction. In this thesis, both global correction and specific position correction are both studied.

1.2 Research Motivation

It is noted that for the electron beam orbit correction problem, there are generally two problems: (1) to control the beam to stay on the design orbit to minimize the orbit deviation at 45 Hz updating rate (i.e., global correction) and (2) to control the beam to reach a specific position to satisfy a special beamline experiment (i.e., local correction or specific positions correction). The two problems are coupled; that is they need to be controlled at the same time, which is a challenge.

The state of technologies for electron beam orbit correction at CLS is such that only the so-called Singular Value Decomposition (SVD) method is available. It is noted that the SVD is not meant for a mathematical approach but for a particular control method in synchrotron radiation technology. The so-called SVD will be illustrated in detail in Chapter 4. The SVD method was considered not an enabler to solve both problems, especially problem 2, based on the literature of synchrotron technology. Moreover, the effectiveness of a particular control method for the electron beam orbit correction quite depends on individual synchrotron facilities owing to considerable differences in disturbances to and structures of individual synchrotron facilities. That said: an algorithm that works for the Japanese synchrotron facility may not be suitable to CLS.

The **general research question** to this study is: what was the most suitable control algorithm or method among the existing algorithms for electron beam orbit correction at CLS to solve the two problems as mentioned above?

Given the then situation at CLS where there was only SVD available, a more **specific question** is: what was the best algorithm among the Eigen Vector method with Constraints (EVC) and SVD plus Proportional integral derivative (PID) called SVD+PID to solve the two problems in the CLS environment?

1.3 Research Objective and Scope

This research was designed to generate answers to the aforementioned questions. The general methodology is simulation due to the limited possibility of performing the experiment at CLS. The following are specific research objectives defined for this research:

Objective 1: Develop dynamic models for the systems such as BPM, OCM and Vacuum Chamber (VC). The models refer to the transfer functions of these systems.

Until now, there is no literature about the model development for BPM, OCM and VC. It is further noted that some other auxiliary systems, e.g., cooling system, ventilation system, were not included in this study due to their minor effects to the overall beam system at the storage ring. It is clear that these models are necessary to be built to make a legitimate simulation study.

Objective 2: Identify the nature of the noises in the SR.

Indeed, noises in the SR are the main factor to deviate the electron beam. The model for noises is necessary to be built to make a legitimate simulation study.

Objective 3: Implement and perform a comparative study of the electron beam orbit correction algorithms, which were SVD, EVC and SVD+PID by simulation.

There are many methods available in the current literature for orbit correction in the SR. However, no method can be claimed to be good for every synchrotron facilities, which is owing to different noises at different synchrotron facilities and the inherent sensitivity of the SR to the noises. In fact, there has been a consensus among the synchrotron researchers in the world that the best method for beam orbit correction depends very much on fine-tuning of the control system in a particular synchrotron facility. Therefore, there is a high need to conduct a comparative study on the existing orbit correction methods in the SR at CLS in order to solve the two problems in CLS. As a pilot study, the methods of EVC, SVD+PID and SVD were chosen for a much closer examination in the context of CLS (see the objectives), which is the core of this thesis.

Due to the restriction of measurement in CLS, this research was largely based on simulation. Nevertheless, wherever possible, tests or measurements on the real system were taken, e.g., in the development of the transfer functions of BPM, OCM, and identification of the noise model.

1.4 A Brief Comment on Related Work

Several orbit correction methods have been developed. The harmonic correction was a popular method proposed in 1990s, and the method was described in detail by Schlueter et al. (1996). In this method, the orbit was decomposed onto a sinusoidal set of basic functions and each component was corrected independently. This method has a solid physics foundation because the orbit typically contains sinusoidal harmonic components centered at the Betatron tunes. This method has been used in PEP-II I.R with some great success (Humphries et al., 1997).

The most effective corrector (MICADO) was found from the Householder transformation. In 1973, B. Autin and Y. Marit explained this algorithm in their paper (Autin and Marit, 1973). This corrector can make the Orbit Correction Magnet (OCM) in the least number. After each correction cycle, the next most effective corrector was found. This algorithm was used in Fermilab Recycler Ring (Gattuso and Tecker, 1999).

The Eigenvector (EV) correction is a typical global corrector and it has been applied to the orbit feedback system for many SR sources. It was first introduced by Lambertson and laslett (1965). There is a detailed illustration of this method in the work of (Nakamura et al., 2006). The main idea of the method is to decompose the response matrix of a plant system onto a set of eigenvectors for the response matrix. But the drawback is that it requires a square response matrix. The response matrix is a representation of the relation between the variable of BPM and the variable of OCM, and it will be given in later discussion further.

The Least square (LS), which was described in detail in the work of (Golub and Reinsch, 1970), can be used when the number of BPMs exceeds the number of OCMs and the response matrix becomes tall (more rows than columns). However, if there is degeneracy in the response matrix that significantly compounds the effects of rounding errors in numerical computations, it is difficult to solve the matrix, e.g., LSSOL (Gill et al., 1986). SVD performs the same functions as EV or weighted LS but is much more general, mathematically manageable and numerically robust. In addition, Lagrange multipliers (Bassetti et al., 1998; Liu et al., 2008; Kamiya et al., 1999; Nakamura, 2010) and linear programming techniques (Allen et al., 1995; Pandit et al., 2001; Sarma et al., 2001) have been used for solving the problem of the inverse of the response matrix and for orbit correction.

In the current literature, SVD and EVC are two basic algorithms in the synchrotron facilities worldwide. Many algorithms are built upon or around them, such as PID controller (Steier, 2001), neural network (Atanasova and Zaprianov, 1999), and hybrid numerical method (White, 1997).

SVD is a fundamental algorithm for orbit correction. The general idea of SVD is to find a way to calculate the correction at OCM from the measured orbit deviation at BPM. This is the most straightforward thought for any “feedback” control but it cannot deal with disturbances or time delay. The SVD is the most popular method in the synchrotron technology. It is noted that in the synchrotron literature, the relation from the variable at BPM to that at OCM is called response matrix. The SVD is essentially a way to come up with an inverse of the response matrix.

EVC differs from SVD in their different ways to obtain an inverse of the response matrix. As such, EVC suffers from the same shortcoming as SVD. EVC was successfully implemented and performed well in KEK (Ninomiya et al., 2004), ALS (Nishimura et al., 1996) and LNLS (Farias, 1997). The detailed explanation for these two methods will be presented in Chapter 4.

To improve the robustness of beam orbit correction, the PID controller is a natural choice. The advantage of the PID controller is its computational efficiency and easy implementation, as it does not need the response matrix (in the specific context of synchrotron technology) and a plant dynamic model (in a general and broad context). However, the PID suffers from the problem such as the inherent difficulty in dealing with non-linear dynamics of the plant. The PID with the response matrix was successful in TSL (Chiu et al., 2007), PSI (Schlott, 2002), APS (Jeffrey, 1996), and SRCC (Kuo et al., 1996). Most recently, there was an effort on developing fuzzy neural controllers for beam orbit correction; see the work of Meier et al. (2012).

In beam orbit correction, corrections at a certain segments of the ring (e.g., the straight segment) may need to be done as quick as possible termed “fast”, while corrections at other segments (e.g., the bending segments) may need to be done “slow”. In the terminology of control, corrections in synchrotron technology thus have a mixed spectrum of bandwidths. A combined or integrated method has received some attention recently. Such methods were successful in orbit correction in ALS (Steier et al., 2004), NSLS-II (Pinayev, 2008) and Max IV (Sjöström et al., 2011).

1.5 Organization of the Thesis

There are five chapters in this thesis. The remaining chapters are outlined as follows:

Chapter 2 presents a detailed description of the Storage Ring at CLS. Basic concepts and functions of the hardware in the SR will be explained. The related physical theories will also be illustrated. The model to obtain the response matrix is developed, which serves as a plant model from a point of view of the control system.

Chapter 3 presents development of the transfer functions or models for Beam Position Monitor (BPM), Orbit Correction Magnet (OCM) and Vacuum Chamber (VC). Details of the experiment, calculation and validation are presented in this chapter.

Chapter 4 presents the implementation of the methods for electron beam orbit correction (i.e., the methods such as SVD, EVC, SVD+PID) and compares them using the simulation technique. The results of comparisons of these methods are discussed in this chapter.

Chapter 5 provides conclusion and future work.

Several appendixes are provided in light of the completeness of this document.

CHAPTER 2 STORAGE RING

2.1 Introduction

In this chapter, the basic concept and function of hardware in Storage Ring (SR) will be discussed. The related physical theories will be illustrated. At the end, the model to obtain the Response Matrix will be developed. All the parameters and devices that build the response matrix will be presented; while the response matrix will be presented together with the control system in Chapter 4.

2.2 Devices in SR

Figure 2.1 shows a layout of the synchrotron facility. The SR is a type of circular particle accelerator. Charged particles are accelerated in the E-gun and linear accelerator into beams for a period of time in the SR. Most commonly, charged particles (i.e. electrons, positron, or protons) are stored in this ring. The CLS has a range of energy from 1.5 to 2.9 GeV to operate its SR. Its basic parameters are shown in Table 3.1.

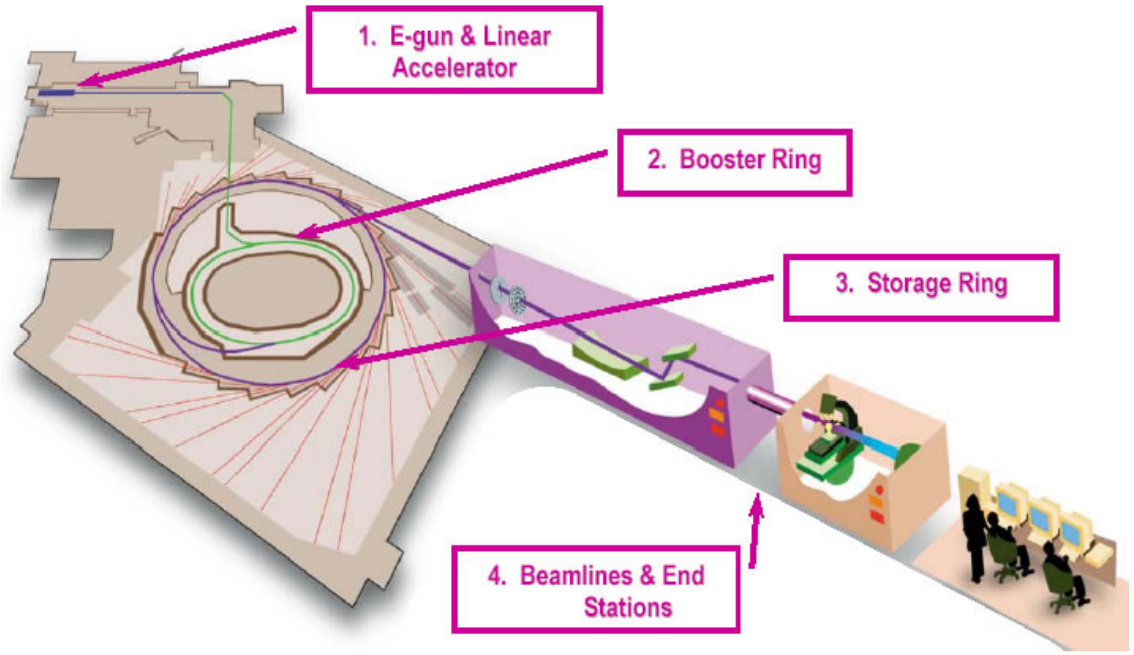

Figure 2.1 The composing of the Synchrotron facility
(http://dmttest.usask.ca/education/images/Synchrotron_new1.jpg)

Table 2.1 Basic parameters of the CLS SR (Dallin, 2004)

Parameter	Symbol	Value
Beam Energy	E	2.9 GeV
Electron Current	A	300 mA
Circumference	C	170.88 m
Horizontal Beam Size	X	480 μm
Vertical Beam Size	Y	13 μm
Emittance	ε_x	18.3 $nm\,rad$
Energy Spread	σ	0.0011
Momentum Compaction	α	0.0038
Betatron tunes	ν_x/ν_y	10.22/3.26
Radiation Damping Time	$\tau_x/\tau_y/\tau_E$	2.4/3.8/2.7
RF Frequency	f_{RF}	500 MHz
Harmonic Number	h	285

In CLS, the SR has a fairly compact structure and it is composed of 12 identical lattices (Dallin et al., 2004). The structure of the cell is a Double Bend Achromat, which gives the largest number of straight segments in the circumference (Dallin, 2000). The full lattice in CLS is shown in **Error! Reference source not found.**. Each cell has 2 dipoles, 6 quadrupoles and 3 sextupoles, which are made of AISI1010 steel (Dallin, 2000), and they will be described in the next section. In addition, there are 4 BPMs and Vacuum Chamber (VC) in the lattice. While the function of BPM was to measure the deviation of beam at a specific position, the function of VC is storage of the high-speeding electrons Both BPM and VC will be presented in Chapter 3.

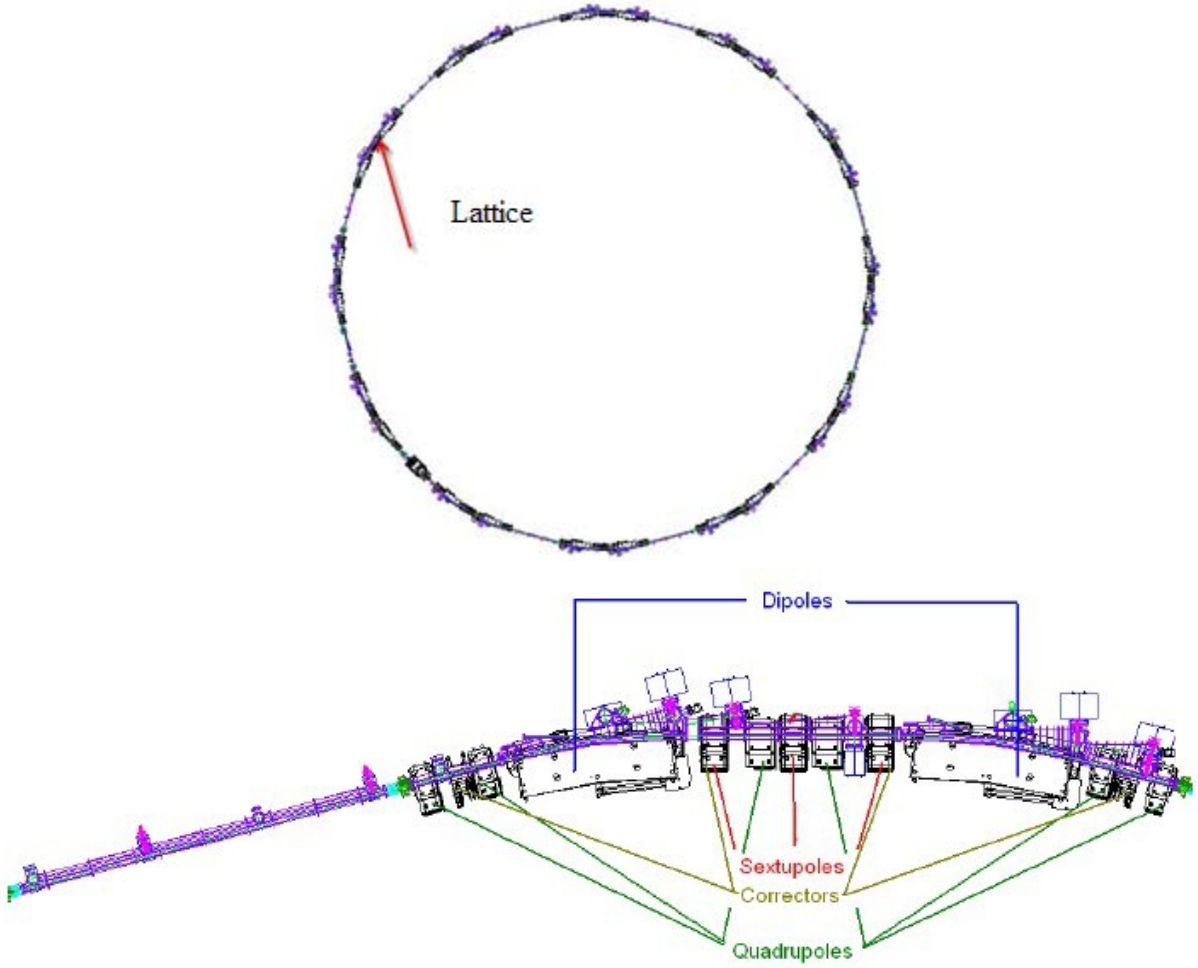

Figure 2.2 Schematic of full lattice showing the location of the Magnets (CLS internal CAD file)

2.1.1 Dipole Magnet

The dipole magnet (Figure **2.6**) is a gradient magnet which has a 15º bend angle. Its field strength is 1.3543 T (Dallin, 2001). Each magnet has a "C" configuration in order that the

radiated photons can leave the magnet unimpeded by the iron (Lowe, 1999). The dimension of the dipole is 146 mm by 89 mm. Its parameters are shown in Table 2.2.

The dipole magnet in SR is responsible for bending the beam 15 degrees so as to it can run in the ring.

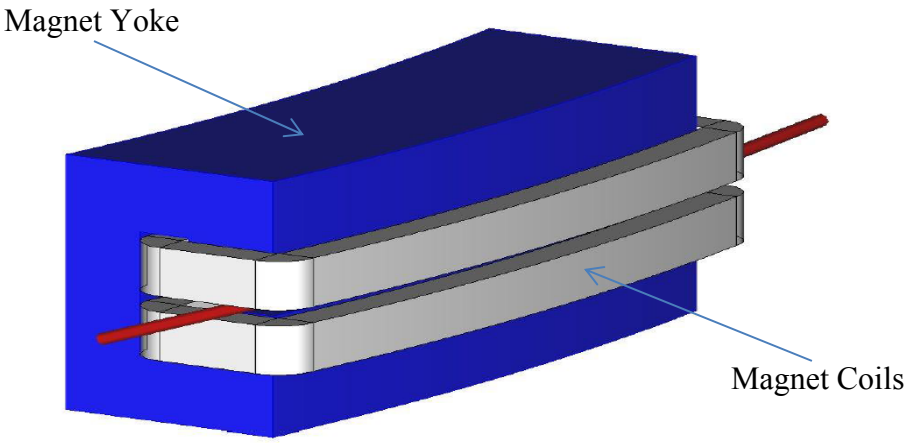

Figure 2.3 Dipole Magnet (Bilbrough and Sigrist, 2011)

Table 2.2 Dipole magnet parameters at 2.9 $\boldsymbol{GeV}$(Dallin, 2001)

Parameter	Value	Unit
Number of magnets	24	
Field strength	1.354	$\boldsymbol{T}$
Gradient	-3.87	$\boldsymbol{T/m}$
Magnet arc length	1.87	$\boldsymbol{m}$
Magnet gap on orbit	45	$\boldsymbol{mm}$
Good field width	50	$\boldsymbol{mm}$
Current	625	$\boldsymbol{A}$
Conductor area	183	$\boldsymbol{mm^2}$
Conductor length per coil	179	$\boldsymbol{m}$
Voltage drop per magnet	21.9	$\boldsymbol{V}$
Power per magnet	13.7	$\boldsymbol{kW}$

2.1.2 Quadrupole Magnet

There are three types of quadrupole magnets in the SR of CLS (Dallin, 2004), which have same shape (Figure 2.7). Further, all quadrupole magnets have an open side configuration in order to allow synchrotron radiation to exit from the magnet easily (Lowe, 1999). A summary of the parameters of quadrupole magnet is listed in Table 2.3.

The Quadrupole magnet is responsible for acting as a focusing lens in one plane and a defocussing lens in the perpendicular plane.

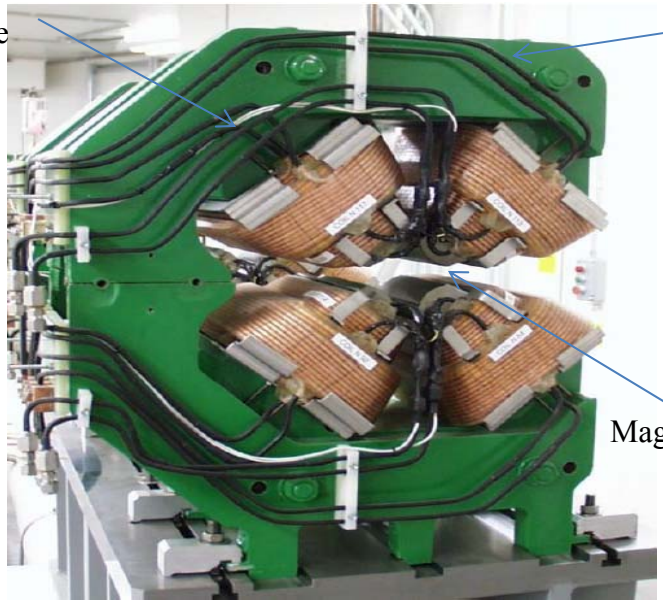

Figure 2.4 Quadrupole Magnet (Bilbrough and Sigrist, 2011)

Table 2.3 Quadrupole parameters at 2.9 GeV (Dallin, 2001)

Parameter	Value			Unit
	Q1	Q2	Q3	
Number of magnets	24	24	24	
Magnet length	0.170	0.170	0.253	m
Magnet aperture radius	32.5	32.5	32.5	mm
Gradient, K1	1.806	1.670	2.083	m^{-2}
Gradient	17.46	16.14	20.14	T/m
Good field radius	30	30	30	mm
Number of coils	4	4	4	
Ampere-turns	7465	6900	8611	
Number of windings per coil	104	104	104	
Current	71.8	66.4	82.8	A
Conductor area	14.7	14.7	14.7	mm^2
Conductor length per magnet	288	288	356	m
Resistance per magnet	0.35	0.35	0.44	Ω
Power per magnet	2.92	2.92	3.67	kW

2.1.3 Sextupole Magnet

There are two types of sextupole magnets (denoted as S1 and S2), and they have the same type of shape (Figure **2.8**). They are constructed as a "C" configuration. The S1 sextupole magnets serve as an orbit corrector in the lattice, and they have separate coil windings for each function. S2 is used to excite the quadrupole. A summary of the parameters of sextupole magnet is listed in **Error! Reference source not found.**.

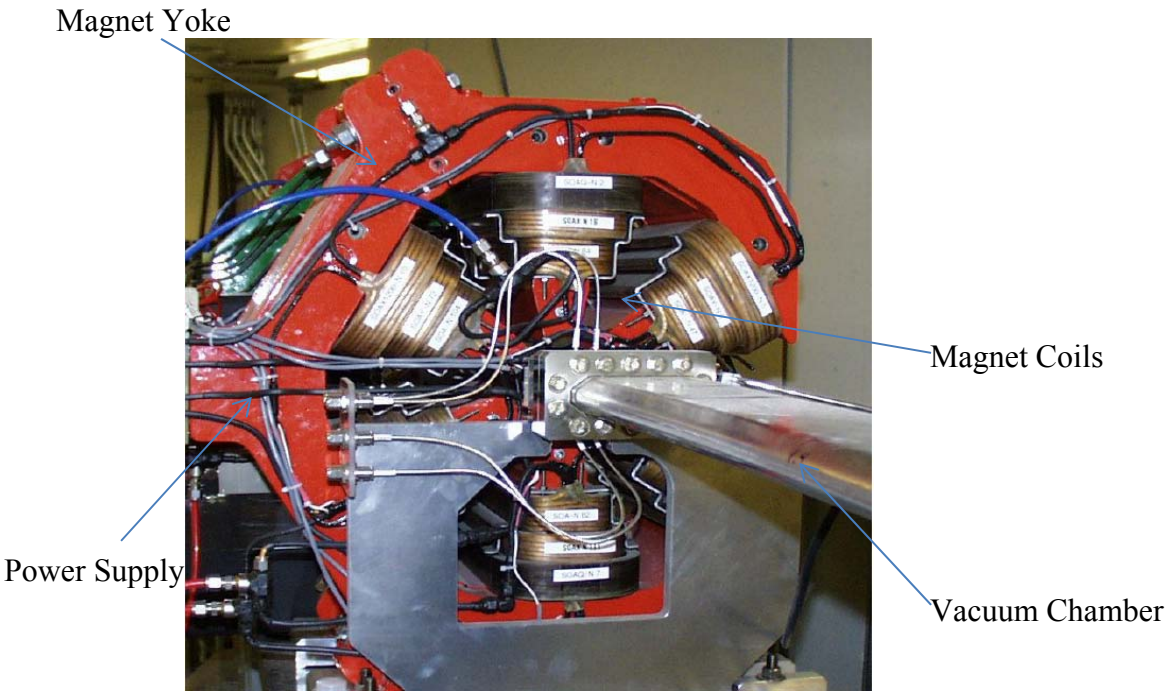

Figure 2.5 Sextupole Magnet (Bilbrough and Sigrist, 2011)

Table 2.4 Sextupole Parameters at 2.9 $\boldsymbol{GeV}$ (Dallin, 2000)

Parameter	Value	Unit
Number of magnets	48	C
Magnet length	0.192	$\boldsymbol{m}$
Magnet aperture radius	39	$\boldsymbol{mm}$
Gradient	267.8	$\boldsymbol{T/m^2}$
Good field radius	30	$\boldsymbol{mm}$
Number of coils	6	
Ampere-turns	4320	
Number of windings per coil	104	
Current	120	$\boldsymbol{A}$
Conductor area	14.7	$\boldsymbol{mm^2}$
Conductor length per magnet	21.5	$\boldsymbol{m}$
Resistance per coil	0.026	$\boldsymbol{\Omega}$
Power per magnet	2.25	$\boldsymbol{kW}$

2.3 Physics Theory of the Synchrotron System

2.3.1 Maxwell Equations

Maxwell Equations are a set of integral and differential equations including Gauss's law for electricity and magnetism, Faraday's law of induction and Ampere's law. This study was focused on the Faraday's law only, because this equation was used for the orbit beam stabilization methods.

Faraday's law governs the behavior of a magnetic-electric system such that a time varying magnetic field B can create an electric field I, and then the electric field subsequently generates a field $B_{induced}$ which is opposite to the varying magnetic flux through a loop (Figure 2.6). The Maxwell Equation describes how a varying magnetic field can induce an electric field, and it has

both an integral form and differential form, as shown in Equation 2.1 and Equation 2.2 (Signell, 2001), respectively.

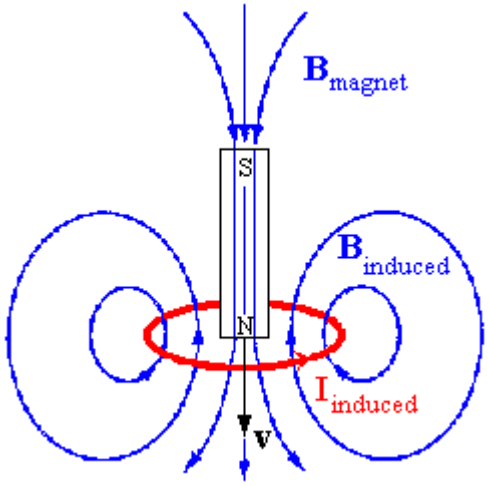

Figure 2.6 Varying magnetic field with its electric field
(http://labman.phys.utk.edu/phys222/modules/m5/images/lenz.gif)

$$\oint \vec{E} \cdot \overrightarrow{ds} = -\frac{d\,\Phi_B}{dt} \tag{2.1}$$

$$\nabla \times E = -\frac{\partial B}{\partial t} \tag{2.2}$$

where E : Electric field;
s : Path length;
Φ_B : Magnetic flux; and
t : Time.

2.3.2 Hill's Equation

In electromagnetism physics, a charged particle experiences a Lorentz force due to electromagnetic fields. This force is given by Equation 2.3 (Jackson, 1999). It is also illustrated by Figure 2.7.

$$\vec{F} = q\left(\vec{E} + \vec{v} \times \vec{B}\right) \tag{2.3}$$

where F : Lorentz force;

q : Quantity of electricity;

E : Electric field;

B : Magnetic field; and

v : Velocity of the particle.

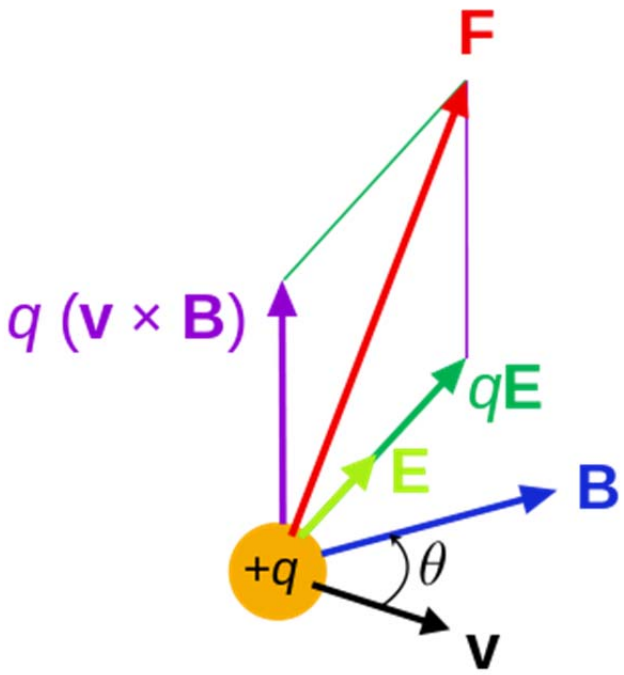

Figure 2.7 Lorentz force of charged particle in the magnetic field (https://upload.wikimedia.org/wikipedia/commons/thumb/7/7c/Lorentz_force_particle.svg/325px-Lorentz_force_particle.svg.png)

When the particle follows a closed orbit, its movement is periodic. The path of the particle can be expressed by the Hill's equation as follows (Magnus and Winkler, 1966):

$$\ddot{x} - 2\,\Omega\,\dot{y} - 3\,\Omega\,\dot{x} = -\frac{\partial\,\Phi}{\partial x} \tag{2.4}$$

$$\ddot{y} + 2\,\Omega\,\dot{x} = -\frac{\partial\,\Phi}{\partial y} \tag{2.5}$$

where x and y are the local coordinates of the particle; Ω is the angular velocity; and Φ is the disturbance due to noise.

2.3.3 Beta Function

It is well known that beam particles perform Betatron Oscillations around a closed orbit. The beta function (β) represents an envelope for all these oscillations. The beta function at CLS is shown Figure 2.8. The detailed mathematical expression of $\beta(s)$ will be given in Chapter 4. The size of beam can be calculated by:

$$\sigma(s) = (\varepsilon \cdot \beta(s))^{1/2} \tag{2.6}$$

where ε is the emittance of the beam; σ represents the diameter of the beam.

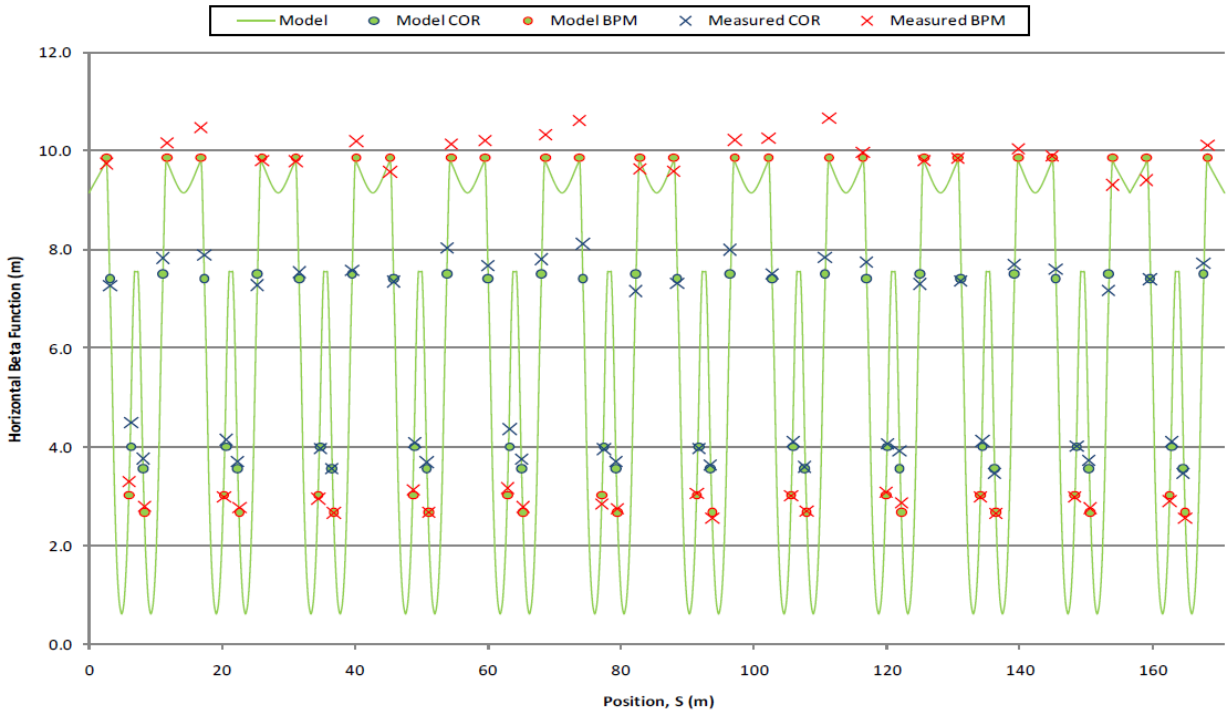

Figure 2.8 Beta function of the Storage Ring in CLS (Horizontal) (CLS internal file)

2.4 Concluding Remarks

The response matrix is the relationship between BPM and OCM, and its detailed information will be presented in Chapter 4. In Appendix II, there is a description of how the response matrix is determined experimentally. The lattice model for giving both the structure and physics behind the response matrix was given. The detailed Matlab codes are shown in Appendix I.

CHAPTER 3 SYSTEM MODEL DEVELOPMENT

3.1 Introduction

For the convenience of discussions, the control system for beam stabilization in the SR is called SROC (Storage Ring Orbit Control System) for short. In the CLS, the SROC was expected to provide a stable global orbit beam correction up to 45 Hz (Summer et al., 2009). The SROC and beam correction can be viewed as a control system where the SROC is a plant, and the SVD, PID and so on are control methods or controllers. The goal of this chapter is to describe the plant, i.e., SROC, and in particular to prepare the background knowledge for simulation of the behavior of the SROC.

The hardware components of the SROC are: BPMs, OCMs, Digital I/O modules. The software components are: IPICS (Experimental Physics and Industrial Control System), core correction manager, and VME (Versa Module Eurocard) device access. It is noted that the control method was within the core manager module (which was coded in the Matlab environment). Data acquisitions are performed via the EPICS (Dalesio and Kraimer, 1993).

There are 48 BPMs (X and Y) and 48 OCMs (X and Y) involved in the SROC. The distribution of them is shown in Figure 3.1. The corrections are also including horizontal and vertical directions. The present study focused on the horizontal correction only (without loss of generality due to the same devices and principles on both).

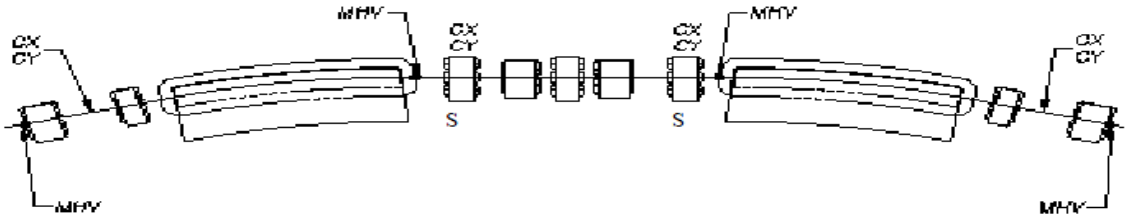

Figure 3.1 Schematic of the distribution of BPM and OCM in the SR (CX: Horizontal OCM CY: Vertical OCM; MHV: H/V BPM) (Dallin, 2000)

It may be clear that the SROC is a large Multiple-Input and Multiple Output (MIMO) system (Figure 3.2). The inputs of this system are 48 BPMs and outputs are 48 OCMs. First, several key sub-systems need to be identified, and they are BPM, OCM and VC and discussed in the next section.

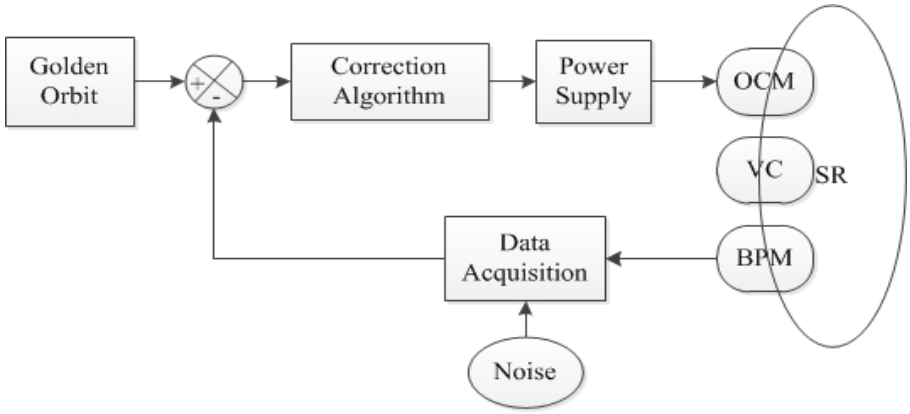

Figure 3.2 Control Block diagram for orbit correction in SR

3.2 Sub-systems Identification

3.2.1 Bergoz Beam Position Monitor Modeling

3.2.1.1 System Overview

Bergoz Beam Position Monitor (BPM) was supplied by BERGOZ Instrumentation Company. It is the most popular product used for monitoring the position in synchrotron facilities all over the world. There are several product models available with the system. At the CLS, the MX 45º

button BPM was used, as shown in Figure 3.3. In this figure, there are four buttons A, B, C and D to get voltage signals with which to calculate the horizontal and vertical offsets.

The equations for determining the horizontal and vertical offsets with the information from A, B, C, D are as follows (Bertwistle, 2001):

$$X = K_x \frac{V_B + V_D - V_A - V_C}{V_A + V_B + V_C + V_D} \tag{3.1}$$

$$Y = K_y \frac{V_B + V_A - V_D - V_C}{V_A + V_B + V_C + V_D} \tag{3.2}$$

where X : horizontal offset from the geometric center of the VC;

Y : vertical offset from the geometric center of the VC;

K_x : horizontal gain;

K_y : vertical gain; and

V_A,V_B ,V_C, V_D : voltage induced on buttons A, B, C and D, respectively.

The block diagram of the BPM is shown in Figure 3.4. In this figure, the BPM button signals are processed into a single signal by the time multiplex device. After this single signal is demodulated, it is demultiplexethed into four button values. The four values are further stored in the analog memories. After that, the beam position is calculated by Equation 3.1 and 3.2. The horizontal and vertical gains are constant for the buttons (Hinkson and Unser, 1995).

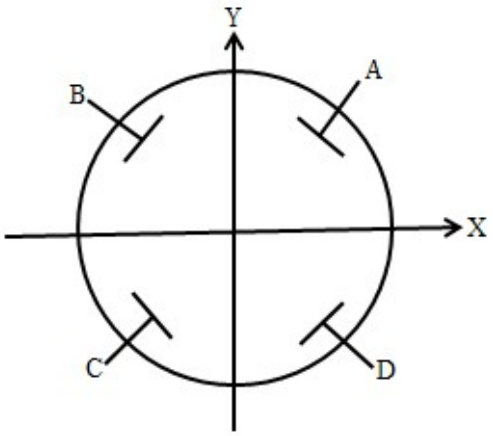

Figure 3.3 Beam Position Monitor (Unser, 1996)

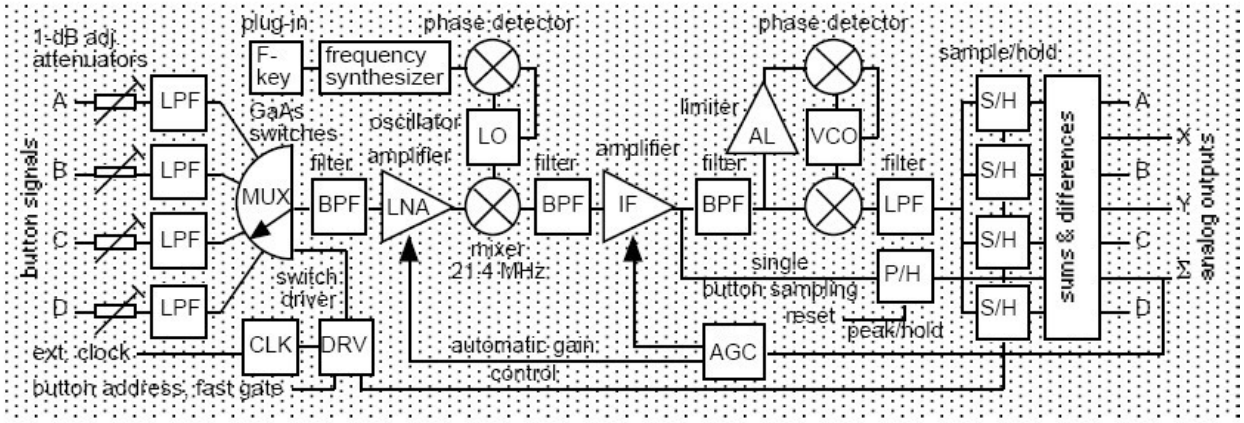

Figure 3.4 MX BPM block diagram

(http://www.bergoz.com/images/stories/bergoz/products/mx-bpm/schema.gif)

3.2.1.2 Test Bed and Data Acquisition

A test bed was built to develop the transfer function or model of BPM (i.e., to identify several parameters of the BPM system). The test bed is shown in Figure 3.5. The signal generator sets up the sampling frequency. The pulse train generator can generates the pulse voltage signal, which is further sent to the mixer. Oscilloscope (OSC) was used for monitoring the output position signal. Only horizontal values were recorded because this study focused on the horizontal orbit correction. All the devices used in the test bed are listed in Table 3.1.

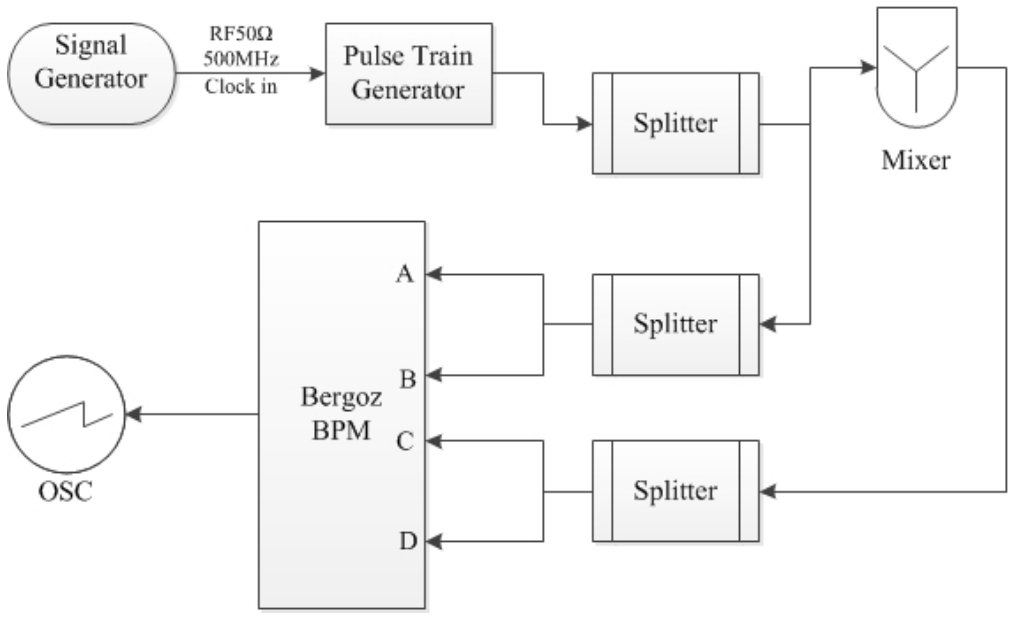

Figure 3.5 Schematic of the test bed for developing the transfer function of BPM

The SR at CLS operated at the nominal RF frequency (Appendix III) of 500 MHz (Sewell, 2007). Thus, the signal generator was clocked in 500 MHz.

Table 3.1 Devices in the BPM transfer function measurement test bed

No.	Name	Model	Number
1	Signal Generator	ROHDE & SCHWRZ (SMC100A) 9KHz~3.2GHz	1
2	Pulse Train Selector	WieNeR UEP15 Plein & Baus GmbH	1
3	Splitter	Mini-circuits ZX10R-14-S+	3
4	Pulse/Function Generator	HP 8116A 50MHz	1
5	Mixer	Mini-circuits ZLW-11R 15542	1
6	BPM Signal Generator	Bergoz BPM BPMC2403.1-01	1
7	Oscilloscope	Tektronix TDS3034B Four-channels color 300MHz 2.5GS/s DPO	1

The step response of the BPM was measured. The 10000 numbers of input and output values were obtained and they were represented as column vectors, respectively. They were further split

into two groups: 5000 were used for identification and the other 5000 were used for validation. The input and output signals are shown in Figure 3.6.

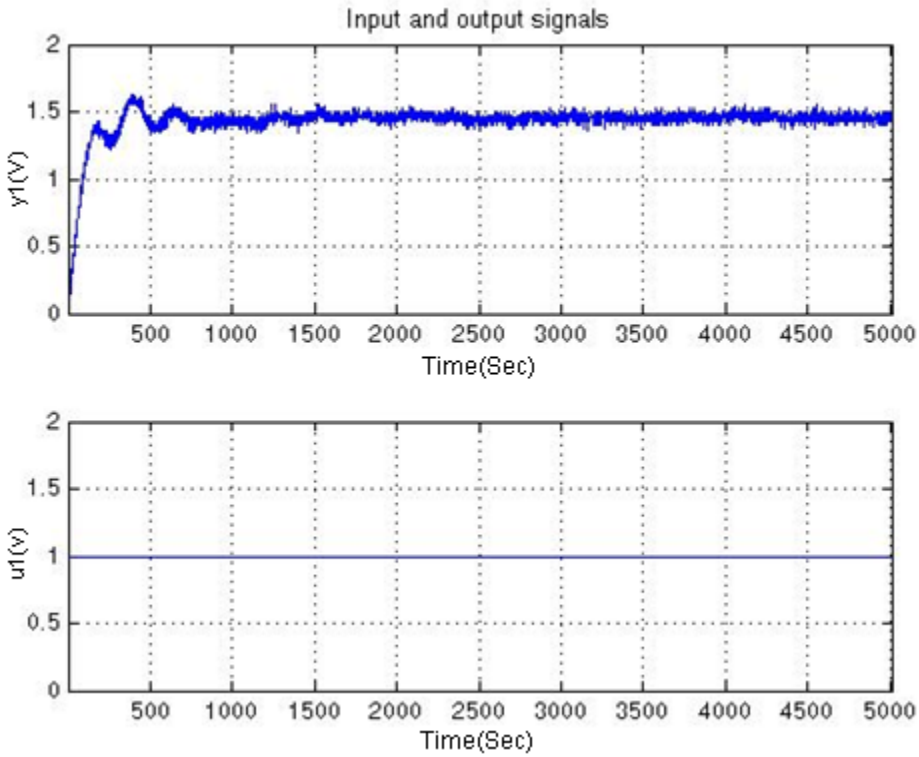

Figure 3.6 Bergoz BPM input and output signal with the sampling rate of 500 MHz

3.2.1.3 Parameter Calculation

Based on the measured data, the grey-box model in Matlab was selected for calculating the parameters of the system. By comparison, the 2nd under-damped model has a much better fitting than the 1st order model. Therefore, the 2nd under-damped model was shown to represent the transfer function, which is given in Equation 3.3.

$$G_{bpm} = \frac{Ke^{-T_d s}}{(1 + (2\zeta T_\omega)s + (T_\omega s)^2} \tag{3.3}$$

where K : Gain;

T_d : Time delay;

T_ω : Time constant of the complex pair of poles; and

ζ : damping ratio.

By Matlab System Identification Toolbox (SIT), the parameters of the model were determined using the SIT. The interface of the SIT with result is shown in Figure 3.7.

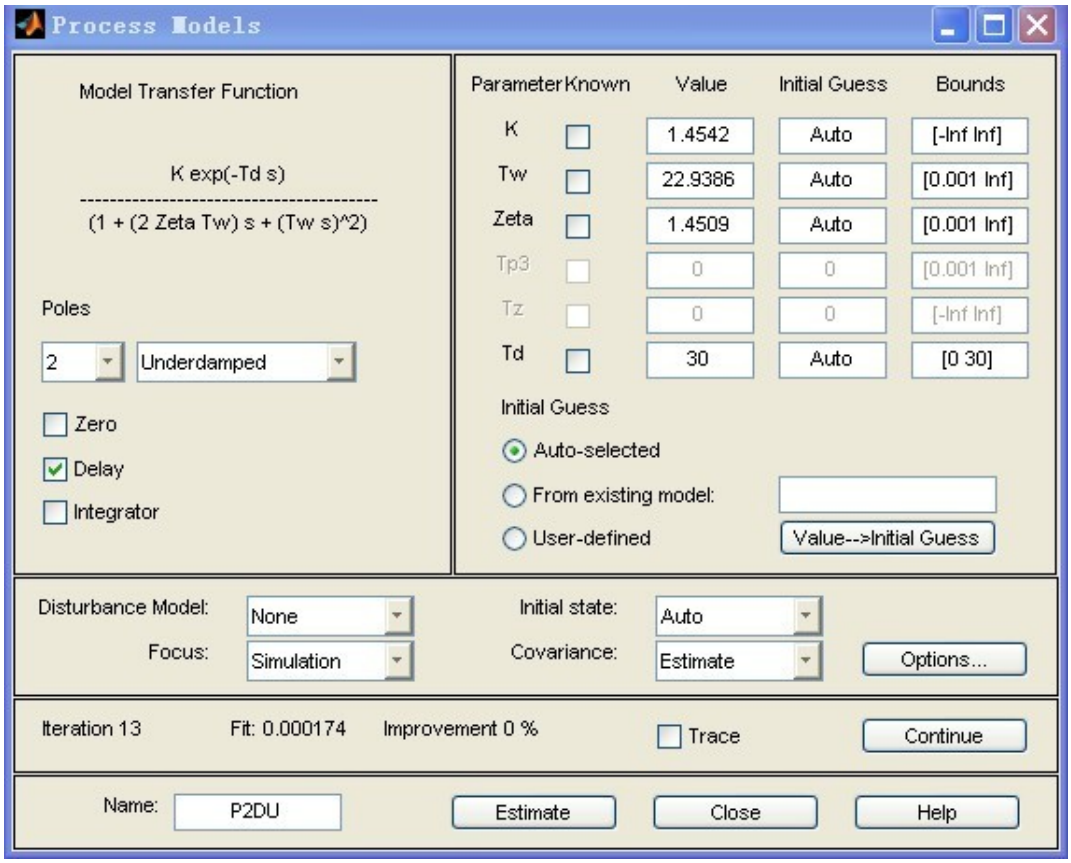

Figure 3.7 Interface of the System identification Toolbox with estimated result

As a result, the parameters are as follows:

$$K = 1.4542$$

$$T_\omega = 22.9386$$

$$\zeta = 1.4509$$

$$T_d = 30$$

Finally, the transfer function of the BPM is given by Equation 3.4:

$$G_{bpm} = \frac{1.4542e^{-30s}}{(1 + (2 \times 1.4509 \times 22.9386)s + (22.9386s)^2} \tag{3.4}$$

3.2.1.4 Model Validation

There are a few validation methods for the model, and they are step response, Bode diagram, residual analysis (see Appendix IV). The step response of the model is shown Figure 3.8. From Figure 3.8, the transient response has a good match to the original experiment data. From the other group data, the frequency function can be obtained, which is shown in Figure 3.9. The Bode plot is shown in Figure 3.10. By comprising these two figures, the Bode plot of the process and grey-box model are consistent with the frequency analysis.

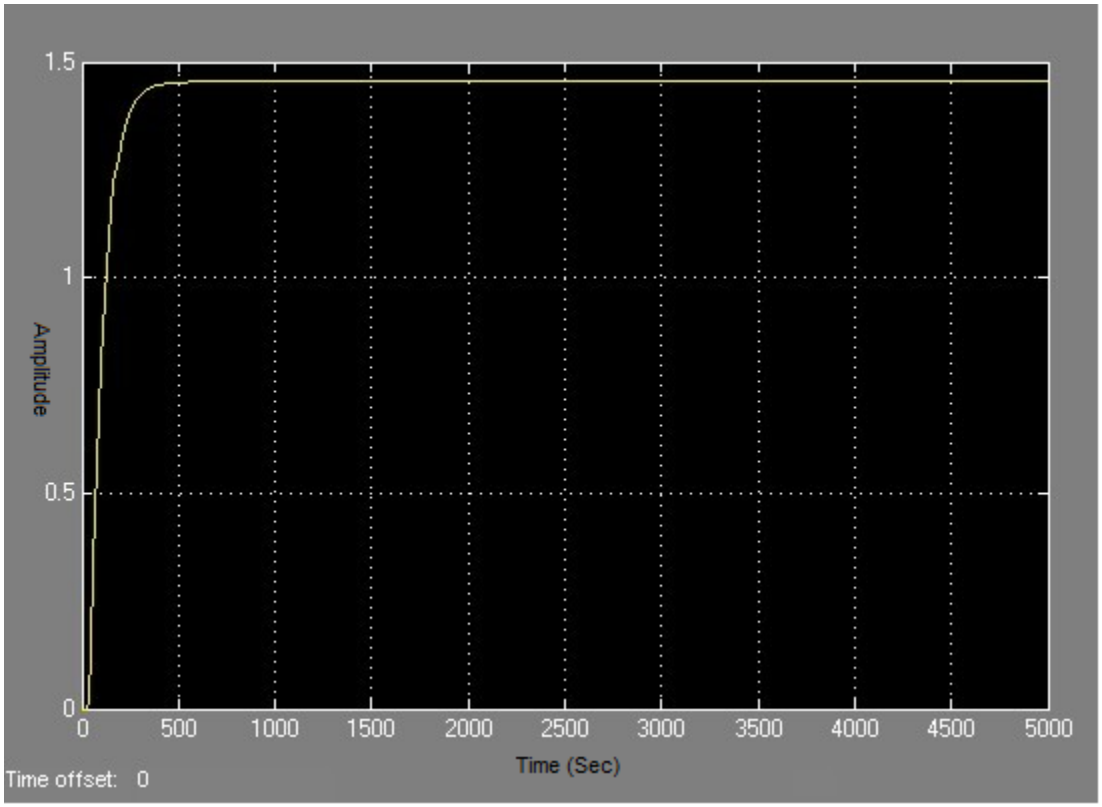

Figure 3.8 Step response of the BPM

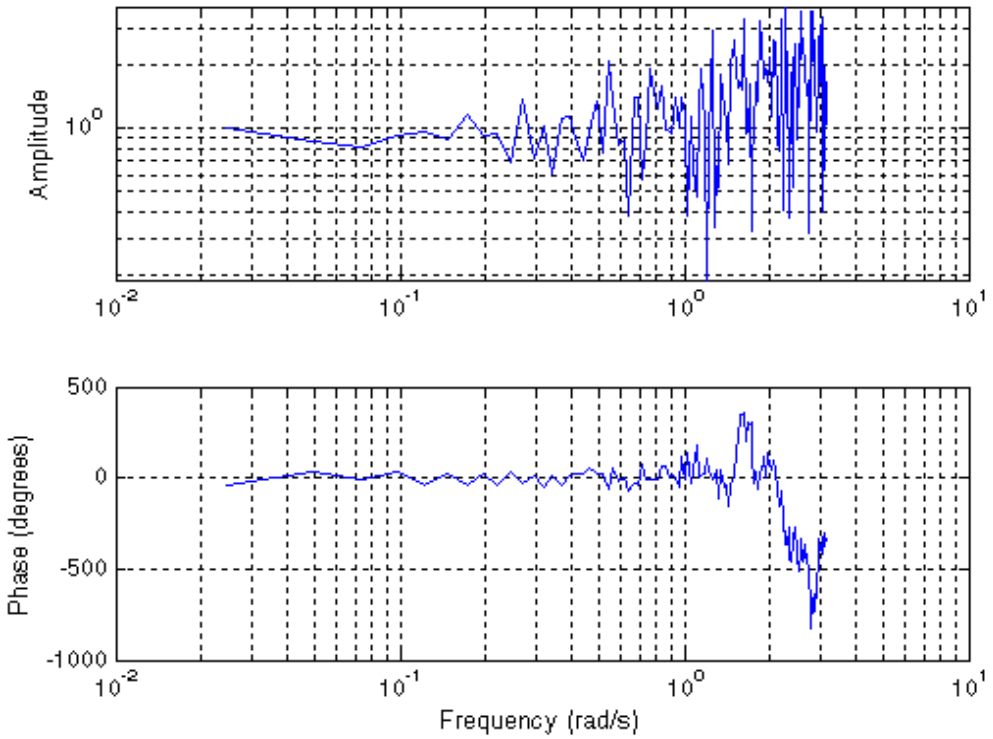

Figure 3.9 Frequency function

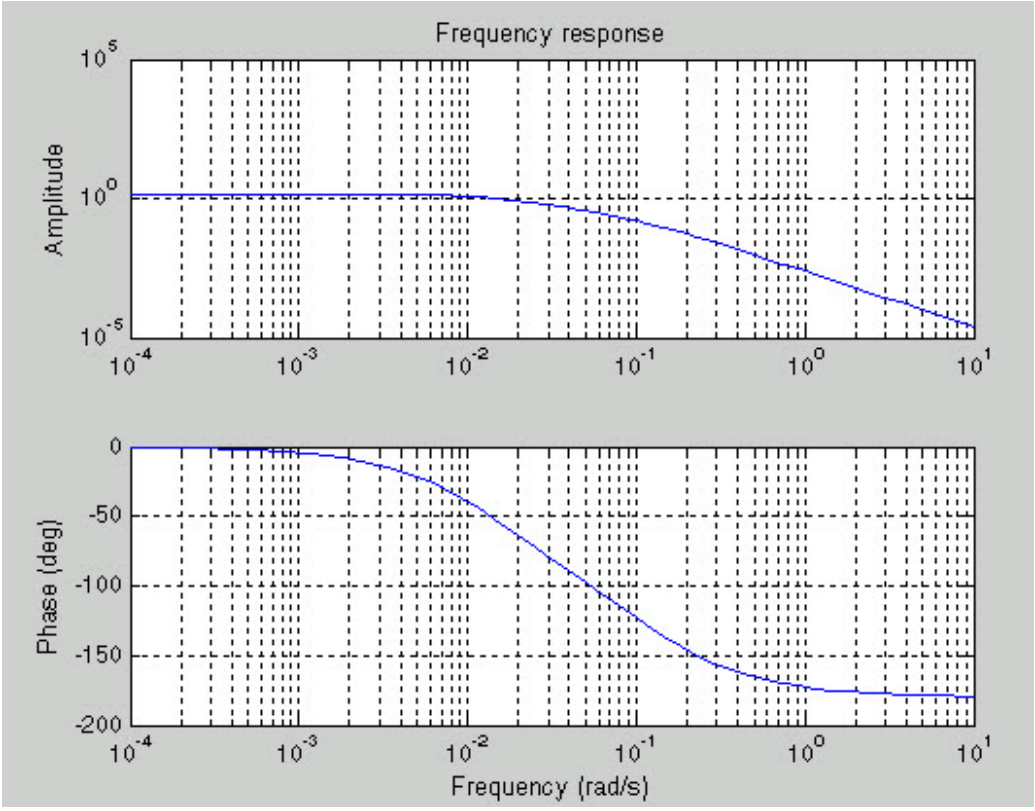

Figure 3.10 Bode plot of the BPM model

The residual analysis is shown in Figure 3.11. By the analysis of the step response, Bode plot and residual plot, it can be seen that the BPM model (transfer function) is valid and can be used for simulating the real plant.

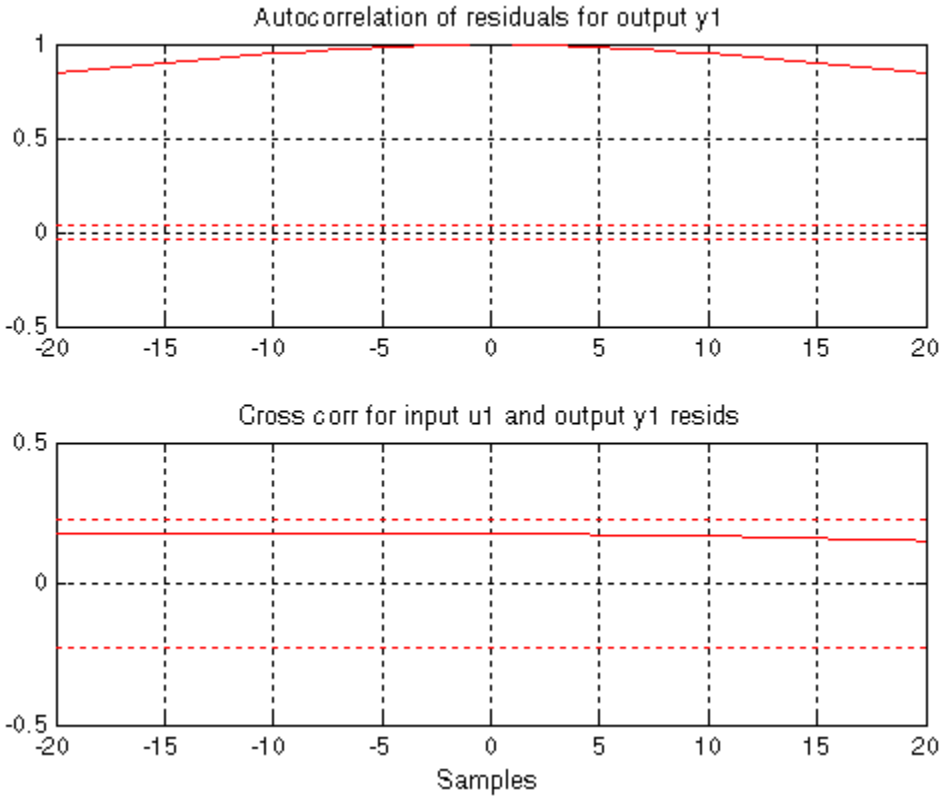

Figure 3.11 Residual analysis of the BPM process and grey-box model

3.2.2 Orbit Correction Magnet Modeling

3.2.2.1 System Overview

The Orbit Corrector Magnets (OCMs) have both horizontal and vertical dipole magnets capable of kicking the SR beam 1.4 mrad at the nominal beam energy of 2.9 GeV (Dallin, 2000). Using a corrector length of 0.2 m, a magnetic field of 0.0822 T is required in each dimension (Dallin, 2001). It is noted that from a control system's perspective, the OCM serves like an actuator.

Each corrector is built in a "C" configuration to allow the radiated photons to leave the magnet unimpeded by iron. Four coils are used to produce a horizontal field (for the vertical kick) and

two coils are used to produce a vertical field (for the horizontal kick). A cross sectional view of the magnet for horizontal kick is shown in Figures 3.12.

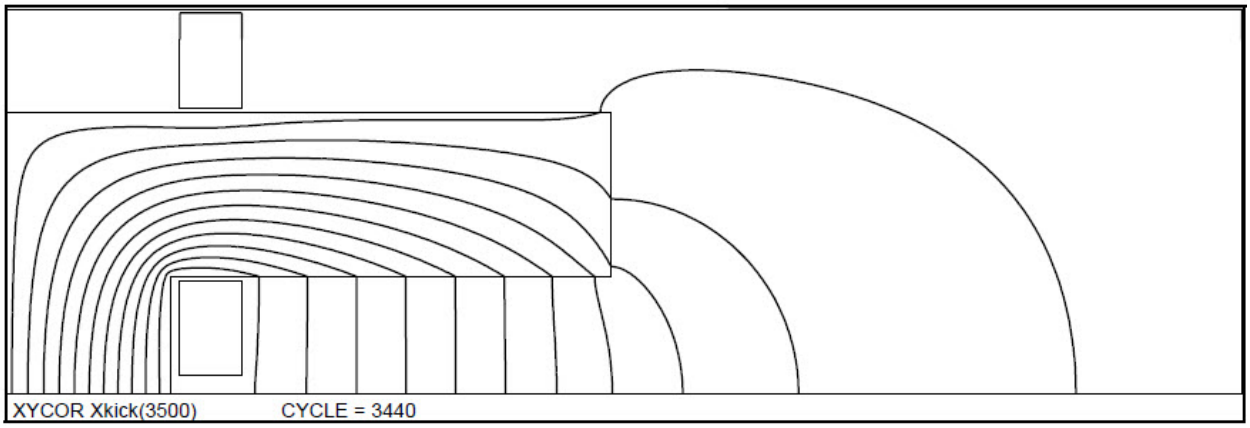

Figure 3.12 Corrector with vertical field (B_y) for X kick 14 (Dallin, 2000)

Details of the corrector (X kick-By) parameters are given in Table 3.2.

Table 3.2 X orbit Corrector Parameter at 2.9 $\boldsymbol{GeV}$ (Dallin, 2000)

Parameter	Value	Unit
# magnets	24	
X kick	1.40	$Mrad$
Maximum Field strengths	0.090	T
Length	0.15	M
Good field width	>80	Mm
#coils	2	
Ampere-turns	3884	
Current	162	A
Conductor length	34.6	M
Resistance per magnet	0.018	Ω
Voltage drop per magnet	2.92	V
Power per magnet	473	W

3.2.2.2 Test Bed and Data Acquisition

Figure 3.13 shows the test bed for developing the transfer function or model of the OCM, which primarily includes a Proportional-Integral (PI) compensation circuit for the PS.

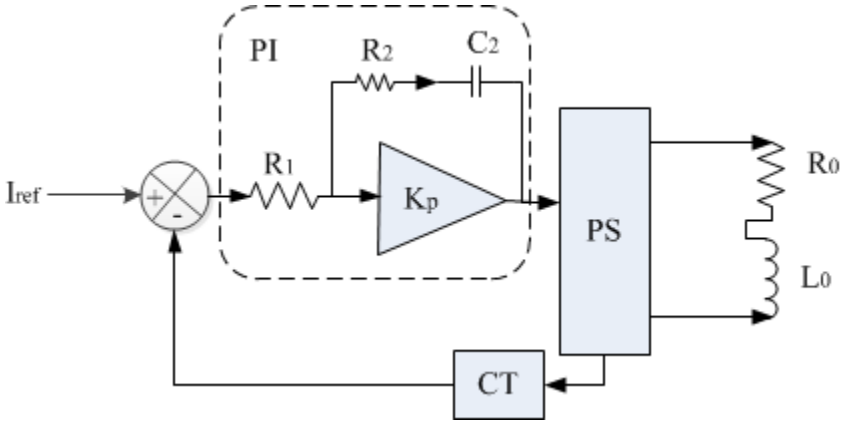

Figure 3.13 Circuit diagram for measuring the CLS correction magnet (adapted from Bellomo, 2004).$\boldsymbol{R_0}$ and $\boldsymbol{L_0}$ contains the load circuit, PS: Power Supply; $\boldsymbol{R_1}$, $\boldsymbol{R_2}$, $\boldsymbol{C_2}$: PI controller parameters

The block diagram of the circuit of Figure 3.13 is shown in Figure 3.14.

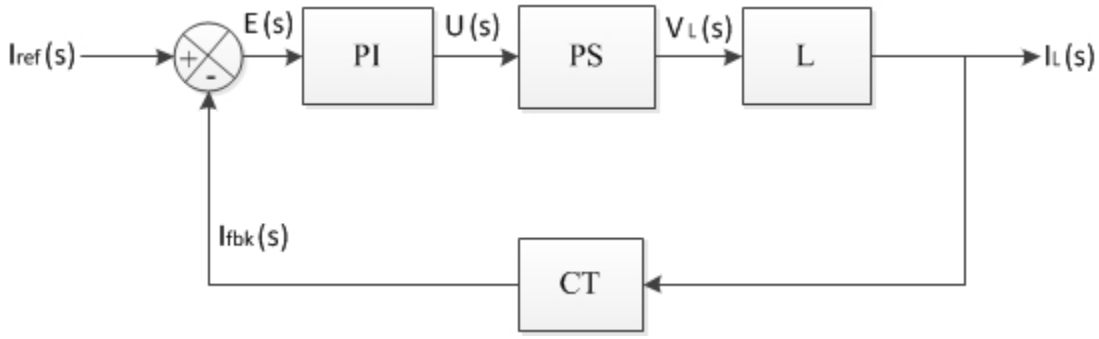

Figure 3.14 OCM power supply (PS) control loop block diagram, L: load, CT: current transducer

Based on this diagram, the transfer function of the PI controller (G_{PI}) is given by

$$G_{PI}(s) = \frac{U(s)}{E(s)} = K_{PI}\omega_{PI}\frac{\frac{s}{\omega_{PI}} + 1}{s} \tag{3.5}$$

The gain of the Power Supply (PS) is given by

$$G_{PS}(s) = \frac{V_L(s)}{U(s)} = K_{PS} \tag{3.6}$$

The transfer function of the load is given by

$$G_L(s) = \frac{I_L(s)}{V_L(s)} = K_L \frac{1}{\frac{s}{\omega_L} + 1} \tag{3.7}$$

The gain of the current transducer is given by

$$H_{CT}(s) = \frac{I_{fbk}(s)}{I_L(s)} = K_{CT} \tag{3.8}$$

Table 3.3 lists all the parameters of the test bed.

Table 3.3 Parameters of the devices for measuring the OCM (Horizontal)

Parameters	Symbol	Value
Rated Output of PS	I_O(A)	± 180
	V_O(V)	± 14
	$V_O/I_O(\Omega)$	0.0778
Magnet Load	R_0 (Ω)	0.0273
	L(mH)	2.316
	$\tau = L/R$ (s)	0.0848
	$K_L = 1/R$	36.630
PI Stage	K_{PI}	1
	$\omega_{PI} = 1/\tau$	11.788
PS Stage	K_{PS} (V/dac)	9.10E-06
Current Feedback Stage	R_1 (Ω)	1
	K_{CT} (adc/A)	84000
Closed Loop Gain	Gain	1.1905E-05

3.2.2.3 Parameter Calculation

The model of the OCM is shown by

$$G_{ocm}(s) = \frac{I_L(s)}{I_{ref}(s)} = \frac{1}{K_{CT}} \frac{1}{\frac{s}{2\pi f_c} + 1} \tag{3.9}$$

where

$$f_c = \frac{K_{PI}\omega_{PI}K_{PS}K_L K_{CT}}{2\pi} \tag{3.10}$$

Finally, the transfer function of the OCM is given by Equation 3.11 (the information in Table 3.3 substitutes all the parameters in Equation 3.9 and 3.10):

$$G_{ocm}(s) = \frac{0.0039}{s + 327.6} \tag{3.11}$$

3.2.2.4 Model Validation

The Bode plot of the OCM model is shown in Figure 3.15 (Red line is auxiliary line, and the blue line the Bode plot line.). From the Magnitude plot, one can see that the slop of the magnitude is -20 $dB/decade$, and from the Phase angle plot, one can see that it goes through -90º phase angle and the break-point at -45º. This means the system is a 1st order system.

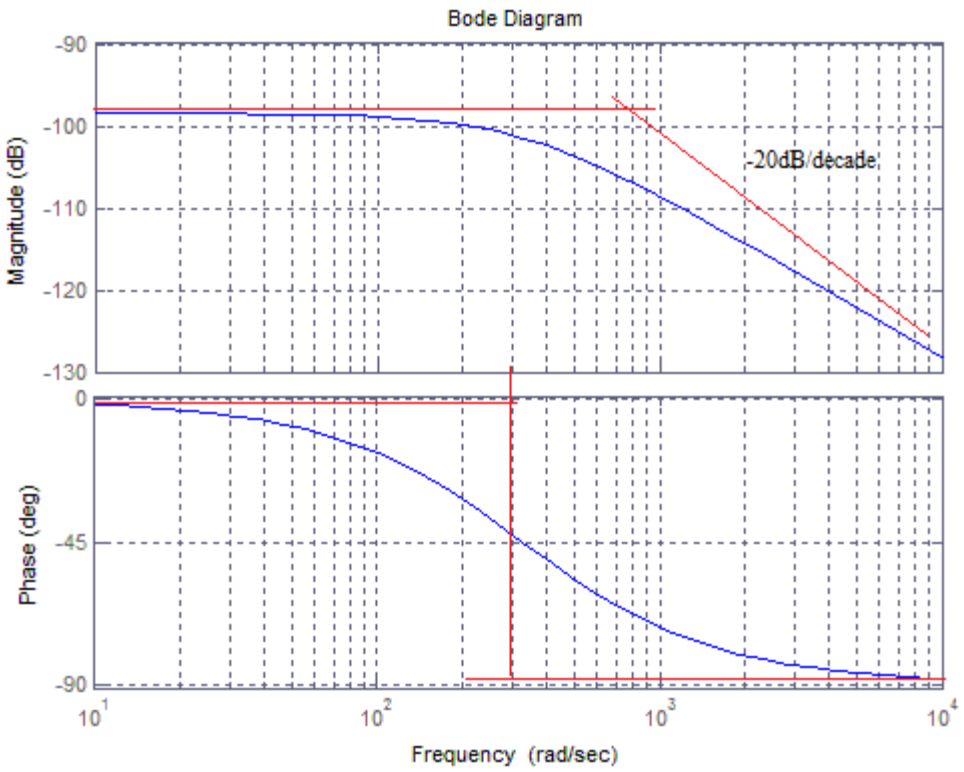

Figure 3.15 Bode plot of the OCM model

The frequency function of the OCM is shown in Figure 3.17. From the figure, one can see that the slop of the gain in the stop-band area is -20 $dB/decade$. This means the system is a 1st order system. The cut-off frequency is uniform from the result calculated with Equation 3.9. From Figure 3.15 and 3.16, it is seen that the model of the OCM is acceptable.

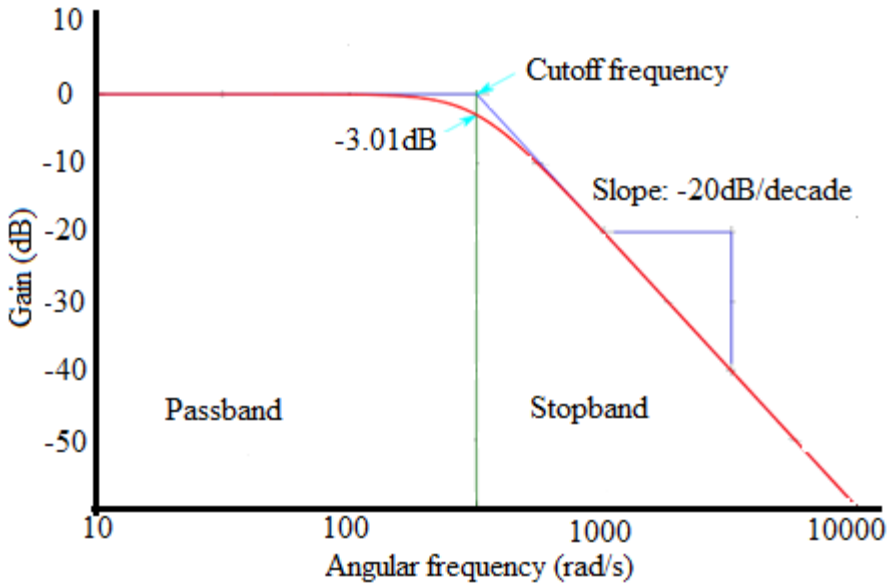

Figure 3.16 CLS correction magnet PS current loop frequency function

3.3 Vacuum Chamber Modelling

Vacuum Chamber (VC) is an ultra-high vacuum vessel system. It is used for storing the high speed electronics circuits or electronics for short. During the normal operation in the SR, specific requirements on the VC are as follows (Lowe, 2001):

- The pressure inside vessel is expected to be less than $133nPa$. The pressure when the SR operation is in a normal situation is shown in Figure 3.17.
- The normal ambient temperature of the SR tunnel should be 27ºC.
- The magnetic permeability inside the magnet of chambers should be less than 1.01.
- The support girders should have a maximum vibration movement of less than 0.4 microns at frequencies less than 100Hz.
- The range of humidity of the components should be between 25% and 50% depending on the seasons.
- There should be a water cooling system to cool the chamber. The velocity of the cooling water roughly between 1.5 and 2.0 m/s.

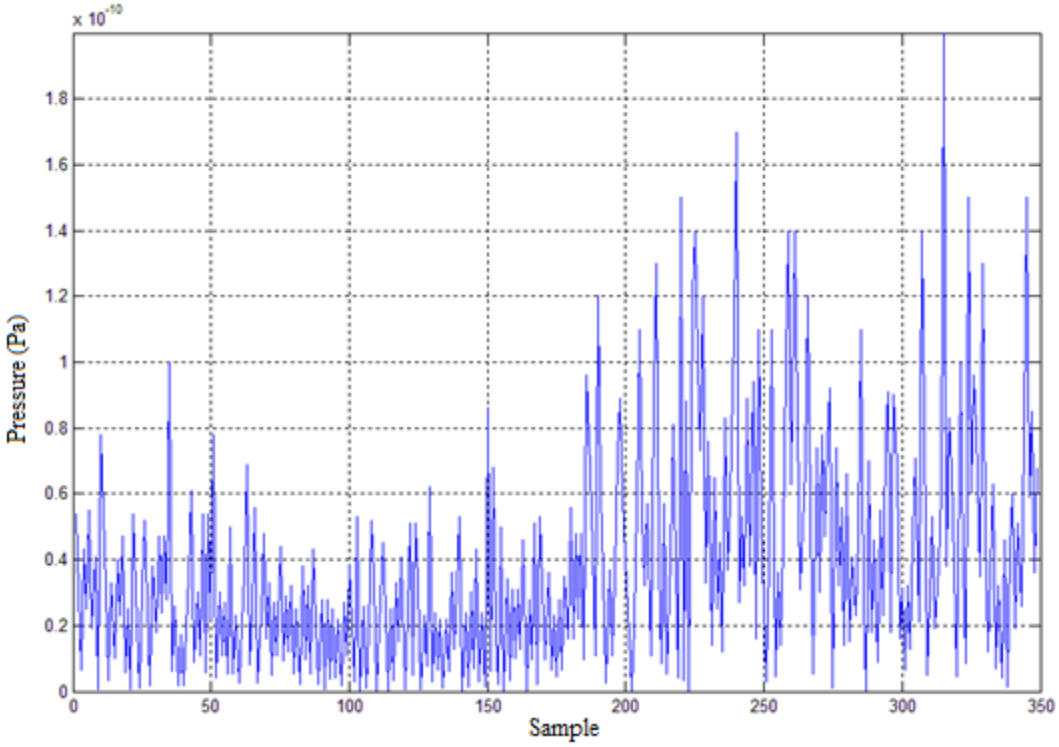

Figure 3.17 Pressures inside of VC when the SR is under the normal operation

It is extremely difficult to have a test-bed to meet the above requirements to build the model of the VC. In this study, a simulation system was employed. The simulation system was offered by Dr. Montse Pont and Marc Munoz from the Consortium for the Exploitation of the Synchrotron Light Laboratory (CELLS). The model was built upon Finite Element Method Magnetics (FEMM), which is a suite of programs to solve low frequency electromagnetic problems on 2D domain (Meeker, 2010). The model for the horizontal correction is shown in Figure 3.18.

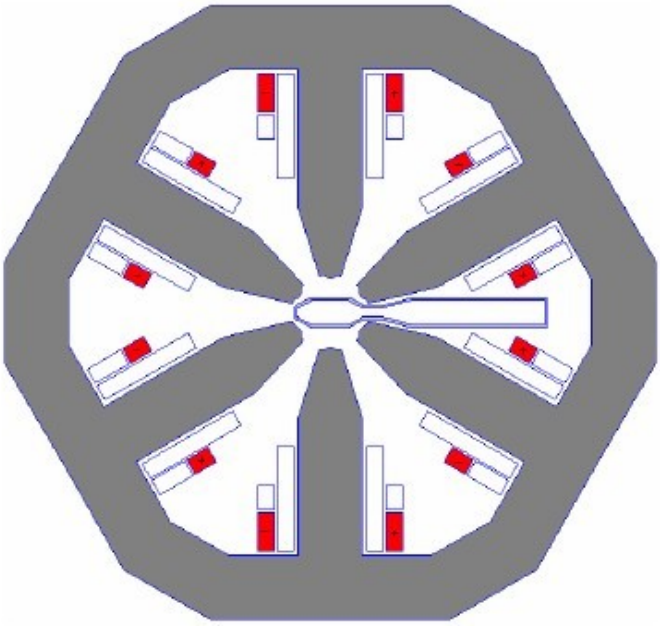

Figure 3.18 Horizontal correction coil configuration on FEMM, CELLS (adapted from Lopes, 2005)

The magnetic field attenuation with varying thicknesses at x=0 mm is shown in Figure 3.19.

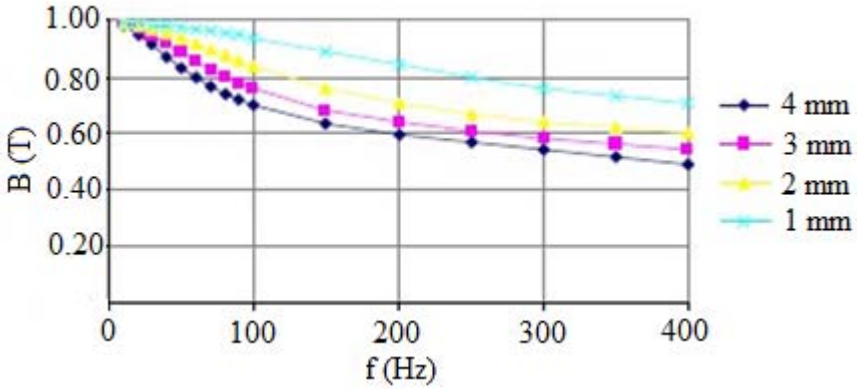

Figure 3.19 Magnetic Field attenuation of the VC varying on thickness at x =0mm (adapted from Lopes, 2005)

The cut-off frequency of the VC for the horizontal correction measured is 235 Hz (Beltran and Munoz, 2007). From the last section for OCM identification, the cut-off frequency of the OCM is 52.529 Hz. Thus, the VC cut-off frequency is greater than the OCM's. This means that there is no attenuation before OCM starts attenuating. Based on this observation, the transfer function of

the VC can be assumed to be 1. It is noted that CELLS did not have this assumption. At CELLS, the transfer function of the VC can be found by Equation 3.12.

$$H_{CV} = \frac{1/(2\pi \times 218)s + 1}{1/(2\pi \times 235)s + 1} \tag{3.12}$$

The above equation suggests that the influence over the correction by VC is little. Its step response is shown in Figure 3.20. From this figure, one can see that it is reasonable to assume that the transfer function of the VC is 1.

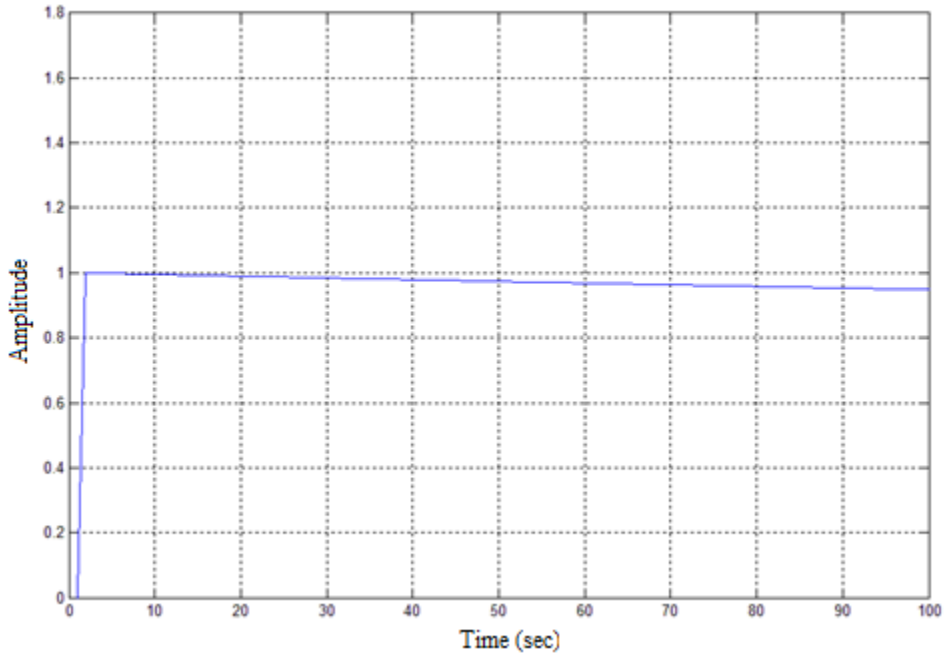

Figure 3.20 Step response of VC in SR of CELLS

3.3.1 Noise Identification

When the SROC is shut down, the beam orbit off correction which is named “bare orbit” can be obtained, which is shown in Figure 3.21. The sampling rate is 10 kHz.

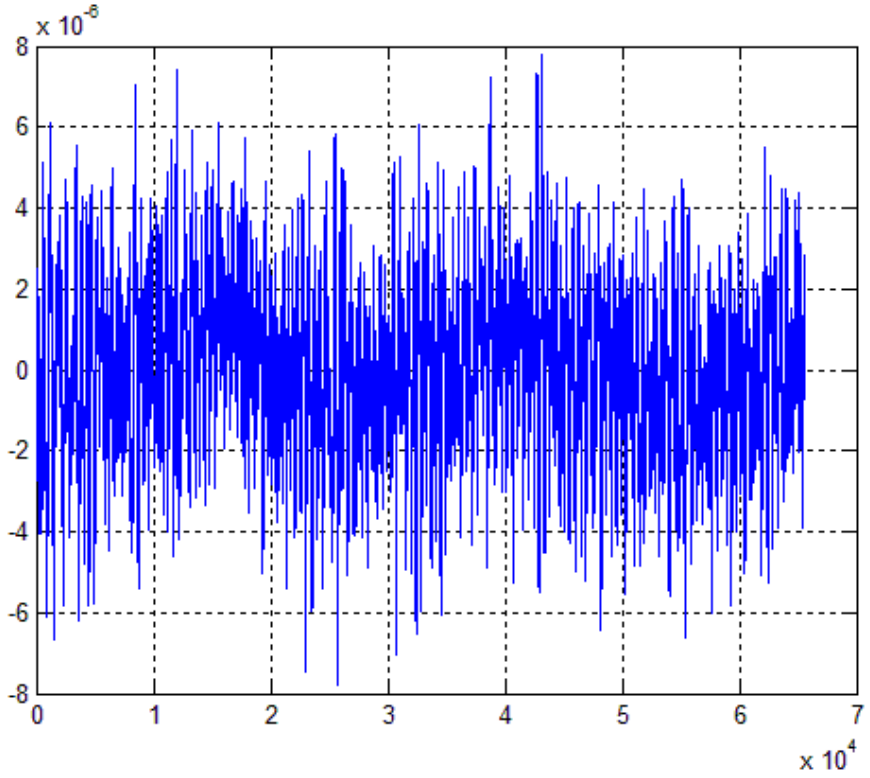

Figure 3.21 Bare orbit of SR in CLS when the correction system is off

The group of data can be named “system noise”. Next, the data will be analyzed with SPSS. Its histogram is shown in Figure 3.22.

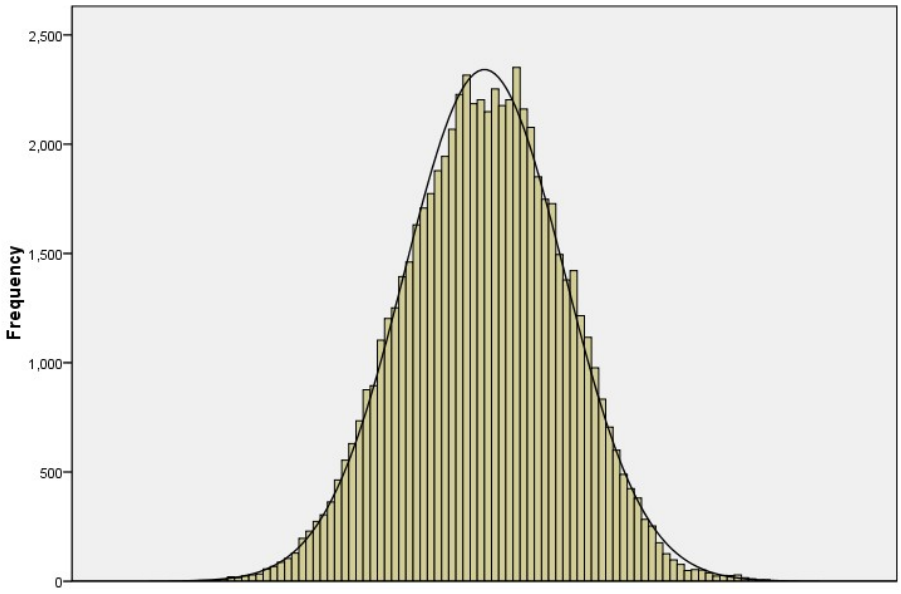

Figure 3.22 Histogram of the system noise

The Q-Q plot is shown in Figure 3.23, and the descriptive analysis is shown in Figure 3.24.

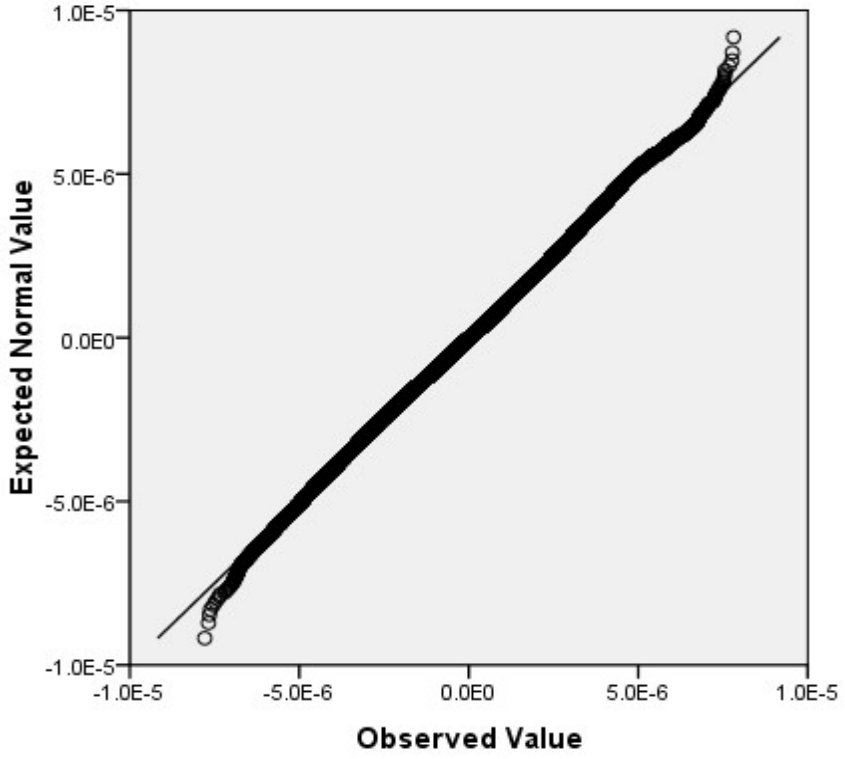

Figure 3.23 Q-Q plot of the system noise

Descriptives

			Statistic	Std. Error
y	Mean		...	...
	95% Confidence Interval for Mean	Lower Bound	-1.643E-8	
		Upper Bound	1.643E-8	
	5% Trimmed Mean		4.758E-9	
	Median		2.780E-8	
	Variance		.000	
	Std. Deviation		2.146E-6	
	Minimum		-7.789E-6	
	Maximum		...	
	Range		...	
	Interquartile Range		...	
	Skewness		-.033	.010
	Kurtosis		-.138	.019

Figure 3.24 Descriptive analysis of the system noise

Through the above SPSS analysis, the noise data is a Normal distribution. Therefore, the system noise is Gaussian noise and its mean is: $\mu = 2.0728 \times 10^{-22} \approx 0$, and its standard deviation is: $\sigma = 2.14691 \times 10^{-6}$. In Matlab, the auto-correlation and its power spectrum of the system noise can be obtained. The autocorrelation of the system noise is shown in Figure 3.25. Its power spectrum is shown in Figure 3.26. The related program and the method of calculating these data are illustrated in Appendix V.

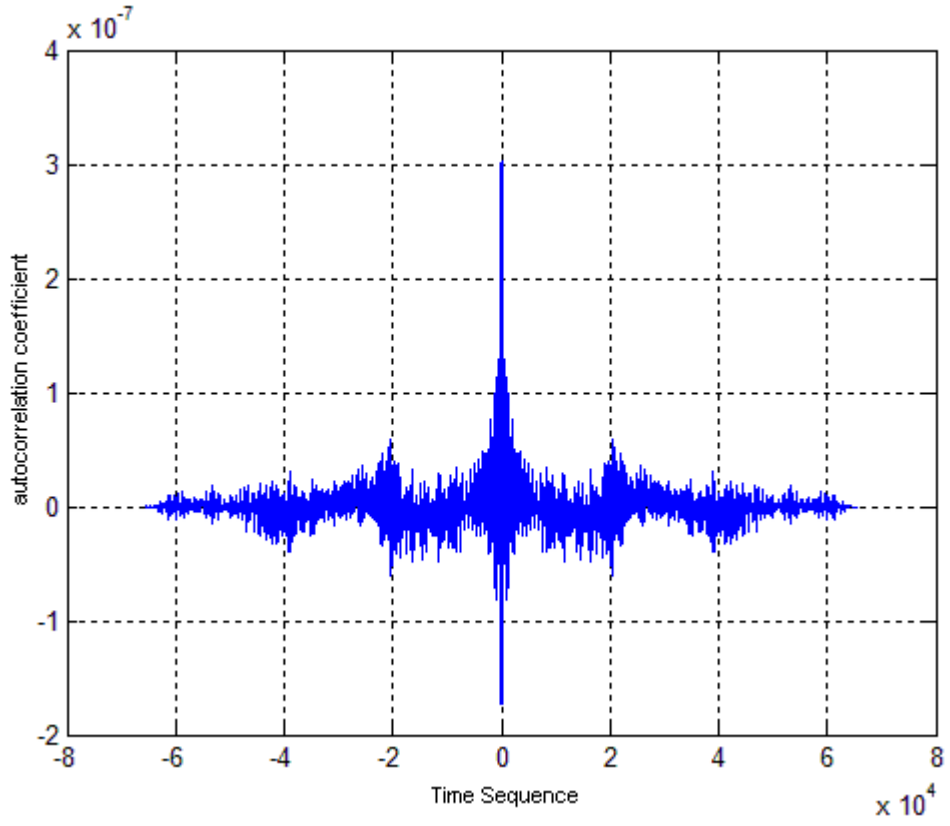

Figure 3.25 Auto-correlation of the system noise

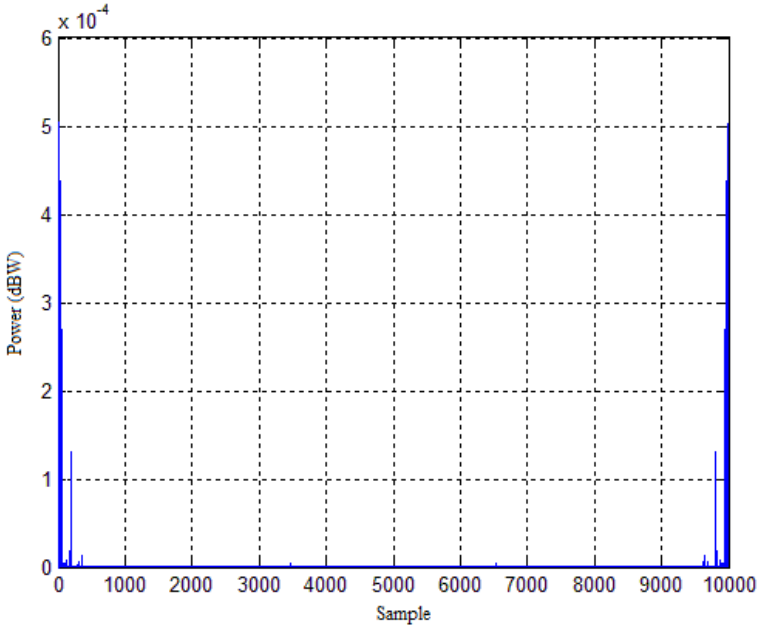

Figure 3.26 Power spectrum of the system noise

From Figure 3.26 and Figure 3.27, the system noise can be recognized as Gaussian white noise (Appendix VI).

3.4 Conclusions

The SROC system can be viewed as a control system. In this control system, the storage ring is the plant. There are three important components or systems in the storage ring, namely, BMP, OCM, and VC, and their dynamics, which are represented by transfer function, need to be understood. This chapter presented work to develop their transfer function. Further, for a more reliable simulation study, the noise of the plant system needs to be identified, which was also described in this chapter. The following conclusions can be drawn:

1. The transfer function of the BPM is a 2^{nd} order function.
2. The transfer function of the OCM is a 1^{st} order function.
3. The transfer function of the VC can be assumed to be 1.
4. The noise in the SR of CLS is approximately a Gaussian white noise.

CHAPTER 4 MODEL DEVELOPMENT AND SIMULATION STUDY

4.1 Introduction

In this chapter, implementations of several methods for orbit correction are described, and they are SVD, EVC, and SVD+PID. Base on the motivation and objective, the updating rate in the simulation is set at 45 Hz. The all simulations are worked in Matlab. At the end, comparisons for them are discussed.

4.2 SVD Method for Orbit Correction

4.2.1 Response Matrix

The SVD method is built upon the concept of response matrix. The response Matrix is a matrix which represents the relationship between the movement of the beam measured by BPM and the "kick strength" provided by OCM. The term "kick strength" is used in synchrotron technology, representing a magnetic force to correct the beam movement in case of the presence of orbit deviations. The response matrix is expressed by Equation 4.1 (Chung et al., 1993).

$$\Delta x = R \cdot \Delta\theta \tag{4.1}$$

where R : response matrix;

Δx : orbit difference between the reference or design orbit and current orbit measured by BPM; and

$\Delta\theta$: kick strengths.

The elements of the response matrix are found by Equation 4.2 (Sands, 1970).

$$R_{ij} = \frac{\sqrt{\beta_i \beta_j}}{2sin\pi\nu} \cos\left(|\psi_i - \psi_j| - \pi\nu\right) \tag{4.2}$$

where R_{ij} : the element of the response matrix;

β_i : i^{th} BPM beta function;

β_j : j^{th} OCM beta function;

ψ_i : i^{th} BPM phase function;

ψ_j : j^{th} OCM phase function; and

ν : Betatron tune of the machine.

In practice, the response matrix is found through the measurement instead of Equation 4.2.That is, giving the kick strength from OCM and then getting the related beam movement from BPM as shown in Figure 4.1.

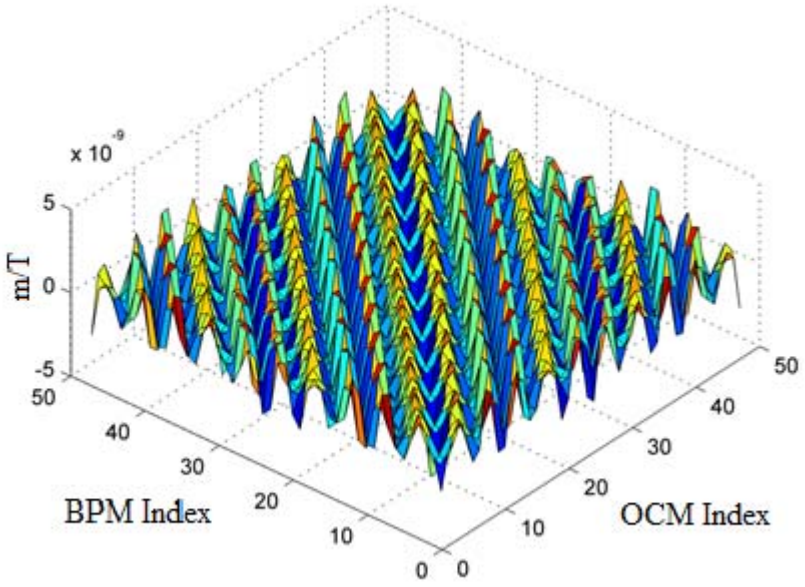

Figure 4.1 Response matrix on the 3D mode of CLS (Horizontal kick, T is the unit of Magnetic field intensity; m is the unit of orbit offset)

From a point of view of beam stabilization or orbit correction, one needs to compute $\Delta\theta$ from Δx. So the response matrix needs to be inversed; see Equation (4.3). The inverse of the response matrix is denoted as R_{inv}.

$$\triangle \theta = R_{inv}\Delta x \tag{4.3}$$

When the response matrix is a square matrix and non-singular, the inverse of the response matrix has a unique solution. However, when the response matrix is singular, there will be no solution at all, and in this case, one can consider that the response matrix is degenerated to a non-square matrix. In general, for a non-square response matrix, the procedure to find $\triangle \theta$ from Δx follows the so-called singular value decomposition (SVD).

4.2.2 Singular Value Decomposition

A real or complex matrix M can be factorized (Golub and kahan, 1965) as:

$$M = U\Sigma V^T \tag{4.4}$$

where M: $m \times n$ real or complex matrix;

U: $m \times m$ real or complex unitary matrix;

Σ: $m \times n$ real or rectangular diagonal matrix without negative real number on the diagonal; and

V^T: conjugate transpose matrix of V, an $n \times n$ real or complex unitary matrix.

The pseudo-inverse matrix of M can be found by (Chung, 1992)

$$M_{inv} = V\Sigma_{inv}U^T \tag{4.5}$$

where M_{inv}: the pseudo-inverse matrix of M;

U^T: the conjugate transpose matrix of U, an $m \times m$ real or complex unitary matrix;

Σ_{inv}: the pseudo-inverse matrix of Σ ; and

V: an $n \times n$ real or complex unitary matrix.

For the orbit correction, the R is M in the foregoing discussions. This means that R_{inv} in Equation 4.3 can be found from Equation 4.5. In particular, first, the R can be factorized as follows:

$$R = U\Sigma V^T \tag{4.6}$$

where R: the $m \times n$ response matrix;

U: an $m \times m$ real or complex unitary matrix;

Σ: an $m \times n$ real or rectangular diagonal matrix without negative real number on the diagonal; and

V^T: the conjugate transpose matrix of V, an $n \times n$ real or complex unitary matrix.

Then, there is:

$$R_{inv} = V\Sigma_{inv}U^T \tag{4.7}$$

where R_{inv}: inverse matrix of R;

U^T: conjugate transpose matrix of U, an $m \times m$ real or complex unitary matrix;

Σ_{inv}: inverse matrix of Σ ; and

V: $n \times n$ real or complex unitary matrix.

Figure 4.2 shows R_{inv} graphically.

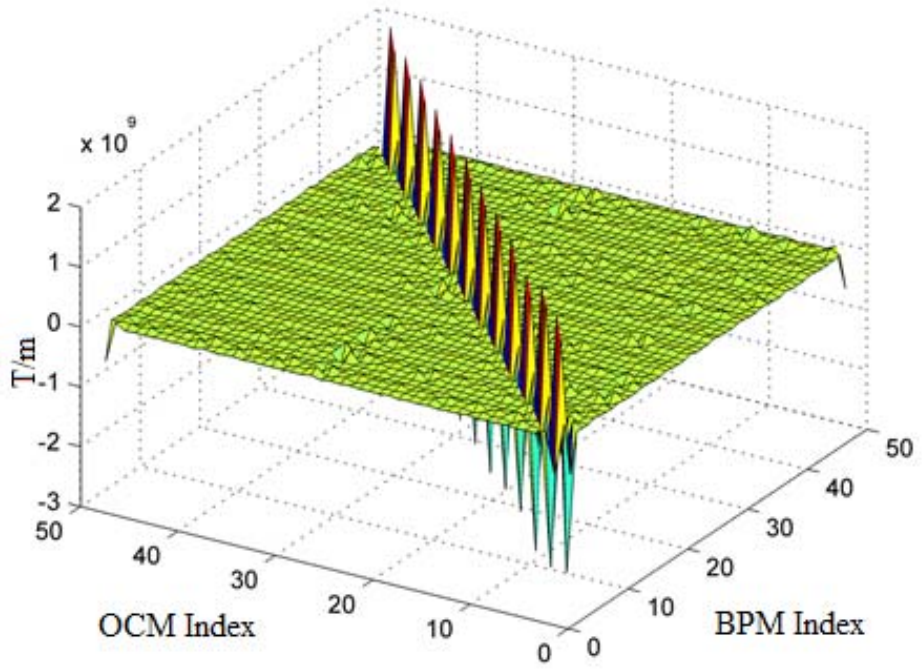

Figure 4.2 Inverse response matrix of CLS (Horizontal kick, T is the unit of Magnetic field intensity; m is the unit of orbit offset)

4.2.3 Flow Chart and Simulation

Figure 4.3 is a flowchart of the SVD orbit correction method, which is self-explanatory. Further, Figure 4.4 shows a control block diagram for the SVD method. In this figure, the noise is Gaussian White noise. During the simulation, the standard deviation can be varied in order to examine the sensitivity of the model. In this study, the noises were divided into 10 groups with each having its own standard deviation (Table 4.1). In Table 4.1, the first row represents the group number, and the second row gives the standard deviation of the group. The simulation result is shown in Figure 4.5. In this figure, the horizontal axis is the BPM index; the vertical axis is the RMS value. The RMS results are listed in Table 4.2.

Table 4.1 Standard deviations ($\boldsymbol{\sigma(m)}$)

	1	2	3	4	5	6	7	8	9	10
$\sigma(10^{-6})$	0.215	0.5	1	2.15	4	8	10	15	20	21.5

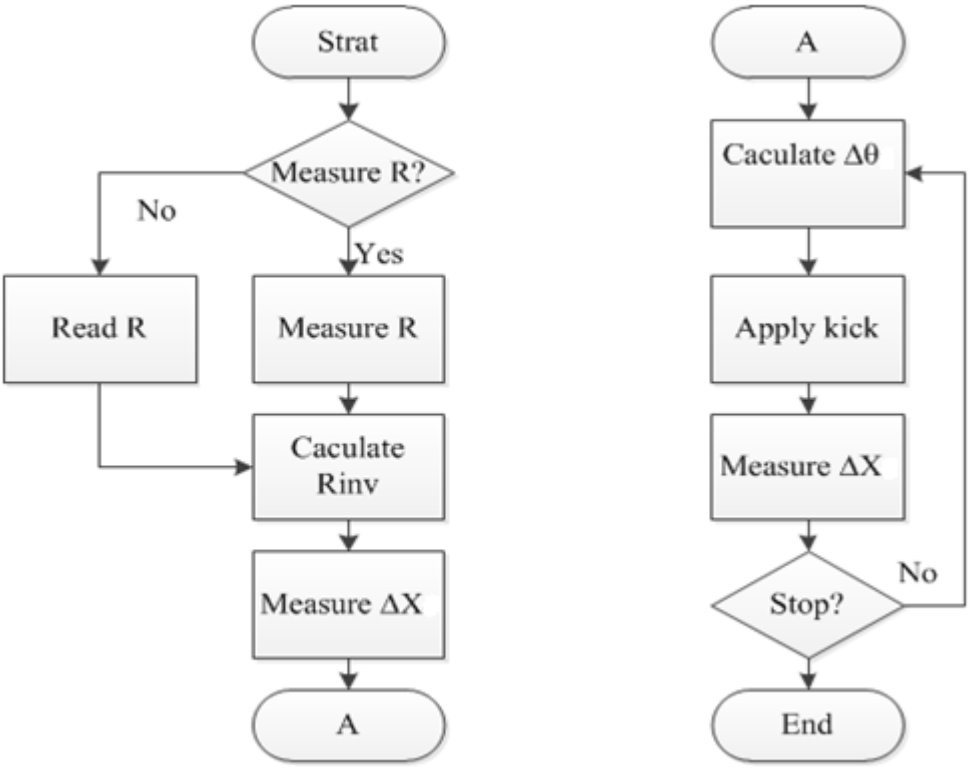

Figure 4.3 Flow chart of SVD algorithm for orbit correction (adapted from Chung et al., 1992)

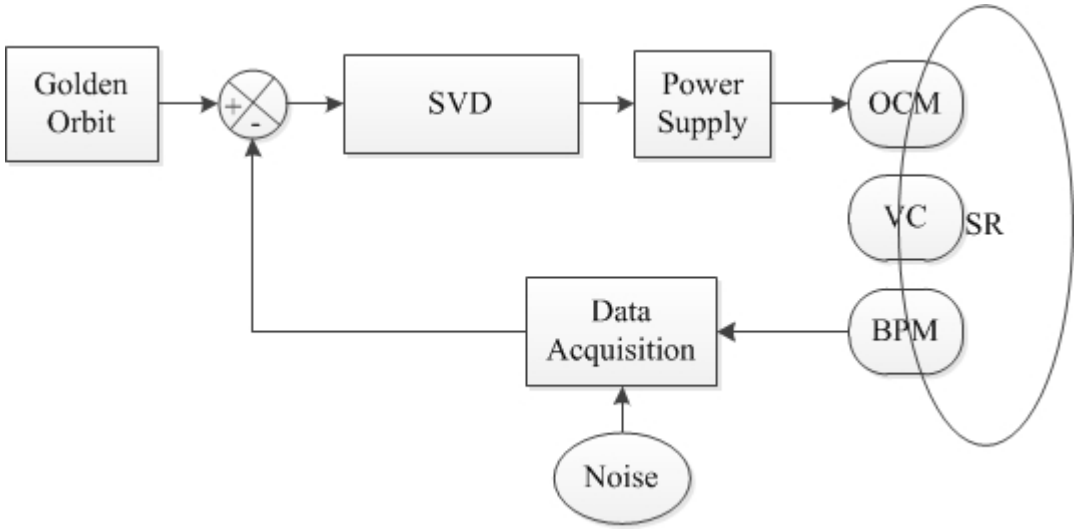

Figure 4.4 Control diagram of SVD model

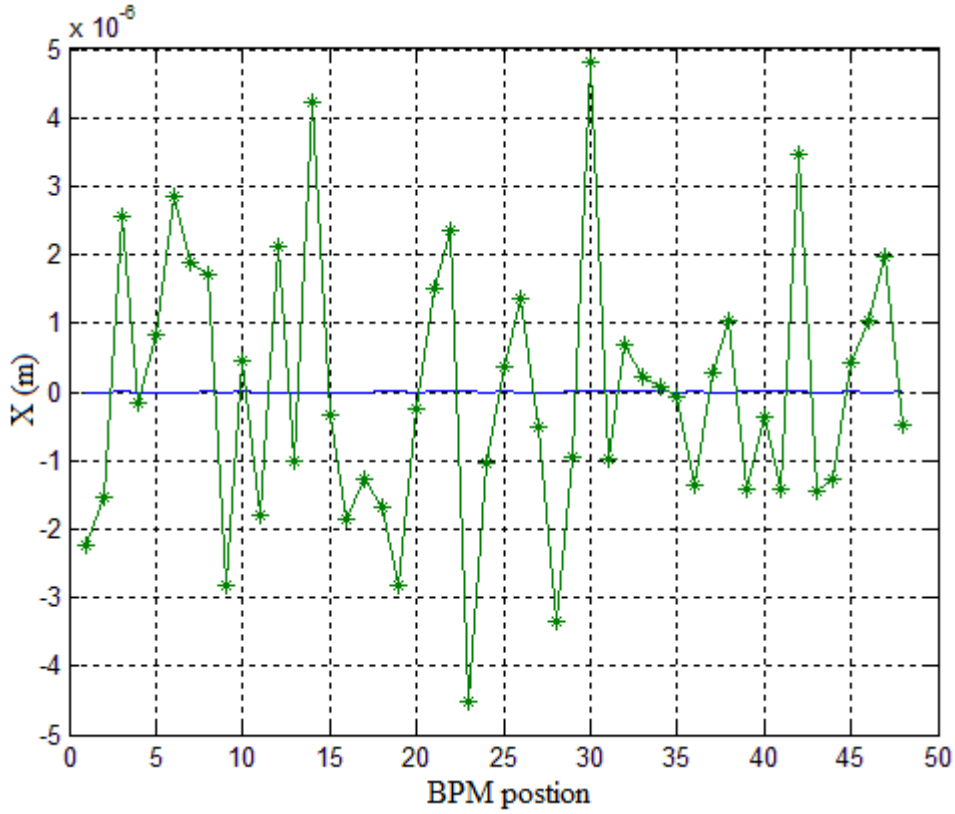
x 10^-6
X (m)
BPM postion

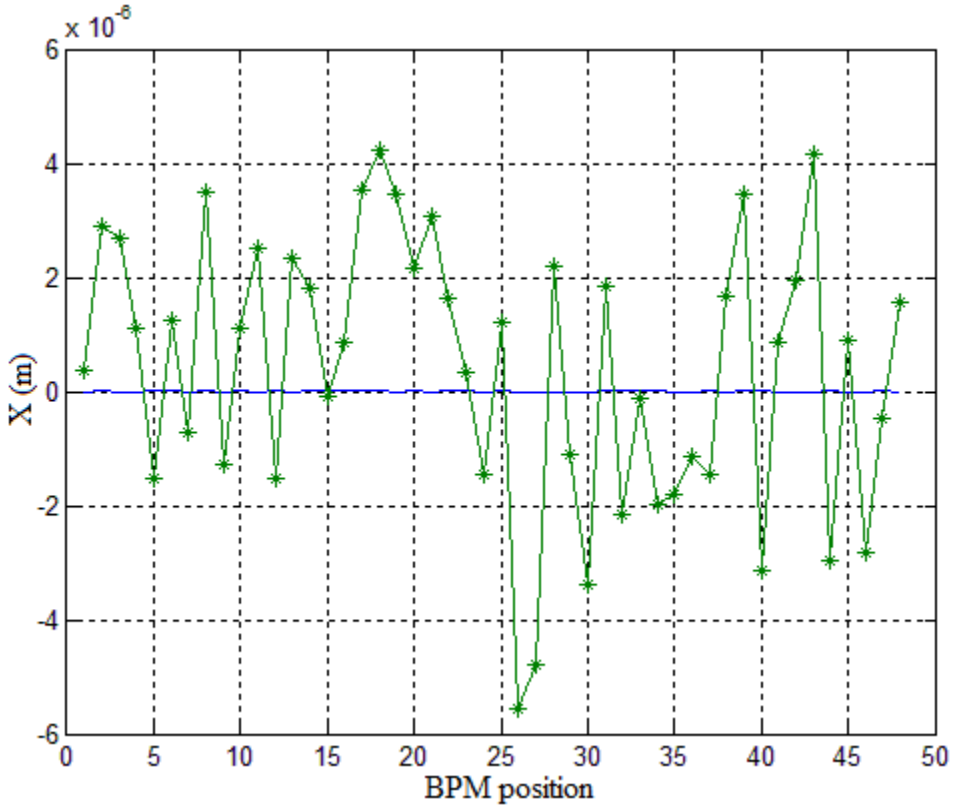
x 10^-6
X (m)
BPM position

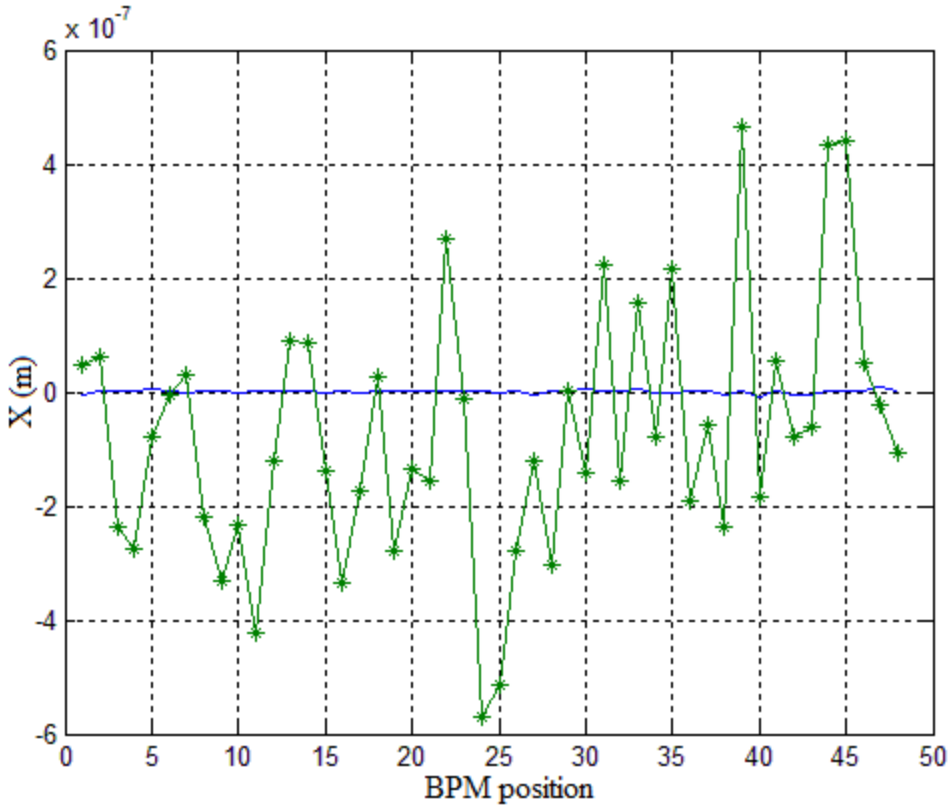

Figure 4.5 Result of the SVD simulation. Top: $\boldsymbol{\sigma = 0.215}$; Middle: $\boldsymbol{\sigma = 2.15}$; Bottom: $\boldsymbol{\sigma = 21.5}$

Table 4.2 RMS values of the SVD method ($\sigma(m)$)

	1	2	3	4	5	6	7	8	9	10
$\sigma(10^{-10})$	0.239	0.761	1.94	4.72	5.52	12.75	12.03	31.76	20.99	33.54

4.3 EVC Method for Orbit Correction

The motivation of the EVC method was to trade-off between the global and local orbit corrections. The global and local orbit corrections may have conflicts (Harada el at., 2009). The evidence was further provided where there may be some leakage of a local orbit bump (Plouviez et al., 2005). The EVC method was proposed by Nakamura et al. (2006), which aims to provide both global and local orbit corrections by having one single feedback loop only. It is noted that the concept of global and local orbit correction was discussed before in Section 1.1.4.

Let Δx,$\Delta\theta$ and Rdenote the measured orbit by the BPM, the kick angle strength by the OCM, and the response matrix, respectively. The norm of Δ defined by Equation 4.8 is required to be zero or as small as possible in light of beam stabilization.

$$\Delta = R(\Delta\theta) + \Delta x \tag{4.8}$$

The norm of Δ has a minimum value when its derivatives with respect to θ_j (j=1 2… N) are zero. The $\Delta\theta$ is determined by Equation 4.9.

$$A(\Delta\theta) + R^T(\Delta x) = 0 \tag{4.9}$$

where $A = R^T R$ (A is a square matrix). This equation can be decomposed as:

$$A = U\lambda U^T \tag{4.10}$$

λ is the eigenvalues of the matrix A.

A $l \times m$ matrix P is defined to select the l BPMs where the zero error is desired. The i^{th} row and j^{th} column of P is equal to 1 for indicating that the constraint i is set to the j^{th} BPM reading. The other elements are 0. The auxiliary matrices B and D are defined as:

$$B = (ZR)^T \tag{4.11}$$

$$D = \tilde{A}^{-1}B\left(B^T\tilde{A}^{-1}B\right)^{-1} \tag{4.12}$$

where $\tilde{A}^{-1}$ is the inverse of A obtained with the filtered reciprocal of the eigenvalues of λ.

The correction matrix C is obtained with the filtered singular values and zero error constraints for a set of BPMs by the following equation (Tavares et al., 2011):

$$C = DZ - (DB^T - I_n)\tilde{A}^{-1}R^T \tag{4.13}$$

where I_n: n × n identity matrix.

Figure 4.6 shows a block diagram of the EVC method. Suppose that the response matrix is 48 × 48, and the 7th and 16th BPM are set 'zero error'. So the auxiliary matrix Z is shown as follows: the 7th element in first row is 1, and the 16th element in second row is 1.

$$Z = \begin{bmatrix} 0 & 0 & 0 & 0 & 0 & 0 & 1 & 0 & 0 & \cdots & 0 \\ 0 & 0 & 0 & 0 & 0 & 0 & \cdots & 0 & 1 & \cdots & 0 \end{bmatrix} \tag{4.14}$$

The correction matrix C can be determined. The input noise was set to be the same as that for the SVD model, which implies the same μ and σ. The simulation result is shown in Figure 4.7. The RMS values are listed in the Table 4.3. In order to determine the performance of setting "zero error", 48 group simulations for each standard deviation were processed. The result is shown in Figure 4.8. The RMS values of 7th BPM and 16th BPM in the SVD Model are listed in the Table 4.4. The RMS values of 7th BPM and 16th BPM in the EVC Model are listed in the Table 4.5.

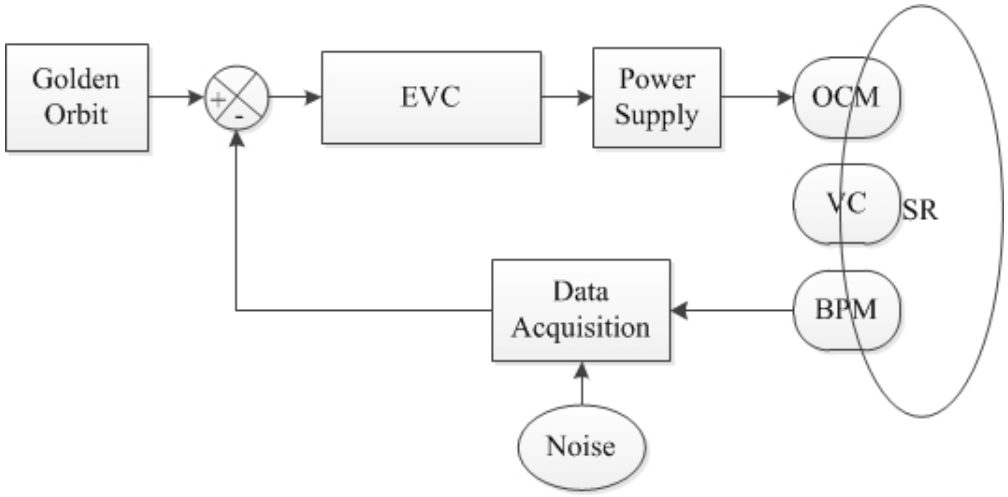

Figure 4.6 Control diagram of the EVC model

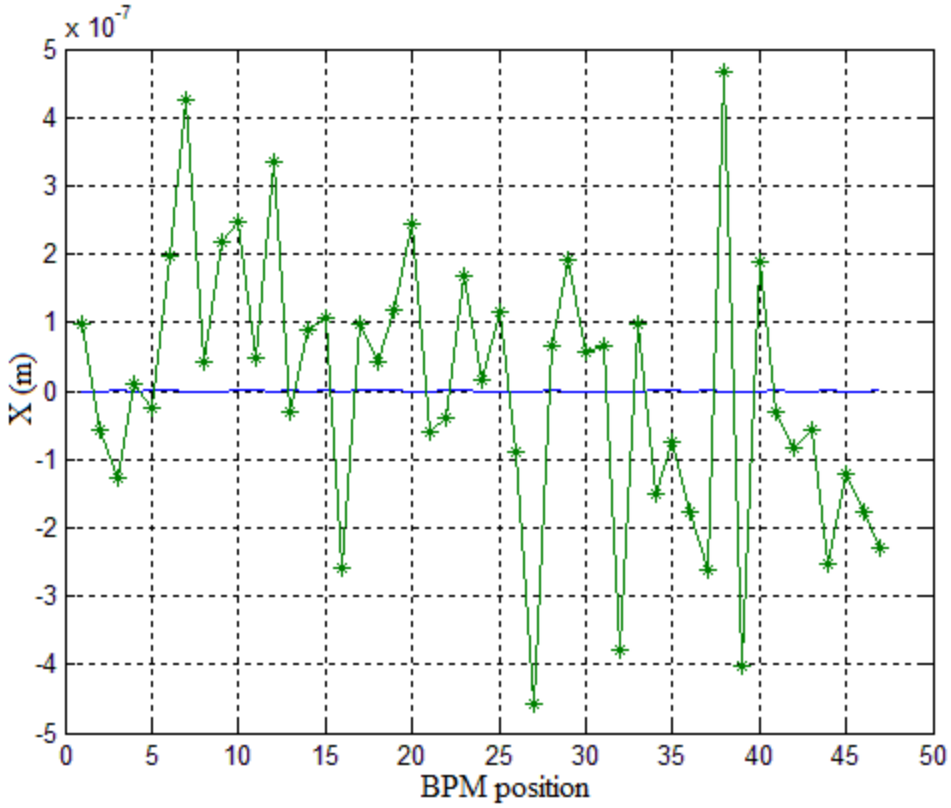
x 10^-7
X (m)
BPM position

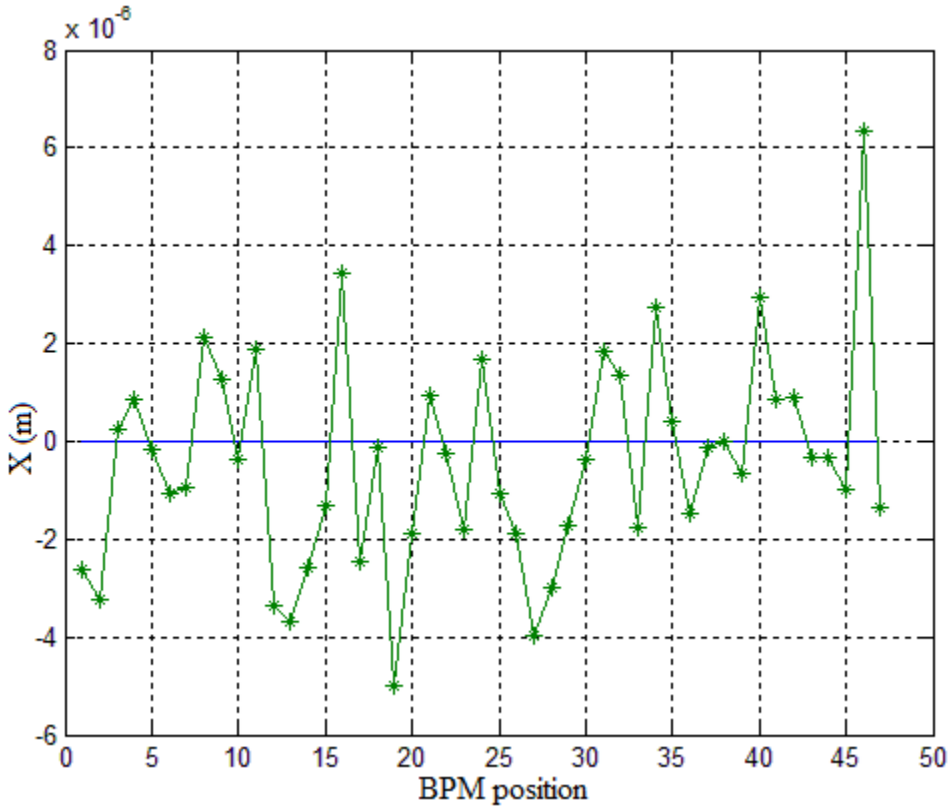
x 10^-6
X (m)
BPM position

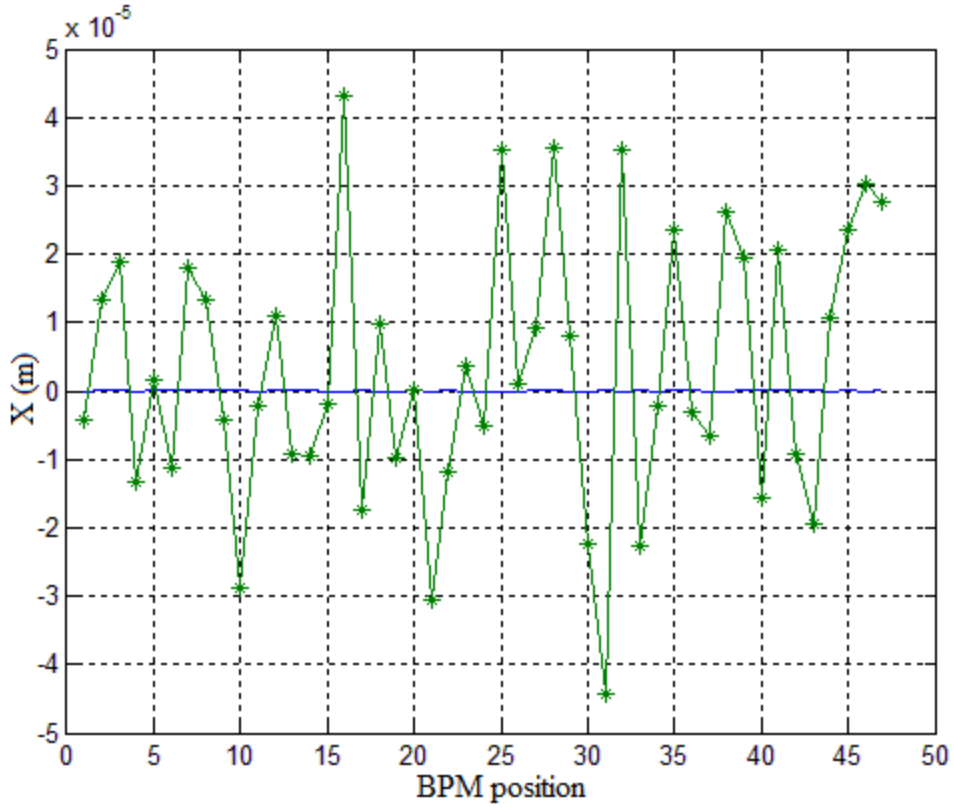

Figure 4.7 Result of the EVC simulation. Top: $\boldsymbol{\sigma = 0.215}$; Middle: $\boldsymbol{\sigma = 2.15}$; Bottom: $\boldsymbol{\sigma = 21.5}$

Table 4.3 RMS values of EVC model ($\boldsymbol{\sigma(m)}$)

	1	2	3	4	5	6	7	8	9	10
$\sigma(10^{-10})$	0.642	0.918	2.616	5.518	8.076	16.324	31.095	46.558	41.331	58.096

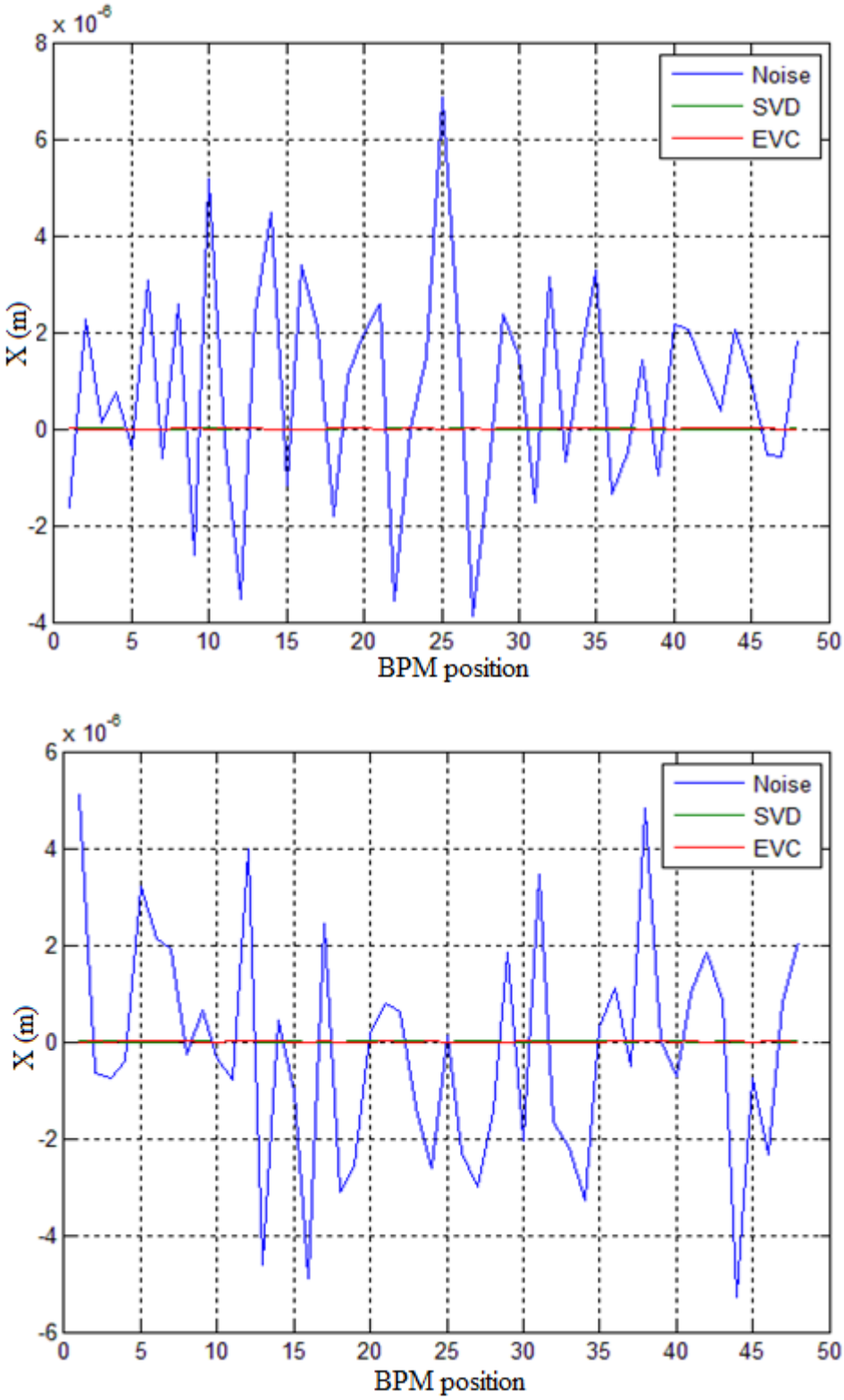

Figure 4.8 Beam orbit on the 7th and 16th BPM, respectively (Top: 7th BPM; Bottom: 16th BPM). The standard deviation of the noise is $\boldsymbol{\sigma = 2.15 \times 10^{-6}}$

Table 4.4 RMS value of 7th and 16th BPM in the SVD model ($\boldsymbol{\sigma}$: $\mathbf{10^{-10}}(\boldsymbol{m})$)

BPM Position	1	2	3	4	5	6	7	8	9	10
7th	0.303	0.832	2.135	4.908	7.347	13.936	20.375	34.271	31.903	43.794
16th	0.291	0.792	2.071	4.833	6.386	11.975	18.334	30.581	29.096	39.157

Table 4.5 RMS value of 7th and 16th BPM in the EVC model (σ: $10^{-10}(m)$)

BPM Position	1	2	3	4	5	6	7	8	9	10
7th	0.218	0.533	1.801	3.216	5.322	11.259	33.134	39.073	37.887	42.113
16th	0.274	0.581	1.737	3.019	5.037	10.989	35.096	28.573	40.009	41.358

4.4 SVD+PID Method for Orbit Correction

4.4.1 PID controller

First, a PID controller (Appendix VII) was developed. This is achieved through a SISO model (Figure 4.9). Three methods to determine the gains of the PID controller were used, and they are: Ziegler-Nichols, OEC PID controller design and Output constraint tuning. The detailed algorithms of them are put in Appendix VIII.

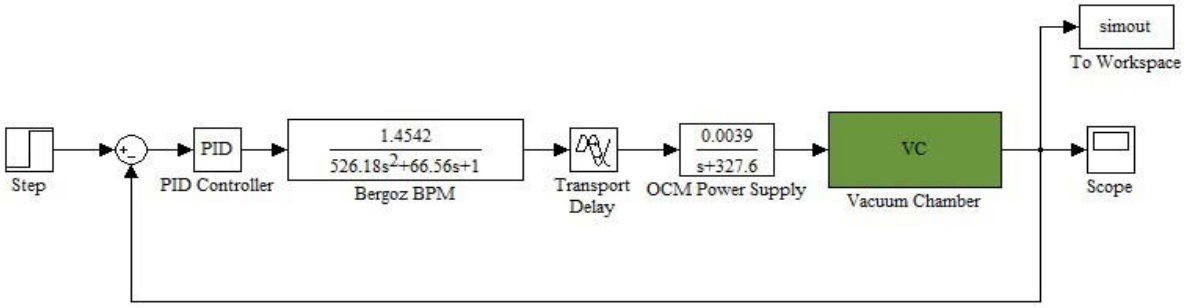

Figure 4.9 PID tuning model of SR in CLS

Ziegler-Nichols tuning: From the PID tuning model, the transfer function of the SR is:

$$G_{SR} = G_{bpm}G_{ocm} \tag{4.15}$$

The PID controller was designed using the Matlab statements in the Appendix VIII. The parameters of the controller are, respectively:

$$K_p = 0.7301$$
$$T_i = 0.02304$$
$$T_d = 0.008356$$

The PID controller designed by Ziegler-Nichols method is:

$$G_{PID} = 0.7301(1 + \frac{1}{0.02304s} + 0.008356s)$$

Its closed-loop step response is shown in Figure 4.10.

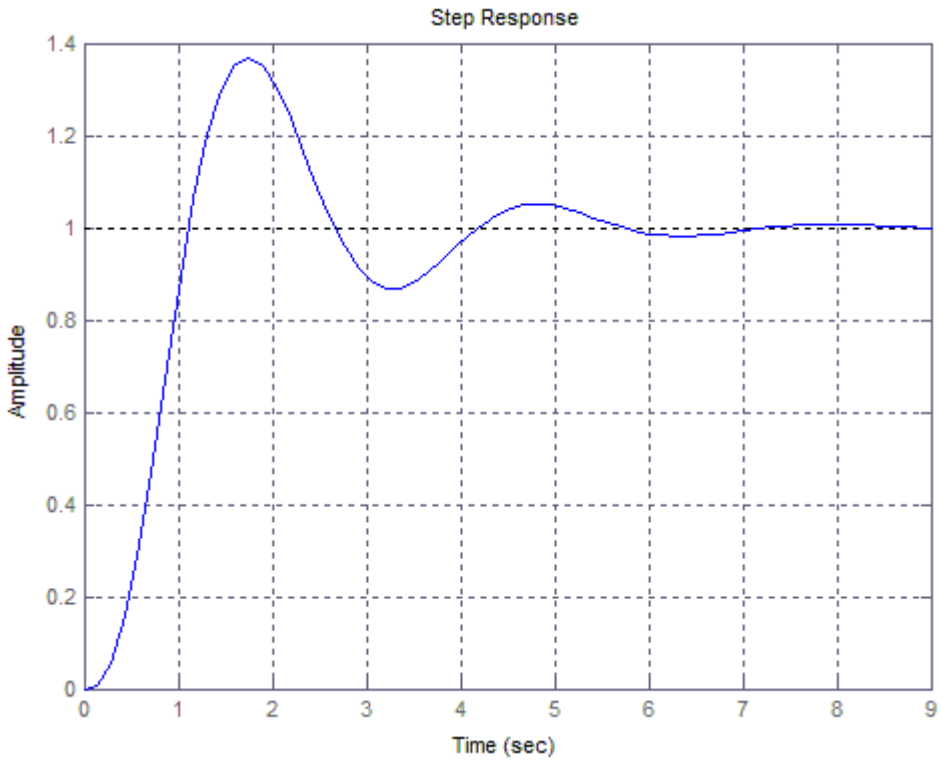

Figure 4.10 closed-loop step response of SR with PID controller by Ziegler-Nichols formula

OEC PID controller design: Based on the Matlab statements of OEC method in the Appendix VIII, the parameters of the controller are, respectively:

$$K_p = 0.8027$$
$$T_i = 0.03142$$
$$T_d = 0.009053$$

The PID controller designed by OEC method is:

$$G_{PID} = 0.8027(1 + \frac{1}{0.03142s} + 0.009053s)$$

Its closed-loop step response is shown in Figure 4.11.

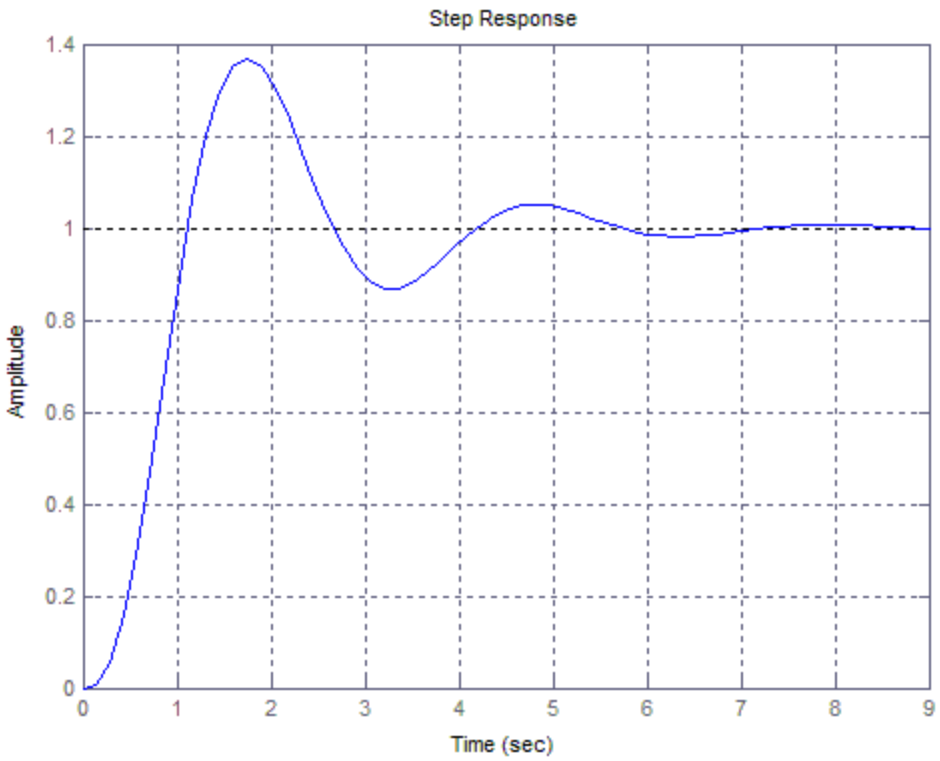

Figure 4.11 closed-loop step response of SR with PID controller by OEC formula

Output constraint tuning: The tuning model in Simulink is shown in Figure 4.12. In the model the only output constraints is that the final value is 1.

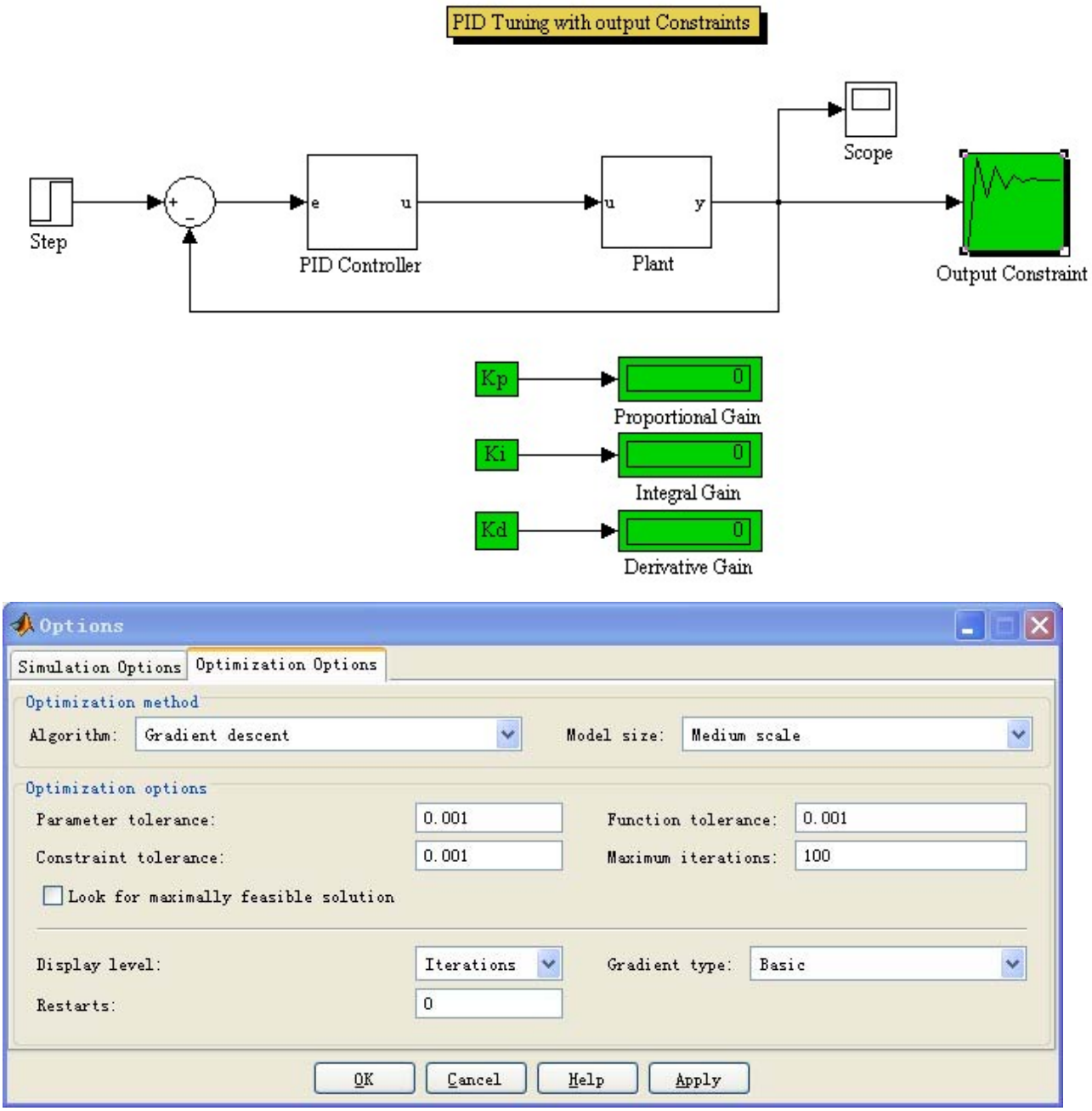

Figure 4.12 Simulink model for PID tuning with output constraint (Top); option of the optimization for PID tuning (Bottom)

The process of the fitting is shown in Figure 4.13.

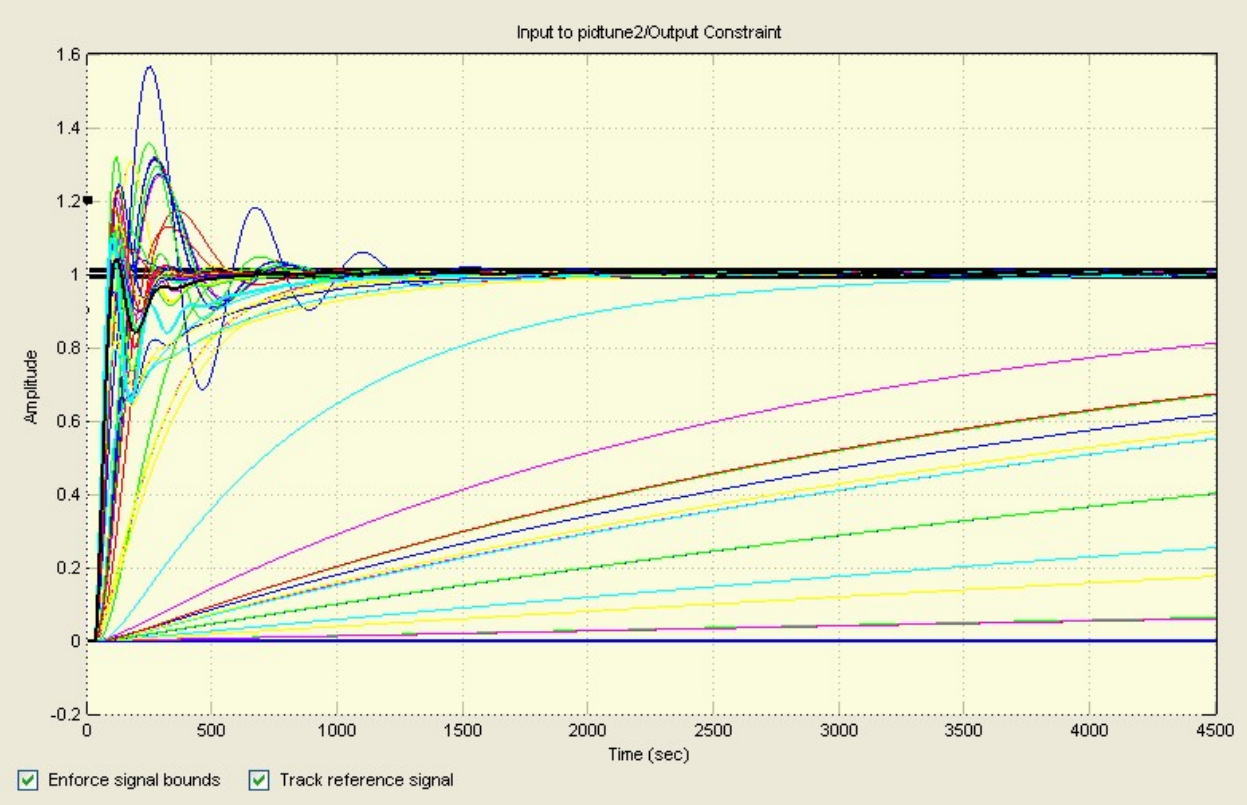

Figure 4.13 Fitting process of the PID tuning with output constraints

The parameters of the controller are, respectively:

$$K_p = 0.8596$$

$$T_i = 0.04018$$

$$T_d = 0.009378$$

The PID controller which is designed by optimum method is:

$$G_{PID} = 0.8596(1 + \frac{1}{0.04018s} + 0.009378s)$$

Its closed-loop step response is shown in Figure 4.14.

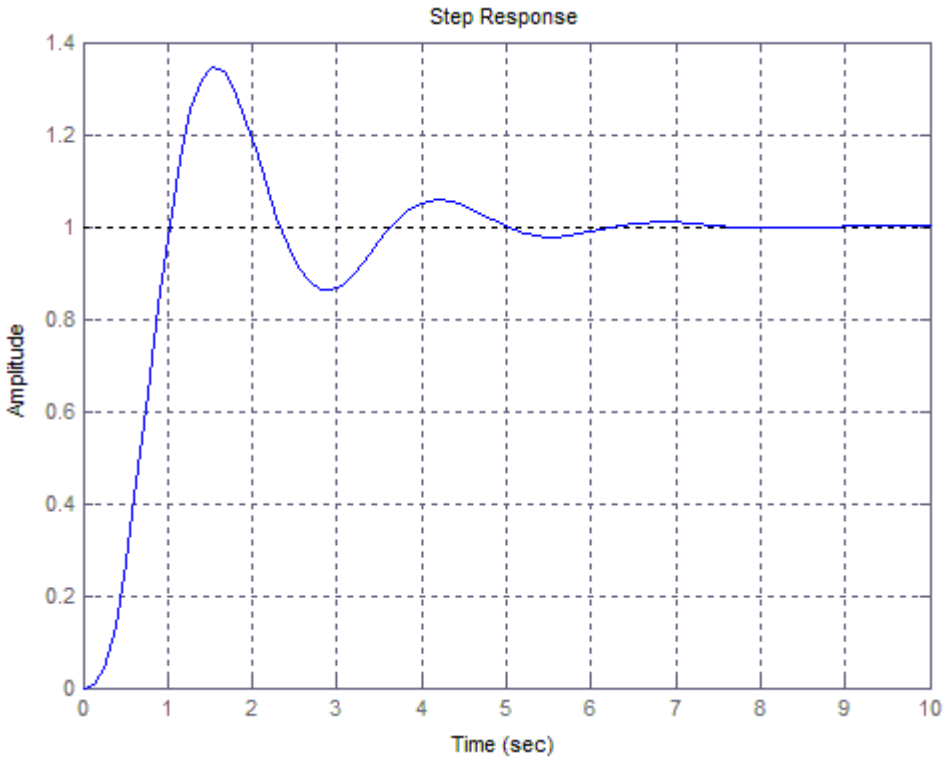

Figure 4.14 closed-loop step response of SR with PID controller by output constraints method

4.4.2 Results and Discussion

The closed-loop step response of the comparing model is shown in Figure 4.15.

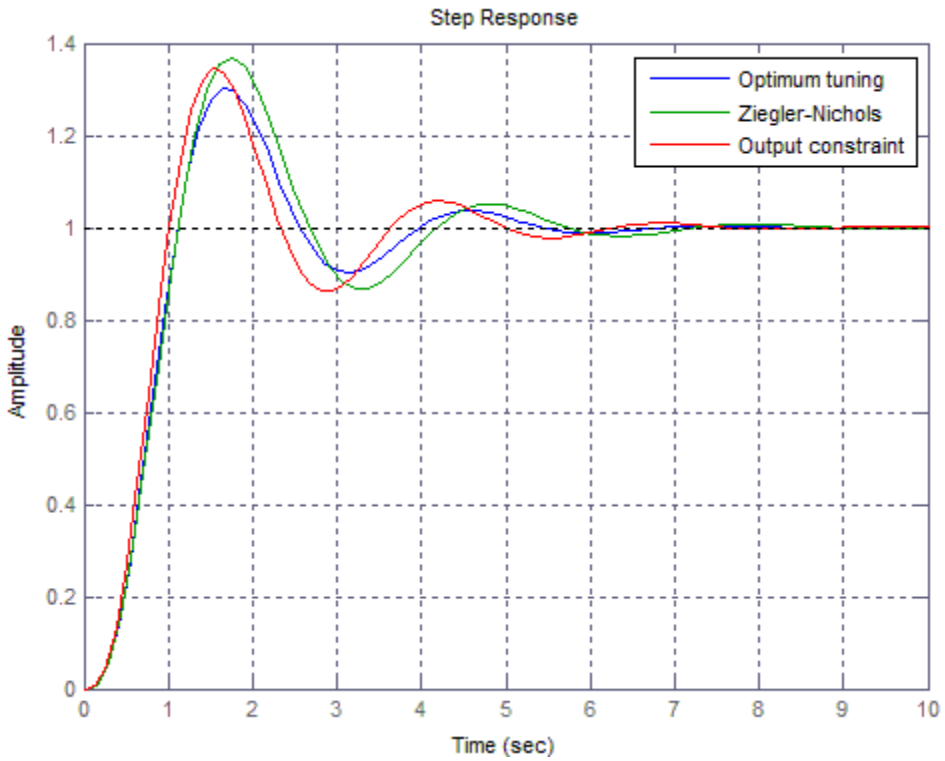

Figure 4.15 Comparison of step responses of three methods

Based on the comparison in Figure 4.15, the performance of the OEC tuning is much better than the other two. In conclusion, the PID controller for the SR model is:

$$G_{PID} = 0.8027(1 + \frac{1}{0.03142s} + 0.009053s) \tag{4.16}$$

4.4.3 Simulation

Figure 4.16 shows a control diagram of the SVD+PID model.

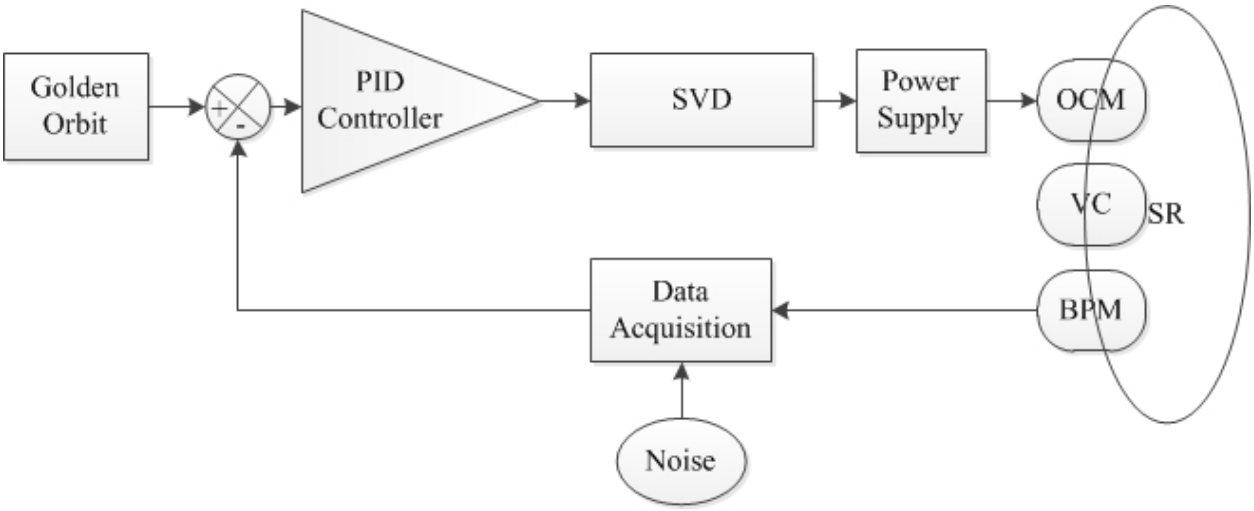

Figure 4.16 Control diagram of the SVD+PID model

The simulation result of the SVD plus PID method is shown in Figure 4.17.

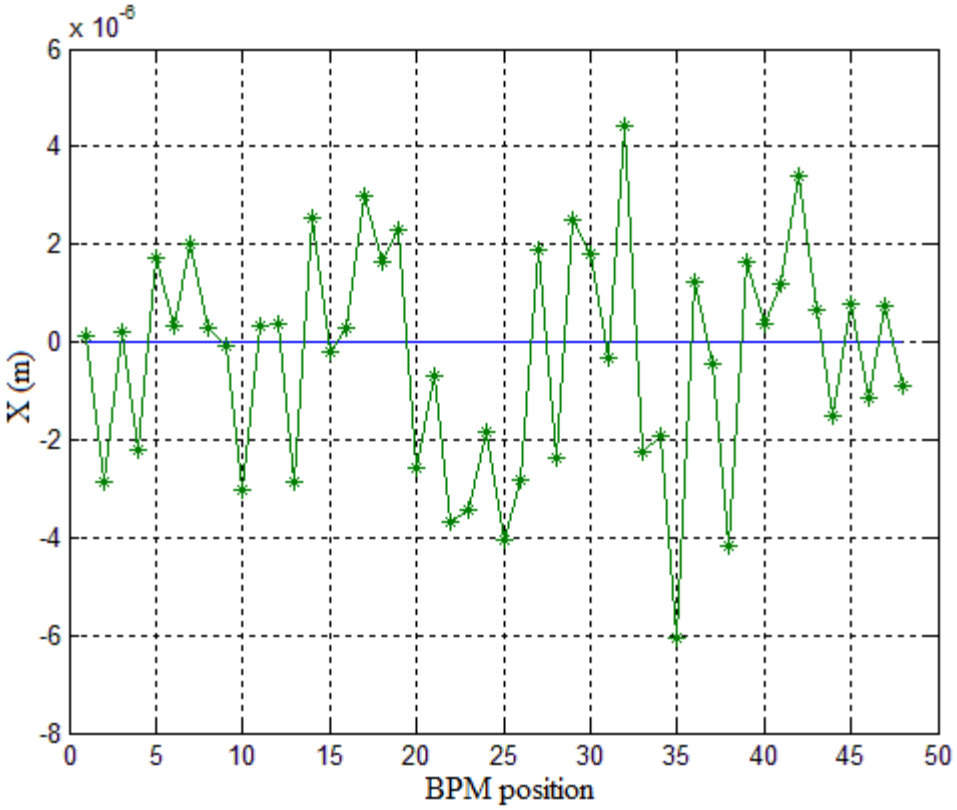
x 10^-6
6
4
2
0
-2
-4
-6
-8
X (m)
0
5
10
15
20
25
30
35
40
45
50
BPM position

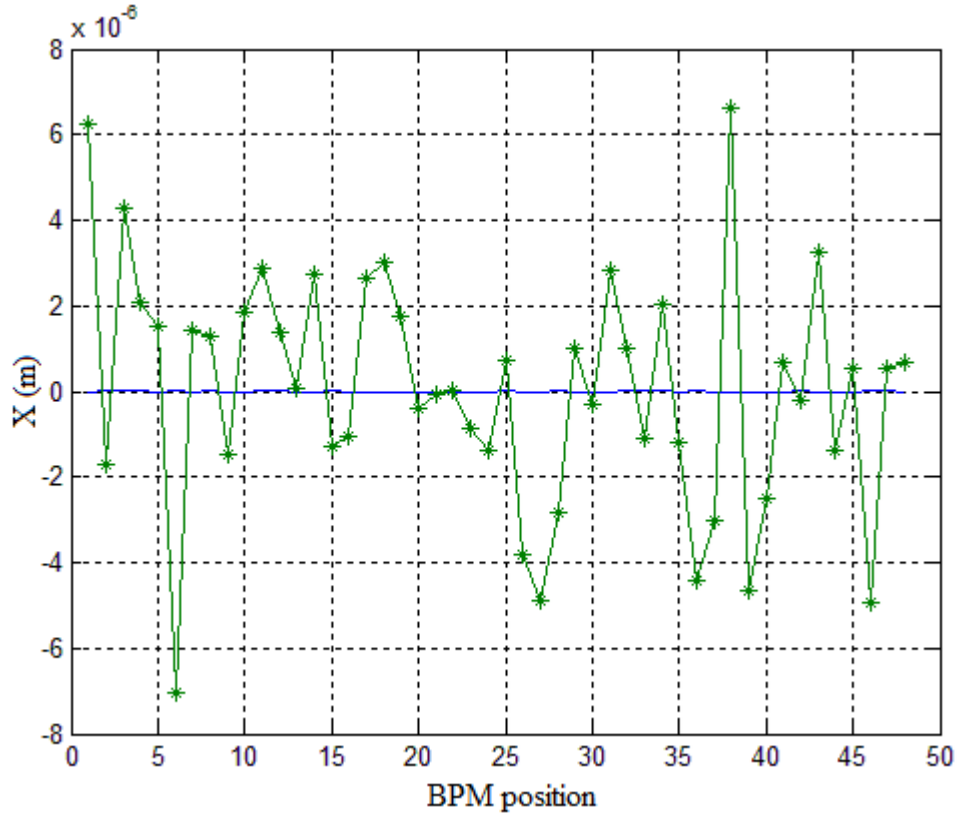
x 10^-6
8
6
4
2
0
-2
-4
-6
-8
X (m)
0
5
10
15
20
25
30
35
40
45
50
BPM position

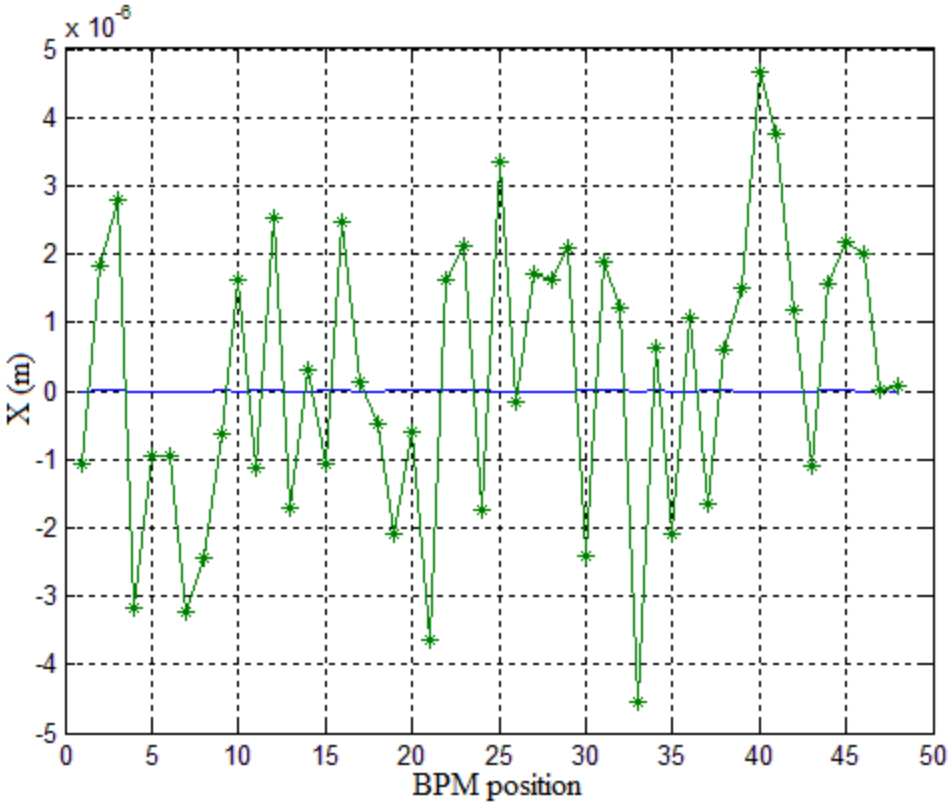

Figure 4.17 Result of the SVD plus PID simulation. Top: $\boldsymbol{\sigma = 0.215}$; Middle: $\boldsymbol{\sigma = 2.15}$; Bottom: $\boldsymbol{\sigma = 21.5}$

The RMS values are listed in the Table 4.6.

Table 4.6 RMS values of SVD+PID method ($\sigma(m)$)

	1	2	3	4	5	6	7	8	9	10
$\sigma(10^{-10})$	0.101	0.428	0.988	2.14	3.94	8.39	10.22	18.69	25.92	39.13

4.5 Comparison with Discussion

4.5.1 EVC versus SVD

The comparison of the RMS between the EVC and SVD model is shown in Figure 4.18. In the figure, the horizontal axis is the number of the simulation with varying standard deviation noises; the vertical axis is RMS value.

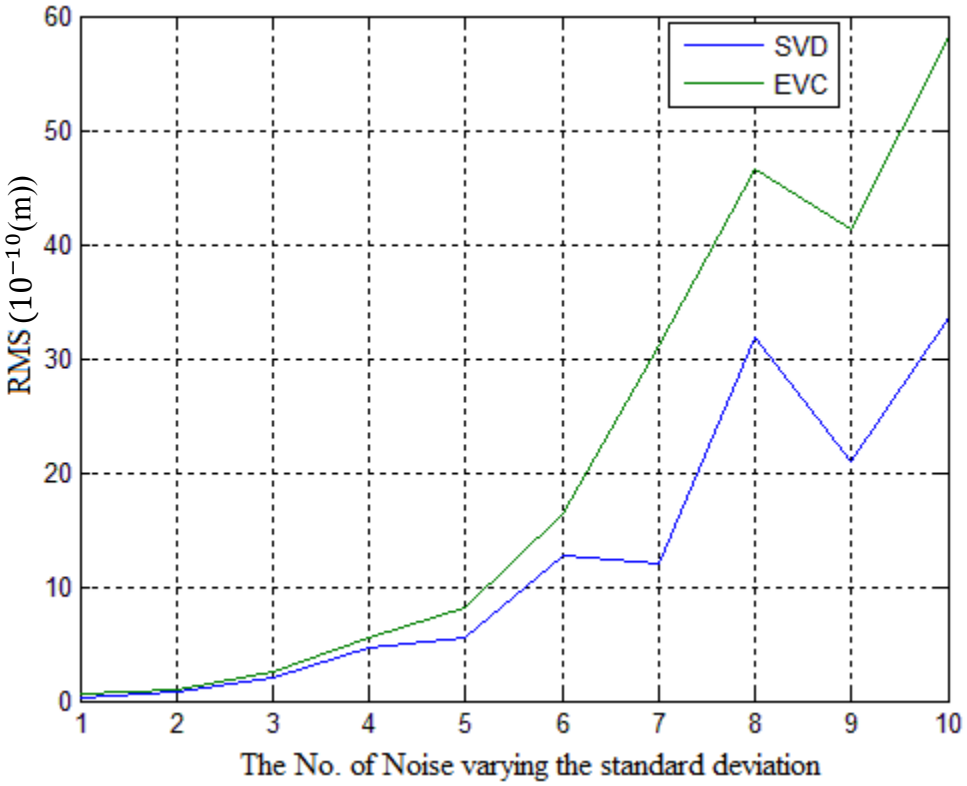

Figure 4.18 RMS values comparison between SVD and EVC model with varying standard deviation noise

Figure 4.18 suggests that the overall performance of the EVC method is worse than that of the SVD method, while the orbit correction control of the EVC is much more smooth when the noise is varying. When the noise signal is much smaller (standard deviation is from 0.215 to 2.15), there is no obvious difference between these two methods. When the standard deviation is greater than 2.15, the SVD algorithm is better than EVC. However, the two methods can meet the needs of the orbit correction requirment in CLS.

At the 7^{th} and 16^{th} BPM position, the simulation is shown in Figure 4.19. Based on this figure, when the noise is smaller than 8, the correction performance of the EVC method is better than SVD, and the control is smoother when the noise is varying. When the noise standard deviation is greater than 8, the performance of the SVD is better than EVC.

In conclusion, when the zero error is required in a specific positon in the SR, EVC is a good choice. In addition, the noise in the SR should be controled under a certain range. If the standard deviation of the noise is much larger, neither the EVC nor the SVD method can correct the devation properly. The key point is that the response matrix need to be updated when the noise is much larger.

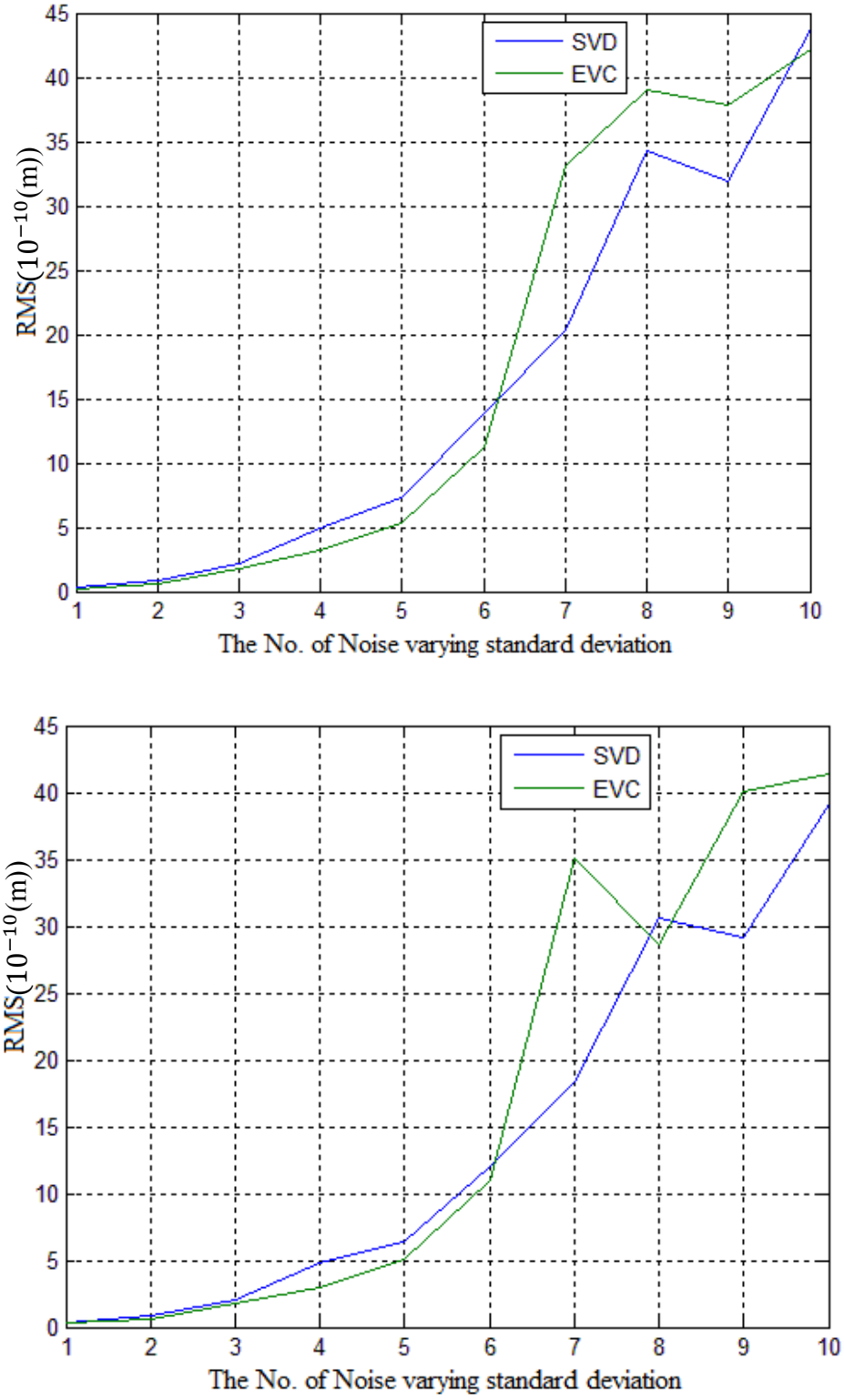

Figure 4.19 RMS values comparison between SVD and EVC at 7th and 16th BPM (Top: 7th BPM; Bottom: 16th BPM) with different standard deviation noise.

4.5.2 SVD+PID versus SVD

The comparison between EVC and SVD model is shown in Figure 4.20. From this figure, it can be seen that when the PID controller is added, the correction performance turns to be better obviously, and when the noise is varying, the performance is still good. However, when the noise is greater than 20, the correction performance is getting worse than the SVD method. The possible reason may be that in this case the response matrix is no longer accurate. The added PID parameters further worsen the inaccuracy of the relation between Δx and $\Delta\theta$.

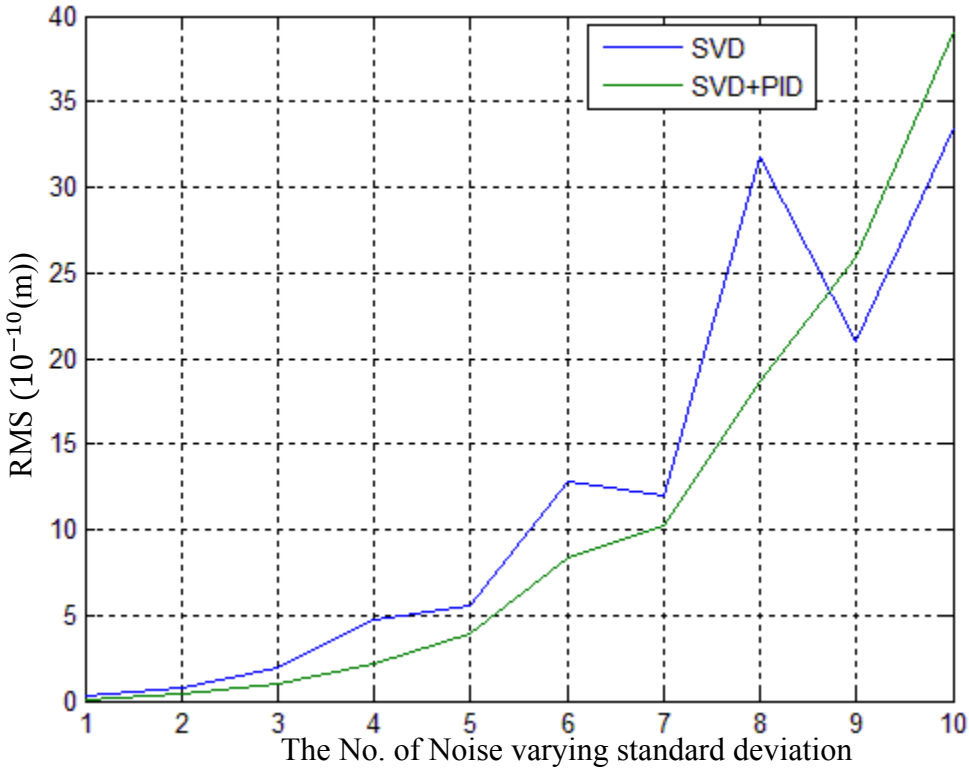

Figure 4.20 RMS comparison between SVD and SVD+PID model with varying noises.

4.5.3 SVD+PID versus EVC

The comparison of the RMS values between the EVC and SVD+PID model is shown in Figure 4.21. From the figure, it can be seen that the correction performance of SVD+PID is much better than that of EVC.

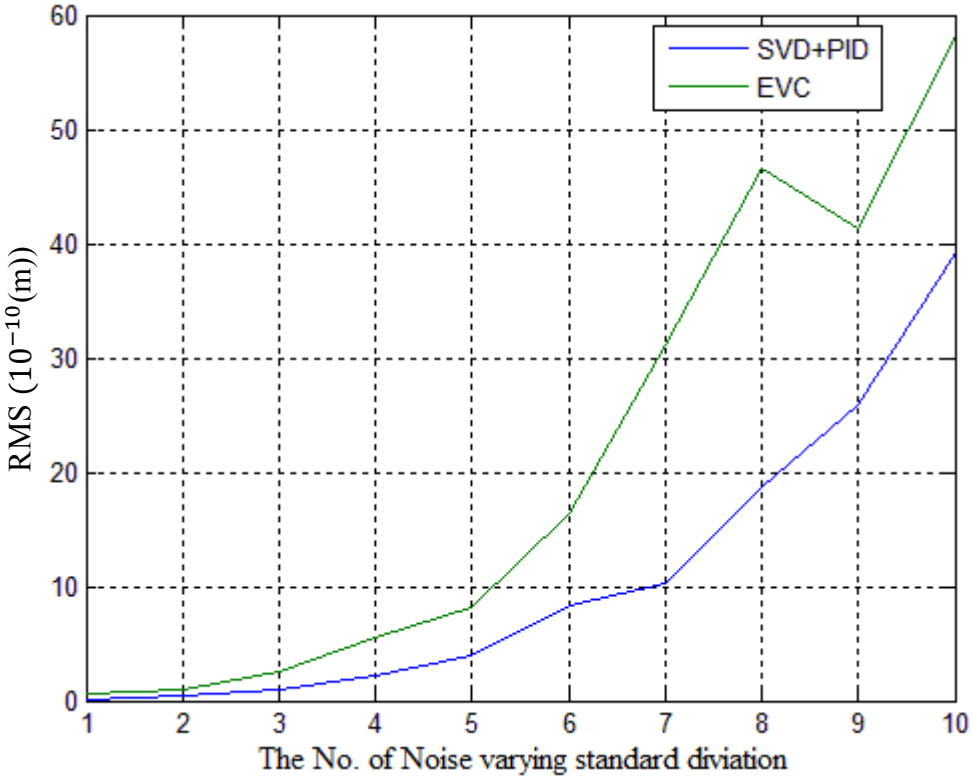

Figure 4.21 RMS comparison between EVC and SVD plus PID model with varying noises

At the 7th and 16th BPM position, the comparison of the performance is shown in Figure 4.22. From this figure, when the noise is smaller than 7, the correction performance of EVC algorithm is almost as same as that of SVD+PID, and the control performance of the SVD+PID algorithm is much smoother when the noise is varying. When the noise standard deviation is greater than 7, the performan of EVC is better than SVD+PID.

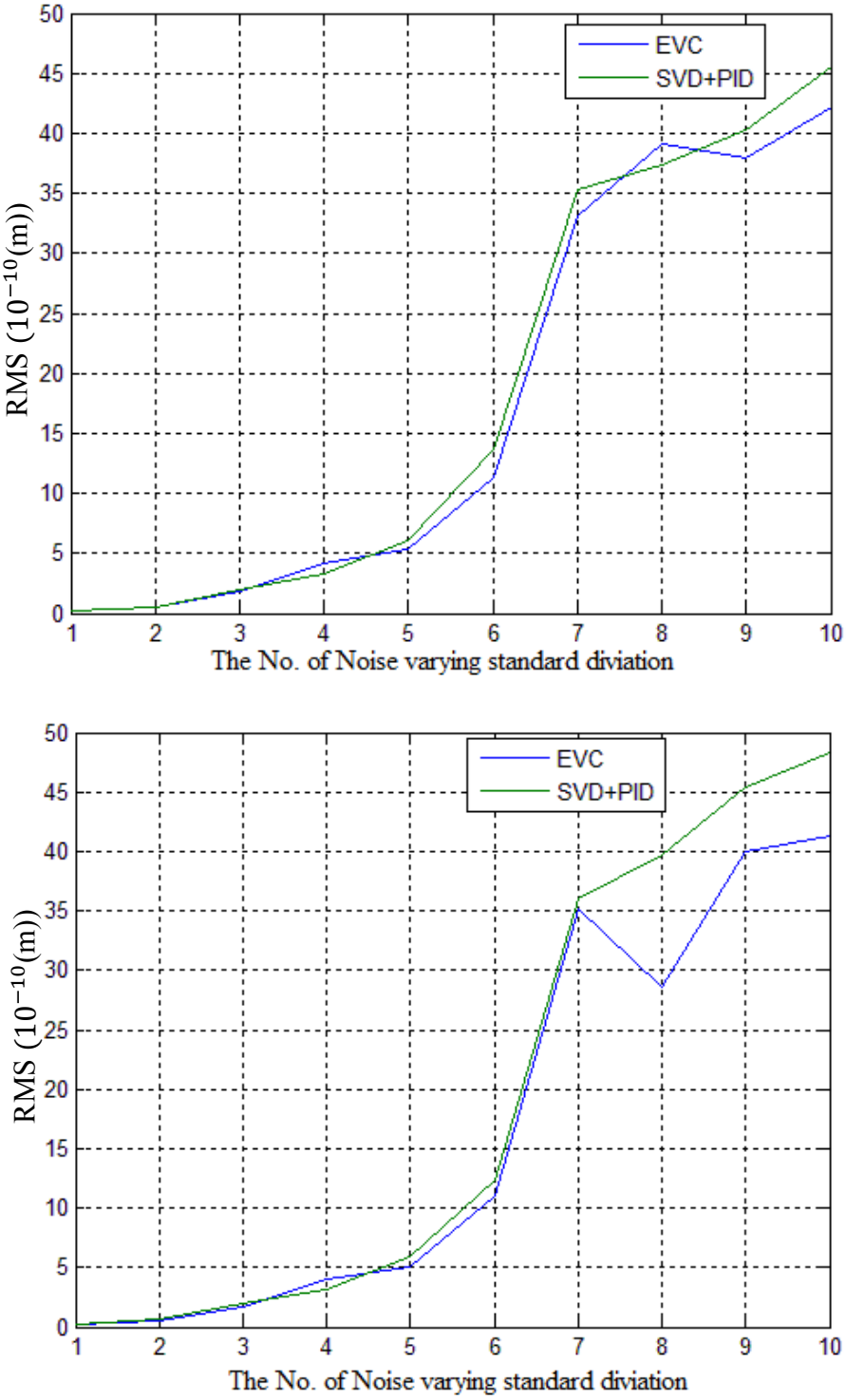

Figure 4.22 RMS comparison between SVD+PID and EVC at 7th and 16th BPM (Top: 7th BPM; Bottom: 16th BPM) with varying noises.

4.6 Conclusions

There is no significant difference between the EVC and SVD method on the overall orbit correction (Table 4.7). They both can meet the needs of the CLS. But the EVC method is much better than the SVD method at a specific position orbit correction (Table 4.8). The SVD+PID controller method is much better than the SVD as well as EVC method on the overall orbit correction (Table 4.7). The SVD+PID is excellent at the performance of specific position orbit correction, comparable with that EVC (Table 4.8). Therefore, the SVD+PID is the best method for the orbit correction at CLS.

Table 4.7 RMS values comparison of SVD, EVC and SVD plus PID

	1	2	3	4	5	6	7	8	9	10
SVD	0.239	0.761	1.94	4.72	5.52	12.75	12.03	31.76	20.99	33.54
EVC	0.642	0.918	2.616	5.518	8.076	16.324	31.095	46.558	41.331	58.096
SVD+ PID	0.101	0.428	0.988	2.14	3.94	8.39	10.22	18.69	25.92	39.13

Table 4.8 RMS values comparison of SVD, EVC and SVD plus PID on 7th BPM position

	1	2	3	4	5	6	7	8	9	10
SVD	0.303	0.832	2.135	4.908	7.347	13.936	20.375	34.271	31.903	43.794
EVC	0.218	0.533	1.801	3.216	5.322	11.259	33.134	39.073	37.887	42.113
SVD+PID	0.253	0.547	2.017	3.222	6.081	13.736	35.279	37.393	40.257	45.516

CHAPTER 5 CONCLUSION AND FUTURE WORK

5.1 Overview and Conclusions

This thesis presented a study on electron beam orbit correction in a particular synchrotron facility that is CLS (Canadian Light Source). The study was focused on beam stabilization in the Storage Ring. There are generally two problems with beam stabilization: (1) to control the beam to stay on a design orbit and (2) to control the beam to reach a specific position. These two problems are coupled - that is they need to be controlled at the same time in the operation of synchrotron. In the current literature, the Singular Value Decomposition (SVD) algorithm is the main method in most synchrotron facilities worldwide. It is however noted that more accurately speaking, the SVD was only a solver for the so-called response matrix which represents the relation between the deviation of the beam and actuation of the beam. The SVD method was considered not an enabler to solve these two problems, especially Problem 2, based on a preliminary literature review of the synchrotron technology. Therefore, investigation of other methods for the beam stabilization problem was considered to be necessary.

In the synchrotron technology literature, there are several other methods that are useful in one way or another, and they are: Eigen Vector method with Constraints (EVC) and Singular Value Decomposition plus Proportional Integral Derivative controller (SVD+PID for short). Their suitability to CLS was also to be examined. It is noted that the effectiveness of a particular control method for electron beam orbit correction depends on individual synchrotron facilities, as there are considerable differences in geographical situations and disturbances among them. This means that an algorithm that may work for one synchrotron facility may not work for others.

Based on the above observation, this research was designed to have the following specific research objectives:

Objective 1: Develop models for the systems such as BPM, OCM and Vacuum Chamber (VC). The models refer to the transfer functions.

Objective 2: Identify the noise in the SR. This will make simulation more reliable.

Objective 3: Implement and perform a comparative study of the electron beam orbit correction algorithms including SVD, EVC and SVD+PID using the simulation at the Matlab environment.

Research was carried out and research results were documented in Chapter 3 for Objective 1 and in Chapter 4 for Objective 2, respectively. In particular, the transfer functions or models for Beam Position Monitor (BPM), Orbit Correction Magnet (OCM), and Vacuum Chamber (VC) were successfully developed, and three methods for orbit beam stabilization were implemented in the Matlab environment.

The following conclusions can be drawn from this study:

(1) In the SR at CLS, noises can be simulated with a Gaussian White noise;
(2) The orbit correction performance of the EVC model is much better than that of the SVD model at specific positions in the SR (i.e., Problem 2). However, the overall performance of the EVC model in the SR is no better than that of that SVD model (i.e., Problem 1);
(3) The SVD+PID is better than the EVC; in particular, the performance of the SVD+PID is greatly better than that of EVC in the overall SR;
(4) The SVD+PID makes a great improvement on the orbit correction performance at the SR of CLS. It can also meet the performance requirement at specific positions at the SR of CLS;
(5) The SVD+PID is a proper alternative method for the SR of CLS, and it is thus recommended to CLS for its future use.

5.2 Contributions

The contributions of this research are as follows: (1) The models for BPM and OCM are unique in the literature of synchrotron technology. The SVD+PID control method may be useful to similar systems in other synchrotron facilities worldwide, as its nature is a combination of feedback (i.e., PID) and inverse of the internal model of the plant (i.e., response matrix). (2) The approach to study noises in synchrotron technology is potentially useful to other synchrotron facilities in the world. The approach in this thesis was to collect noises first and then to study the nature of the noises. This approach is more effective than the existing practice in other synchrotron facilities where several different kinds of noises are simulated and compared to result in the correct type of noise. (3) Knowledge of the performances of SVD, EVC and SVD+PID on one same synchrotron facility is valuable, and it may be useful to other synchrotron facilities in selection of the best methods for orbit correction.

5.3 Limitation and Future Work

The limitation and future work are discussed in the following. First, this research compared the EVC and SVD+PID algorithms based on the simulation only instead of the experimentation on the real SR at the CLS. The knowledge generated based on the simulation is not reliable for such applications with a high degree of uncertainty from the plant's environment. It is worthwhile to test the algorithms further on the real system in the future.

Second, SVD+PID algorithm is a proper alternative for the CLS, but eventually, the specific position should be considered with the Beamlines construction in the future. Therefore, in the further study, EVC+PID controller should be checked for its suitability for CLS.

Third, for more precisely controlling the beam orbit in SR, the integral global feedback (mixing the slow and fast feedback system) is worth to be studied. There are already some kinds of slow corrector distributed in the SR. The further works include determining how many fast and slow correctors should be distributed in the whole SR and modeling them to understand their performance.

Finally, there is a need to study how uncertainties to the SR can be reduced from a redesign of the internal structure of the SR. In the simulation system in this research, it has been found that when the noise level increases, the performance of the orbit beam correction dramatically reduces. To improve the performance, it may be necessary to update the response matrix. This implies that the temperature in the SR and the pressure in the VC may need to be adjusted to improve the robustness of the orbit beam correction system. Further, all the mechanical assemblies in the SR, e.g., assembly of magnets, must be checked up or calibrated regularly to see if they are on right positions, as the mechanical errors seem to be a significant disturbance to the operation of the beam in the SR.

REFERENCES

Antsaklis, P., Atherton, D. and Warwick, K., 1993, MATLAB® toolboxes and applications for control, IEE Control Engineering Series 48, pp. 131-144.

Autin, B. and Marit, Y., 1973, Closed Orbit Correction of A.G. machines using a small numbers of magnets, CERN ISR-MA/73, pp. 17.

Beasley, J. and Miller, G., 2008, Modern Electronic Communication (9th Edition), pp. 4–5.

Beltran, D., Munoz and M., 2007, Initial Design of a Global Fast Orbit Feedback System for the ALBA Synchrotron, Proceeding of ICALEPCS07, RPPA23, pp. 561-563.

Bellomo, P. and De lira, 2004, A., SPEAR3 Intermediate DC Magnet Power Supplies, Proceeding of EPAC2004, WEPRF083, pp. 1798-1800.

Berg, R., Dallin, L. and Vogt, J., 2004, Orbit Control for the Canadian Light Source, Proceeding of EPAC2004, THPKF009, pp. 2275-2277

Bertwistle, D. 2001, CLS Button Position Monitor Sensitivity Analysis, CLS Preliminary Design Note 7.2.38.1 Rev.0.

Bocchetta, C., 1998, Review of Orbit Control, Proceeding of EPAC98, THY01B, pp. 28-32

Caldwell, W., Coon, G. and Zoss, L., 2012, Frequency Response for Process Control, Literary Licensing, LLC, pp. 103-150

Cartwright, K., 2007, Determining the Effective or RMS Voltage of Various Waveforms without Calculus, Technology Interface 8.

Chiu, P., et al., 2007, Fast Orbit Feedback System Upgrade in the TLS, Proceeding of ICALEPCS2007, RPPA38, pp. 597-599

Chung, Y., Decker, G. and Evans, K., 1993, Closed Orbit Correction Using Singular Value Decomposition of the Response Matrix, Proceeding of PAC93, vol.3, pp. 2263-2265.

Chung, Y., Decker, G. and Evans, K, 1993, Global DC Closed Orbit Correction Experiment on the NSLS X-ray Ring. Proceeding of PAC93, vol.3, pp. 2275-2277

Corbett, J., Terebilo, A., 2001, Interactive Orbit Control in MATLAB, Proceeding of PAC2001, MPPH022, pp. 813-815

Dallin, L., 2000, XY Orbit Corrector, CLS Design Note 2.1.48.

Dallin, L., 2000, Canadian Light Source Lattice Performance Analyses, CLS Design Note-8.2.69.1 Rev.0

Dallin, L., 2000, CLS SR1 Dynamic Orbit Correction, CLS Design Note 5.2.69.4

Dallin, L., 2001, CLS SR1 Orbit Corrector Magnet Specification, CLS 5.8.31.4 Rev.0.

Dallin, L., 2001, CLS SR1 Orbit Corrector Magnet Specification, CLS Design Note 5.8.31.4, Rev.0

Dallin, L., 2001, Synchrotron Light Source Magnets, CLS Design Note 5.2.31.2 Rev.0

Dallin, L., 2004, Canadian Light Source Main Ring Lattice, CLS Design Note 5.2.69.2 Rev.3

De Lima, M., 2007, Eddy Current studies on the ALBA SR sextupoles, ALBA Internal report, AAD-SR-MA-SEXT-AN-0009

Gattuso, C. and Tecker, F., 1999, Orbit Correction in the Recycler Permanent magnet storage ring, C99-10-18.3

Golub, G. and Reinsch, C., 1970. Singular value decomposition and least squares solutions, Numer. Math. 14, pp.403-420

Harada, K. el at., 2009, Orbit correction using an eigenvector method with constraints for synchrotron radiation sources, Nuclear Instruments and Methods in Physics Research A 604(2009) pp.481-488

Hofmann, A., 2004, The Physics of Synchrotron Radiation, CAMNRIDGE UNIVERSITY PRESS, pp. 244-256.

Hu, S., 2008, Libera Brilliance Evaluation, CLS Design Note 7.5.39.67 Rev.0

Hu, S. et al., 2012, Global Orbit Feedback System Upgrade at the Canadian Light Source, 11th International Conference on Synchrotron Radiation
Instrumentation Conference, vol. 425, Part 4.

Jackson, J., 1998, Classical Electrodynamics (3rd Edition), Samizdat Press, pp. 47-49.
Meeker, D., 2010, Finite Element Method Magnetics (Version 4.2), FEMM user's Manual.

Jiang, B., Hou, J. and Yin, C., 2012, Status of the SSRF Fast Orbit Feedback System, Proceeding of IPAC2012, WEPPP065, pp. 2855-2857

Johnson, M. and Moradi, M., 2005, PID Control: New Identification and Design Methods, Springer, pp. 102-156

Kirchman, J., Chung, Y. and Bobis, P., 1995, Experimental Result on the Design for the APS PID Global Orbit Control System, Proceeding of ICALEPCS95, ANL/ASD/CP-94983

Kuo, C. et al., 1997, Digital Global Orbit Feedback System Developing in SRRC, Proceeding of PAC97, 6P060, pp. 2374-2376.

Liu, L. et al., 2008. Closed orbit correction at the LNLS UVX Storage Ring, Proceeding EPAC2008, THPC024, pp. 3029-3031

Ljung, L., 1999, System Identification Theory for the User, second Edition, Prentice Hall PTR, pp. 491-518.

Lowe, D., 2001, CLS Storage Ring Vacuum Chambers, CLS Design Specification 5.4.33.1
Matias, E., 2002, CLS Control System Technical Specification, CLS Design Note 7.4.39.1 Rev.2

Meier, E., Tan, Y. and LeBlanc G., Orbit Correct Studies Using Neural Networks, Proceeding of IPAC2012, WEPPP057, pp. 2837-2839

Nakamura, N., et al., 2006, New orbit correction method uniting global and local orbit corrections, Nuclear Instruments and Methods in Physics Research A 566, pp. 421-432.

Nakamura, N., 2010. Application of the eigenvector method with constraints to orbit correction for ERLS, Proceeding of IPAC2010, TUPE085, pp. 2320-2322

Nise, N., 1992, Control System Engineering, The Benjamin/Cummings Publishing Company, INC., pp. 493-550.

Ogata, K, 2003, System Dynamics (4^{th} Edition), Prentice Hall, pp. 522-540.

Plouviez, E., et al., 2005, Upgrade of the Global Feedback of the ESRF Storage Ring, Proceeding of DIPAC2005, POM022, pp. 84-86

Podobedov, B., Ecker, L., Harder, D., and Rakowsky, G., Eddy current shielding by electrically thick vacuum chambers, Proceeding of PAC2009, TH5PFP083, pp. 3398-3400.
Rice, J, 1995, Mathematical Statistics and Data Analysis (Second ed.), Duxbury Press, ISBN 0-534-20934-3), pp.56-89

Sands, M., 1970, The Physics of Electron Storage Rings – An Introduction, SLAC-121

Schlott, V., 2002, Global Position Feedback in SR Source, Proceeding of EPAC2002, THXGB001.

Sitnikov, A., 2005, CLS Vacuum Design Specification, CLS Design Specification 8.4.33.1 Rev.3

Steier, C. et al., 2002, Orbit Feedback Development at the ALS, Proceeding of EPAC2002, THPRI029, pp. 2103-2105.

Summers, T., et al., M., 2009, Orbit Improvement at the Canadian Light Source, Proceeding of PAC09, TU5RFP018, pp. 1129-1131.

Tan, W. et al, 2006, Comparison of Some well-known PID Tuning Formulas, Computer and Chemical Engineering 30 (2006) pp. 1416-1423

Tavares, D., Marques, S., 2011, Performance Optimization for the LNLS Fast Orbit Feedback, Proceeding of PAC 2011, WEOND3, pp. 1485-1487.

Tian, Y. and Yu, L., 2011, NSLS-II Fast Orbit Feedback with Individual Eigen-mode Compensation, Proceeding of PAC2011, WEODN4, pp. 1488-1490.

Tuzlukov, V., 2002, Signal Processing Noise, CRC Press, pp. 61-107

Vladimirov, V. S. (1971), Equations of mathematical physics, Marcel Dekker, ISBN 0-8247-1713-9

Vogt, J., 2008, CLS Beam Monitor System, CLS Detail Design Note 8.2.38.4 Rev.6

Xu, S. et al., 2012, Simulation of the APS Storage Ring Orbit Real-time Feedback System Upgrade Using MATLAB, Proceeding of IPAC2012, WEPPP070, pp. 2870-2872.

Xuan, K., et al., 2011, Application of Integral-separated PID Algorithm in Orbit Feedback, Proceeding of ICALEPCS2011, MOPKS006, pp. 171-173.

Xue, D., Chen, Y. and Atherton, D., 2009, Linear Feedback Control: Analysis and Design with MATLAB, Society for Industrial and Applied Mathematics, pp. 181-231.

Zhuang, M. and Atherton, D., 1993, Automatic Tuning of Optimum PID controllers, IEE, Proceedings of Control Theory and Applications, 140, pp.216–224

Ziegler, J. and Nichols, N., 1942, Optimum Setting for Automatic Controllers, Transaction of the ASME 64, pp. 759-768

Appendix I The CLS lattice Model

The lattice model is a representation of the real lattice of the SR at CLS. Its goal is to determine the response matrix and then to use it for beam orbit correction. The input of the model is the power to make the OCM generate the magnetic strength. The output of model is the beam deviation by the magnetic strength, which is measured by BPM in the real SR. The important thing is that one OCM can make all the BPMs get a deviation value. The relationship between them is response matrix. The theory of the lattice model and the parameters of the devices are described in Chapter 2.

```
function clsat
% ------------------------------------------------------------------------
-------------------
% $Header$
% ------------------------------------------------------------------------
-------------------
% Canadian Light Source
% ------------------------------------------------------------------------
-------------------

disp(['   Loading CLS magnet lattice ', mfilename]);

global FAMLIST THERING
Energy = 2.9e9;
FAMLIST = cell(0);

L0    = 170.88;
C0    = 299792458;
HarmNumber = 285;
CAV   = rfcavity('RF', 0, 2.4e+6, HarmNumber*C0/L0, HarmNumber, 'CavityPass');
COR   = corrector('COR',0.15,[0 0],'CorrectorPass');
AP    = aperture('AP',  [-0.1, 0.1, -0.1, 0.1], 'AperturePass');
BPM   = marker('BPM', 'IdentityPass');
% The parameters are presented in Table 2.1.

% Drifts should match the DIMAD model
D1  = drift('D1' , 2.2500, 'DriftPass');
D1A = drift('D1A', 0.2910, 'DriftPass');
D1B = drift('D1B', 0.0660, 'DriftPass');
D2A = drift('D2A', 0.3390-.15/2, 'DriftPass');  % Was 0.264
D2B = drift('D2B', 0.1950-.15/2, 'DriftPass');  % Was 0.120
D3  = drift('D3',  0.3120, 'DriftPass');  % Was 0.534
D4A = drift('D4A', 0.3095, 'DriftPass');
```

```
D4B = drift('D4B', 0.0975, 'DriftPass');  % Was 0.0375
D5  = drift('D5',  0.3125, 'DriftPass');  % Was 0.3335
D6  = drift('D6',  0.1695, 'DriftPass');
D7  = drift('D7',  0.3975, 'DriftPass');  % Was 0.4185
D8A = drift('D8A', 0.0920, 'DriftPass');  % Was 0.1130
D8B = drift('D8B', 0.2300, 'DriftPass');
D9A = drift('D9A', 0.2100-.15/2, 'DriftPass');  % Was 0.135
D9B = drift('D9B', 0.3240-.15/2, 'DriftPass');  % Was 0.249
D10A = drift('D10A', 0.0700, 'DriftPass');
D10B = drift('D10B', 0.2870, 'DriftPass');
 % The parameters are presented in Table 2.2-2.4.

%Calculated using DIMAD: first order agrees with 'LinearPass' functions
QFAK = 0.19675504817032E+01;
QFBK = 0.14174085779859E+01;
QFCK = 0.20454705915551E+01;
SDK = -0.30555264172985E+02;
SFK =  0.45913109297415E+02;

%Lattice elements
BEND   = rbend2('BND', 1.87, 0.2617994, 0.105, 0.105, -0.3972,
0.05,'BendLinearPass');
QFA = quadrupole('QFA', 0.18, QFAK, 'QuadLinearPass');
QFB = quadrupole('QFB', 0.18, QFBK, 'QuadLinearPass');
QFC = quadrupole('QFC', 0.26, QFCK, 'QuadLinearPass');
SF = sextupole('SF', 0.192  , SFK/2, 'StrMPoleSymplectic4Pass'); %Convention:
divide K2 by two
 % The parameters are presented in Table 2.2-2.4.
%Defocusing sextupoles have windings for corrector and skew quad
SQK = 0.0; %Skew quad strength
SD = sextcorr('SD', 0.192, SDK/2, 0.0 ,'StrMPoleSymplectic4Pass');
FAMLIST{1,SD}.ElemData.PolynomA(2) = SQK; %skew quad component

% Build the lattice
HCELL = [D1 D1A BPM D1B QFA D2A COR D2B QFB D3 BEND D4A BPM D4B SD D5 QFC D6
SF];
HCELR = [D6 QFC D7 SD D8A BPM D8B BEND D3 QFB D9A COR D9B QFA D10A BPM D10B
D1];
CEL   = [HCELL HCELR];
ELIST = [CEL CEL CEL CEL CEL CEL CEL CEL CEL CEL CEL CAV CEL];
buildlat(ELIST);

% Compute total length and RF frequency
L0_tot = findspos(THERING, length(THERING)+1);
%fprintf('   L0 = %.6f     (design length is 170.8800 m)\n', L0_tot)
%fprintf('   RF = %.6f MHz  \n', HarmNumber*C0/L0_tot/1e6)

% Newer AT versions require 'Energy' to be an AT field
THERING = setcellstruct(THERING, 'Energy', 1:length(THERING), Energy);
setcavity off;
setradiation off;
%clear global FAMLIST
% LOSSFLAG is not global in AT1.3
evalin('base','clear LOSSFLAG');
evalin('base','global THERING FAMLIST GLOBVAL');
```

Appendix II The Response Matrix

The response matrix is a matrix that represents the relation between the data measured by the BPM and the data measured by the OCM.

```
                    1.0e-008 *

                  Columns 1 through 6

 -0.195071001887744   0.007102751131712   0.058884777230952
 0.145205934654767  -0.002703727585738  -0.142437600624626
  -0.015192604487365  -0.083503602101033  -0.093173408869526
 0.047798568900194   0.118282838082819   0.002877676615717
 0.037840242090476  -0.089325795531467  -0.068261289670130  -
 0.010808648682360   0.065313689820228   0.041766396877893
 0.146999776849210   0.068363511490723   0.007157310362281  -
 0.207415201581984  -0.252336500885615   0.100253353151149
 0.031787959957991   0.156762742591847   0.099581004921978  -
 0.262936665411037  -0.212086883831790   0.007698041000286
  -0.110913406737884   0.014239718723883   0.043471741246764
 0.071175961290569  -0.010483043876155  -0.076056636701706
  -0.068170284404097  -0.030221957183304   0.000170472274342
 0.109691237371208   0.045010863909633  -0.087495228427254
   0.240731228111794  -0.109685971926022  -0.139614162375596
 0.003228932734254   0.148505098693191   0.056336060318059
 0.210594890541451  -0.013187174628703  -0.066018117128344  -
 0.126080418837098   0.026950556852274   0.140598663998676
-0.123237918910387   0.098897360737834   0.105126401838785  -
 0.052358695563168  -0.117524169066084   0.018038768733551
  -0.124693129964581   0.062067548235177   0.079454500935330
 0.007982427425654  -0.070786438841091  -0.025343968738220
   0.143327430813853  -0.189562558860176  -0.167689631422956
 0.201092191441311   0.247892449202392  -0.106983440599833
   0.227369996653480  -0.164188717307974  -0.174354004402307
 0.099554117034629   0.218311984604508  -0.015136113444507
```

-0.030090827520488 0.110998418858159 0.086576806207851 -
0.138851008682810 -0.130468185080355 0.099525159916384
-0.077072522071500 0.106918007562916 0.097322093813497 -
0.099976187556734 -0.126897629386276 0.059986153716285
-0.067110104227819 -0.121593390626570 -0.063587498226284
0.249883253109763 0.158023318597491 -0.190827505567144
0.059575355672911 -0.176951140834719 -0.136805814780171
0.242804962724763 0.230605261583393 -0.156738533218671
0.086542809020605 0.035773888125811 0.003256967104362 -
0.107732787436311 -0.034033842355763 0.104110810438470
0.032928780252136 0.073310673549737 0.043481828743309 -
0.126989611234218 -0.082641819184984 0.105445986130930
-0.220507820054452 0.046363899261292 0.093407978149970
0.095571616977014 -0.057886156113749 -0.114265486602888
-0.151200714746071 -0.051230223724397 0.007591152349835
0.200110025110028 0.068036769242560 -0.174243922576357
0.131898117292797 -0.057348930947289 -0.072553351286661
0.006681397278309 0.084077663471803 0.033045405483491
0.115899826244827 -0.014227593934980 -0.039258674771609 -
0.051400090518981 0.029205596452420 0.068997591869697
-0.184940315173164 0.173275135551828 0.171429548152115 -
0.130222847122495 -0.216253663705961 0.053795876064924
-0.232519305316511 0.115120774407835 0.142410162510315 -
0.002834264313915 -0.143217845060390 -0.047619239380954
0.075506414959106 -0.104742003815673 -0.091602709036635
0.122116097262641 0.141255544013733 -0.063114237144388
0.108050215837990 -0.086748756775547 -0.086298070593945
0.069340700080234 0.119766173579661 -0.018258327769653
-0.016673972210256 0.178182492706676 0.127577805104004 -
0.260573150598613 -0.219287028438453 0.185591259840744
-0.131728530909199 0.197684539911306 0.172233388719564 -
0.207481026761229 -0.245951034773634 0.122276469626382
-0.045189693476310 -0.053797931140100 -0.022692777179457
0.132431697064828 0.077602157028249 -0.098237652999275
0.012609449650406 -0.079840047109923 -0.055353411200668
0.128931576042451 0.109976716990913 -0.082471180423657
0.194090303921533 0.017351930600742 -0.040879838374872 -
0.163526944988085 -0.013648393622570 0.164912601688731

```
 0.088632363568206   0.112686176793640   0.053023918543007  -
 0.236344094624733  -0.136371764872868   0.192913106882135
 -0.122080396220974   0.038202938274097   0.061792566342106
 0.043265181206372  -0.040523314742846  -0.050187346523469
 -0.091144419571140  -0.006427866918125   0.023563166462332
 0.089252039371382   0.015255817294808  -0.077930862169331
  0.232310821674427  -0.142619075050868  -0.161462418859549
 0.060843922698624   0.189287490801442   0.012284691225985
 0.228116339023455  -0.053163804371167  -0.099238603728586  -
 0.076370436080641   0.076187514965146   0.109361356642843
-0.105551103792377   0.108703372291254   0.105946911091604  -
 0.081156381537164  -0.129608594281909   0.042067776203866
-0.122237879919527   0.078731928617242   0.090640021518524  -
 0.023823760441529  -0.093754091989811  -0.003218143347825
  0.096979000621188  -0.185606720067687  -0.153736748772955
 0.231597727579217   0.244231607076282  -0.140290040107468
  0.201995275604485  -0.188907802476555  -0.184080867727485
 0.158253730923009   0.248488499876512  -0.063036035271306
 0.000677756540830   0.090290453076495   0.064996101491898  -
 0.132564661846889  -0.106033730987491   0.102200990728608
-0.053229807775915   0.107180001813850   0.090888588969043  -
 0.118428164006892  -0.127807211013409   0.079464667294806
 -0.120581419444016  -0.070068444535292  -0.015318393509701
 0.213237808660614   0.097489025284377  -0.174690780813191
  0.006330040993907  -0.153036595175633  -0.109666857716656
 0.252947652242613   0.206909468231164  -0.171895778835753
 0.106895372966319   0.003319844054548  -0.024935480409492  -
 0.074144208768772   0.004809909874703   0.084162670431326
 0.059737829341407   0.047427877708155   0.018732576184506  -
 0.108319829186157  -0.051855400048469   0.097481879387658
 -0.235768613932986   0.106260364177525   0.139308271626129
 0.016006755771024  -0.131435016469958  -0.060217154062564

                  Columns 7 through 12

-0.094578406089007   0.242997463738188   0.197336632045230  -
 0.180361236554153  -0.175875515415528   0.146372433317766
```

-0.031152409865361 -0.080241808395525   0.007328160607142
0.093271339618928   0.061723151500390 -0.137390345319319
 0.011258010306013 -0.106017083166801 -0.046187708574079
0.099503694509271   0.082597034062440 -0.111205334910370
0.143508696064338   0.035710826476740 -0.129458961084976 -
0.074658878635298 -0.012258674963912   0.219668372423986
0.069044211458814   0.154176421436464 -0.005809198722538 -
0.155211221141099 -0.100698066625554   0.257199496894339
-0.086658975968744   0.036876933850309   0.111917484762402
0.006393341191272 -0.024446449834261 -0.078375268743793
-0.070970910928359 -0.019596551063414   0.064329176782073
0.049128665036737   0.015428875062462 -0.110435079092812
-0.006491675533317 -0.191788553630806 -0.245222100149610
0.097713767328483   0.136126396721275   0.029348811987843
 0.088779502737399 -0.238326809652846 -0.201870283859418
0.002847819265054   0.060900049048873   0.149119905002379
0.051201693899722   0.072477031081711 -0.014731618686866 -
0.076729311206921 -0.088594355772750   0.039150594708495
0.006321691126708   0.106545140609321   0.043766080073311 -
0.090193647283594 -0.069124654740073 -0.021113795393362
-0.147901488837453 -0.002495355152229   0.151230805932959
0.055209565216357 -0.004977838965616 -0.194018881758874
-0.076357140803788 -0.127442665186084   0.030356185081246
0.143935820012689   0.088912936495453 -0.243463122358250
 0.111499970856442 -0.050613297574453 -0.123095450428863
0.020372431848509   0.051297604366418   0.074711517689683
0.082674770489602   0.008901969943057 -0.072626068591972 -
0.023902064440666   0.006583347504108   0.106052921159768
-0.177926663681269   0.196543138269211   0.259400019579772 -
0.113600154854989 -0.148425693825794 -0.007716912319414
-0.176273165503543   0.088761781002671   0.216085598202595 -
0.018054187982697 -0.072269958894056 -0.127008518751368
 0.083962398793769 -0.129062823269856 -0.127148134424033
0.099939388229349   0.105587492514985 -0.046275685368761
 0.100688468543074 -0.095888026481611 -0.131434138643012
0.064688737861238   0.082533723366139   0.010186888233260
-0.059966749569676   0.234271481879749   0.156254372193043 -
0.186808908892030 -0.169065886970285   0.183010238355646

-0.139013745643406 0.237376881966627 0.236385672215816 -
0.162826805535913 -0.175473645387593 0.086692419049084
-0.000467153843818 -0.102096634919702 -0.031001345153125
0.103088173176575 0.080057863429905 -0.123179920549455
0.040784186145613 -0.121649113407062 -0.081944939402964
0.105942097360210 0.096178043978211 -0.091662424994141
0.103571918389165 0.079781042952758 -0.069968465277524 -
0.102212892845709 -0.049036461900917 0.218461270274644
0.013459630588517 0.189323308200229 0.063526545883004 -
0.170143718232018 -0.129277769010817 0.223597312681429
-0.080826845035964 0.006590556347968 0.092232720071229
0.030042977763680 -0.001510982812067 -0.105084138471560
-0.046660557635788 -0.047904990357818 0.035540839021476
0.068572993081437 0.038273442506678 -0.120072082626457
0.194601339541528 -0.128665550200534 -0.244232681577652
0.058306708861424 0.106926031479460 0.096915248761069
0.159687033384519 -0.005918625900812 -0.159346608479722 -
0.041703391582155 0.017599162793612 0.190782978409363
-0.087070333516424 0.111120149656859 0.140963193145692 -
0.061194493076002 -0.078328041399263 0.006692650453408
-0.087342716798635 0.062002184719119 0.120843108666367 -
0.018733541868816 -0.043557418088543 -0.046766714989534
0.116005824464029 -0.246340651956342 -0.212823010458511
0.187682138013551 0.187282824845512 -0.132481166345891
0.172576915642622 -0.201007059732670 -0.251455869012916
0.129570500475299 0.158022894123405 -0.010574753880914
-0.020211759452968 0.123141576244717 0.077711012718013 -
0.094124442456814 -0.083805741449164 0.107764405681687
-0.055227312468270 0.125262007132340 0.112145406736639 -
0.083970107258593 -0.086811085551053 0.063027367659849
-0.048681365322129 -0.152827470690432 -0.008617024227482
0.156919774921953 0.109570969671774 -0.236638758219248
0.051639555577209 -0.225242402080157 -0.139192372155961
0.190325909498400 0.168530126243201 -0.190640001766434
0.070190434663670 0.041364750226588 -0.045748285910310 -
0.050041592365519 -0.018729672946250 0.127651425819896
0.029061623699306 0.086981227718073 0.013580001378722 -
0.077153401251966 -0.053757179880774 0.127303567457059

-0.167561897444510 0.053720838941251 0.194478170084041
0.012076026871711 -0.044716144160468 -0.158324005474958
-0.117026552779117 -0.073214867025416 0.092581435151977
0.110220867480374 0.050335791299031 -0.235871511211467
0.104162571581356 -0.073523646386125 -0.126385996317587
0.042361078264841 0.066112228437804 0.041711345136450
0.094892810942251 -0.021909753777937 -0.097371940160071 -
0.000761645807237 0.027824684156810 0.089196277538456
-0.147245866507934 0.221311830248761 0.240456381267499 -
0.142768097381418 -0.163309146679083 0.055285589412003
-0.179458354970954 0.142057325917709 0.243301744815013 -
0.058117787300459 -0.107707336578080 -0.075497096092414
0.057926967617012 -0.127272434719489 -0.102256744376272
0.104912872724163 0.101704819192382 -0.076831658714215
0.084039233709398 -0.107878501045833 -0.121065321418905
0.078242175904984 0.088302872198160 -0.021429224100110
-0.001371567068824 0.202879664885423 0.084840408076866 -
0.176192562950092 -0.141017865315227 0.223362419062227

Columns 13 through 18

0.236121348997774 -0.065454818548539 -0.112027041971073 -
0.066058494834626 0.091750969673352 0.103296293995165
-0.106474344509750 0.113263778170916 0.111174477256709 -
0.086761611891701 -0.132925273670878 0.048074905524636
-0.117849198779799 0.081743221458184 0.091460809884262 -
0.028434152350645 -0.095165434865192 0.002148875672490
0.097547405667358 -0.191122096495809 -0.156541274608940
0.236386073802336 0.242472233876656 -0.147491907252029
0.202335034790972 -0.192615626632202 -0.188440333954183
0.161335686594765 0.248569016429295 -0.069475812811358
0.004079403399851 0.092186150136560 0.063667412662013 -
0.134695092753726 -0.102515500472461 0.105775409733342
-0.049868654739226 0.104532317335974 0.088212241681944 -
0.116283023191754 -0.121126775998185 0.080405499730150
-0.125625726103316 -0.073364270961826 -0.010761023852844
0.211896438632437 0.088927229500545 -0.176902664874084

-0.002303417904496 -0.153099165178924 -0.101179188485972
0.250827507099245 0.192789715519360 -0.180814054354363
0.113950717315367 0.009198303092870 -0.025424647061936 -
0.081908289999284 0.004966328854122 0.091965650930626
0.063477730982027 0.051544354876883 0.018018025463464 -
0.115143128091170 -0.051018301699148 0.103243860197875
-0.237387853001452 0.099105159146209 0.138261537100125
0.024412661845877 -0.126031379974408 -0.066362666949995
-0.197514835033965 0.000926232742137 0.059259962981408
0.150904627578826 -0.003291659004182 -0.150322305541214
-0.015699188892695 -0.081473280607304 -0.092702086887908
0.044429541163723 0.116098689830329 0.004041971029032
0.040097342138385 -0.088109409833392 -0.069944195989084 -
0.017005620378740 0.063907223646797 0.047316081000061
0.151849226005977 0.063420209076283 0.000949738534271 -
0.210377241459320 -0.249904876484471 0.104993077097134
0.029725340024258 0.143738160902980 0.091025608670914 -
0.247160198915302 -0.196110771171693 0.006301087799664
-0.116378239870604 0.017141978151945 0.047980907870576
0.075555647407093 -0.011787535905248 -0.078848160978565
-0.072479456046469 -0.027141121928260 0.004149603465155
0.112471606199808 0.042884575007357 -0.089500012248652
0.242611957668769 -0.103153744610202 -0.140195363613677 -
0.012693906384780 0.137013967620422 0.063590856859303
0.213918248108313 -0.013643279930662 -0.070223913523785 -
0.134620986139634 0.024900276951516 0.146178936886524
-0.119232493411000 0.094991258166528 0.101552596727839 -
0.046276572977942 -0.110066322785276 0.016508449040315
-0.124064144047240 0.060145987226738 0.077996640811440
0.011954653561454 -0.066717688810831 -0.027712930746011
0.131930053718262 -0.176520539958954 -0.157231049226142
0.189255015323302 0.227782374009661 -0.106209964579930
0.217571253119020 -0.151732628327969 -0.165752276179871
0.085994890035523 0.199013120361311 -0.013411773160666
-0.028576259919155 0.107769921271525 0.085184304123777 -
0.134629077593166 -0.123406975508691 0.098383863325154
-0.075376492967218 0.106885393875533 0.096997504044794 -
0.098004086254415 -0.123164764777145 0.062318206326507

-0.071285745777874 -0.120740190369770 -0.059849253855141
0.253440933837027 0.153414965512249 -0.195082857262929
0.054575454700535 -0.174097519732149 -0.132726320459781
0.242530339327327 0.222204721837134 -0.161814897498328
0.090820373229547 0.031594160567729 -0.003052505680358 -
0.104154041436633 -0.027149210377134 0.101254117547459
0.034783578131835 0.068003272584999 0.037381323393926 -
0.121154744954770 -0.074542920856460 0.101814447943067
-0.237004989165396 0.058689958733055 0.110340875984345
0.088855514385668 -0.075198299760720 -0.110889129527339
-0.162329386696857 -0.041591013453244 0.019715220662901
0.193436335203785 0.051914118690865 -0.170761262137005
0.132580796357630 -0.055816220624842 -0.074770410147461
0.005785759455962 0.084635816220048 0.030296547598091
0.118842823713132 -0.016652026736031 -0.044550075839550 -
0.048502663853365 0.033747930258266 0.067089306894306
-0.195936654068377 0.180020446638665 0.181920611824930 -
0.135610624039615 -0.225482286184158 0.061841376310445
-0.238705710138858 0.118031128110545 0.151914746028307 -
0.004127709109714 -0.149467894653117 -0.043013570045305
0.074070743663404 -0.097641124518800 -0.086761342371375
0.117033652240408 0.135691694575855 -0.061775150778398
0.109059862528925 -0.084789091054933 -0.088467415835765
0.068665483831573 0.119698489260769 -0.020129721903458
-0.008257222784497 0.164635656727236 0.116865476017769 -
0.249056416840603 -0.200023546541979 0.183286713383438
-0.133308679133882 0.201035935323180 0.178819949501486 -
0.215467835598791 -0.250011463210394 0.133390531117009
-0.044523838827266 -0.050337784520929 -0.019619510446195
0.128394989520062 0.072119454839934 -0.096151109968120
0.011426351048186 -0.079303837946570 -0.056320674315050
0.133298513846370 0.110308606111309 -0.088654091349557
0.189680682104182 0.013239428278319 -0.044596471983698 -
0.155929911908421 -0.006339356256618 0.158187136226278
0.084907710373709 0.113179438906282 0.053563083519902 -
0.237834539747551 -0.133340138289213 0.195335579707426
-0.123931001640371 0.044438210319684 0.068055110271317
0.036097118214147 -0.047527139660159 -0.045722112736992

-0.091305809985740 -0.002275071823802   0.026385063791562
0.085162171553547   0.010433754279316 -0.074843368408864
 0.230127197543832 -0.147040304095574 -0.167260458584757
0.069234064957986   0.193372480372763   0.002934756367382

Columns 19 through 24

 0.044396245189768 -0.229385322051615 -0.130628812480567
0.189500073905142   0.164875477351019 -0.192673417607606
0.071373199239090   0.034840010820192 -0.054922828070421 -
0.047257999998452 -0.014482942051146   0.126684667539635
0.029804016127301   0.079189949812747   0.004920953696149 -
0.071329803752111 -0.047223734828535   0.119570634409752
 -0.165115116280797   0.067195569562186   0.206273798472531
0.009499759735440 -0.049480653488285 -0.157884868555444
 -0.115059158491363 -0.061815642631831   0.103555251221647
0.105000290735731   0.042926777525016 -0.230552223330843
 0.102695961538066 -0.081760859864814 -0.132684606988017
0.044452403327585   0.068793639962074   0.041301546171671
0.090469225287636 -0.028363088526727 -0.099654382376837 -
0.000904505231757   0.030285473541755   0.084411263968602
-0.142836777715452   0.230038172505360   0.244062492299418 -
0.142829213832666 -0.164114920161482   0.051356930779979
-0.173965130521335   0.156270635417412   0.248057760234111 -
0.065530818444909 -0.111973182455716 -0.071044011801607
 0.062452180527581 -0.136879608612338 -0.110532547230448
0.107740594312724   0.106195806364498 -0.073106315099816
 0.086298186568842 -0.117585870775531 -0.128549295021704
0.081552861035329   0.093091414617310 -0.019423768462997
-0.008063184870989   0.204160809292044   0.089563198389651 -
0.172971782333108 -0.140533194622958   0.210562901600826
-0.099124770501300   0.249967932776142   0.203184144696091 -
0.177657810674924 -0.175541451270903   0.136105596416251
 -0.026312863232820 -0.076292909288016   0.007032213480325
0.090568176616133   0.061761885569673 -0.131972424185295
 0.014801721477506 -0.108519693133978 -0.050541661232316
0.099827212669925   0.084005910255645 -0.107016517718463

0.141866247974803 0.017368595384945 -0.139721393920984 -
0.067206947964045 -0.002789858877337 0.211885513419663
0.059857991403885 0.137863844658765 -0.007532866761662 -
0.141199246961552 -0.091246386216601 0.231355944691771
-0.088188108852200 0.046504390951567 0.118980377908325
0.005034932634268 -0.027902039413143 -0.080138197013834
-0.070019160616207 -0.011600858926078 0.069810741141914
0.045721914806501 0.012969354442891 -0.108482226141330
0.004853821596037 -0.202003374780835 -0.253178588690026
0.095012233386409 0.136254300023072 0.041526971616373
0.091727388236293 -0.252808929327674 -0.211507178243906
0.005999357456336 0.064940820124304 0.148735123848115
0.043647583932005 0.070277726542056 -0.011710383411854 -
0.073937816310369 -0.085447274110178 0.031801002767379
0.002807854315530 0.109685021532668 0.047374889972589 -
0.085657302329241 -0.068686095666872 -0.023504405969116
-0.133349852535285 0.010169041831263 0.148625107676278
0.047857625008678 -0.008687824893343 -0.175556027462557
-0.064212398805574 -0.123385713561852 0.022548915794735
0.133777545533798 0.086861372266414 -0.223696722850290
0.101683867940646 -0.056271343764390 -0.125673627652387
0.020140857813073 0.052343247182057 0.068375826167491
0.078250063744316 0.003806318902555 -0.074842522935467 -
0.021806207078946 0.007736492863986 0.102512163185505
-0.171896149182257 0.210943433660791 0.268203913342012 -
0.112546692238624 -0.149237735364797 -0.010411171730651
-0.168995061873821 0.103933649724509 0.222943891254029 -
0.021054002401494 -0.076520366966563 -0.121893683716843
0.078456364530187 -0.131934817152220 -0.126871495371177
0.096410537307998 0.103809361527559 -0.046054118243783
0.091420650096911 -0.098651411804377 -0.128107588463313
0.061362440963418 0.079335840059663 0.009115426564885
-0.051628683317193 0.243169017895737 0.153268047143165 -
0.186802278993749 -0.167594496441739 0.189103344332205
-0.128175089740808 0.247625542959256 0.235875767513729 -
0.161986864302510 -0.173790305322523 0.090070253372007
-0.001002093468630 -0.097886930080187 -0.029216731725835
0.097785979484716 0.076382594201027 -0.117539623454013

```
  0.037692208795627  -0.121566766546483  -0.079598857049508
 0.101620074788774   0.092876656941946  -0.088893885462841
 0.104610571011177   0.073183601455382  -0.078942820676034  -
 0.099287075050226  -0.044158097697167   0.220145823786677
 0.013678250227953   0.187522900581032   0.062036215572744  -
 0.163561071989454  -0.127259309429559   0.219443491695360
 -0.076409215852062   0.015418312587194   0.095293214032595
 0.027295619820282  -0.005435687756860  -0.097905703220308
 -0.044077247730602  -0.042450176293929   0.038328906469614
 0.064356826210702   0.035176911209067  -0.115553380642775
  0.179149606600023  -0.144781977705725  -0.242452091223529
 0.063805403460355   0.111198107528566   0.085377987753610
 0.160252609711303  -0.025402703391797  -0.175464615558561  -
 0.033613263423083   0.026042092774844   0.188378164542148
-0.082264946130060   0.116236219827361   0.139244838405147  -
 0.059836819799845  -0.077238663676780   0.005663859412247
-0.087752304569387   0.075457063064872   0.128951238336317  -
 0.022394154190205  -0.048070810837604  -0.046725177042249
  0.109533195874638  -0.246164507870807  -0.204874622639009
 0.178557836956157   0.179352535609054  -0.123267643006008
  0.168944316671033  -0.211851016622703  -0.253851908729514
 0.125292220542367   0.157361959370436  -0.002915331761028
-0.015159162295547   0.123774325233696   0.071277210519752  -
 0.092589114967524  -0.079929584369443   0.106180294621814
-0.051722951579347   0.127438099456259   0.109806617812220  -
 0.081871256198197  -0.084199969504549   0.060534809197337
 -0.051197026296699  -0.141687573881545   0.004851207384931
 0.149683673534114   0.099636917966178  -0.228431904681504

                Columns 25 through 30

-0.240543592473520   0.125056121939613   0.158043011129048  -
 0.018780601392939  -0.161062180431623  -0.041500383710194
  0.069109700820571  -0.100614007247004  -0.088637394830212
 0.121894189303975   0.141184777775724  -0.063303157932187
  0.100544695058952  -0.082974090101402  -0.085548891314975
 0.072094656357442   0.119181744201617  -0.019309011627484
```

-0.002467320294266 0.165886240329787 0.118049854963755 -
0.251244553156153 -0.207469237622581 0.185303103199367
-0.124871849867247 0.201008323246524 0.178010276169882 -
0.218471089065069 -0.255975710369636 0.130521461384986
-0.049200967722969 -0.050086878243319 -0.018789197448745
0.127067886110451 0.073552498318200 -0.095798625144013
0.006677239828113 -0.076454348642999 -0.053664684488213
0.128766409169995 0.109033452551807 -0.084361319193489
0.193515379272660 0.012056809058104 -0.045186030372860 -
0.150331843180165 -0.007154985687586 0.158804717243232
0.095262933379245 0.106658231525180 0.048089054462077 -
0.229397199745238 -0.131143153683996 0.193195611680195
-0.130088665224364 0.042786347388006 0.069705937933747
0.039664687752049 -0.047049434474193 -0.052617766721872
-0.098097743953799 -0.003294250714267 0.027624670756691
0.088708015775548 0.012425198150848 -0.080179351000397
0.228605976477623 -0.141040438669189 -0.162413380542401
0.064512494850397 0.189310243252097 0.010919938842112
0.238407768980511 -0.060451395520633 -0.108525443604197 -
0.067466350085534 0.087554029106933 0.109879289708752
-0.104599607344456 0.112795267420803 0.110631944368803 -
0.085687725258568 -0.134017917483642 0.045519648400715
-0.119953429770158 0.079692908211701 0.091275645136795 -
0.025950348989133 -0.093501494068457 -0.003437730991069
0.087162446209692 -0.187377249287194 -0.154643078676426
0.238751279396983 0.246458191697183 -0.149842331059110
0.185568081400163 -0.176461853568382 -0.175089678017932
0.150852499589055 0.234628535029341 -0.061537632642905
0.007779984571575 0.092774442079846 0.064569970288665 -
0.138470746406610 -0.108332670172575 0.111028960460714
-0.046978700672018 0.105525581249109 0.089455751588941 -
0.118737530816600 -0.124914078749289 0.082541574866670
-0.123506328013847 -0.081004626048318 -0.017898656367759
0.218694979213611 0.103502546594822 -0.186869682830749
-0.008686659330125 -0.155156873758008 -0.103465036697209
0.254820040126762 0.202173116650496 -0.184244589489653
0.108259048551434 0.011080113318762 -0.021498374136535 -
0.079824479168634 -0.000051823195899 0.093029324750093

0.062379610146950 0.052780528985059 0.021127511930242 -
0.113683771943289 -0.055644714336156 0.106048319541586
-0.224209171963383 0.091440109138304 0.129696295353467
0.023036437196853 -0.118701797339099 -0.068181281681318
-0.190129637814121 -0.006243081795154 0.052681239009863
0.150345022940853 0.007670886900190 -0.151338185332440
-0.021158797281813 -0.079609480509758 -0.088617771104465
0.043757991708906 0.114510909917194 0.010098568282391
0.037035987855127 -0.085085245325210 -0.067657348074235 -
0.016350791853954 0.061699371492511 0.050552373646109
0.158405296883784 0.065059416054029 0.001469113554734 -
0.206505027872161 -0.251357215680189 0.098476402788175
0.038534479124279 0.140843364846127 0.088369404677101 -
0.242167306657417 -0.194604781046554 0.000063221782213
-0.117399989761439 0.018352780045310 0.047698601003007
0.068177598942168 -0.016093060318247 -0.077609477173617
-0.073726735897472 -0.025147869104293 0.005542530017352
0.103936791881604 0.039325192685927 -0.085560195001607
0.249687876633881 -0.111399340211436 -0.147196532333061
0.004505257587774 0.154252865490047 0.062359749307797
0.220393814274991 -0.018577527025140 -0.073800048183830 -
0.119554514314938 0.035086956153844 0.143811981244452
-0.116593813574192 0.092156656173908 0.099566811914077 -
0.049300717180955 -0.110571691619101 0.015150053627132
-0.124011656174165 0.059225510705324 0.078809628705602
0.005926720958325 -0.070487381478158 -0.027792534369015
0.131505531973819 -0.180858607270815 -0.162714830999643
0.198739445325889 0.241052754755399 -0.107842416406506
0.218226854440430 -0.152689284378266 -0.167619695467370
0.091720106204693 0.206482691423953 -0.009651751023354
-0.022820028399244 0.101726375059914 0.079905409015569 -
0.131014927622875 -0.120441030974726 0.098200164500386
-0.073091515606828 0.103765223801239 0.095919054250277 -
0.099051782753307 -0.125420200815266 0.061829889383475
-0.081227824294004 -0.108608223393049 -0.051544734501379
0.238078766649372 0.143301575335046 -0.188328792390863
0.045467314871578 -0.175474654369197 -0.133728843808697
0.251238197792040 0.231133026073695 -0.166928055973824

```
 0.089653088898560   0.030985907025162  -0.002460024723790  -
 0.099461619817319  -0.026711956280575   0.101988390186328
 0.040996933528540   0.068619468861682   0.037209557612899  -
 0.124681452549363  -0.077080069838666   0.108541650709477
 -0.229505855156596   0.057514446454531   0.107411522500834
 0.080692511006827  -0.073912563881549  -0.111131575822792
 -0.162973887240104  -0.043980441164535   0.019898354303338
 0.191374077727628   0.060526214730945  -0.175661147415818
  0.130105654393596  -0.059320058853563  -0.076198436888833
 0.013703535570662   0.090375512672407   0.029965474832644
 0.117500126904873  -0.017781272762291  -0.043342603198896  -
 0.043968817939026   0.035031102161960   0.068038774820484
-0.185491851526058   0.178188577522941   0.179082147095072  -
 0.142831167182098  -0.229276792264758   0.061841724235136

                  Columns 31 through 36

 0.021863971082503   0.188325819798627   0.059042557964887  -
 0.172204173096664  -0.133659786942830   0.232125963676253
 -0.081087678764761   0.009695445184314   0.093659801019376
 0.029586037442462  -0.006082074618744  -0.101643489323733
 -0.045863951582418  -0.042292330137799   0.035977698224623
 0.064081443044487   0.035374025236760  -0.114652683345125
  0.185722739035199  -0.130077247295820  -0.236613557635382
 0.059486555508434   0.112339233250114   0.091350148741578
 0.163380320473403  -0.012301949188309  -0.166780629353069  -
 0.039426832187006   0.023042415979590   0.195712832395485
-0.083690420650531   0.110562510733418   0.136788588512627  -
 0.059929581161503  -0.080658409280814   0.006646231685336
-0.085249649019772   0.064912968255375   0.120231285939084  -
 0.019857938598047  -0.047504902822615  -0.046620235276496
  0.110274995284326  -0.238226592192107  -0.203954926694961
 0.180572245920845   0.187586427023678  -0.127363376046460
  0.168290165676376  -0.198708141141766  -0.247407121080500
 0.125490366746644   0.161843114190781  -0.007909327352135
-0.019162028908791   0.130043566028410   0.080176469753795  -
 0.099120790242834  -0.091161990510851   0.112451680300431
```

-0.054299897555349 0.129745862732848 0.116254535261820 -
0.085199071594002 -0.092509743294314 0.065617993550651
-0.045560913042252 -0.152854218412111 -0.012025785346168
0.154776602121734 0.113724945390548 -0.234117897689281
0.049605461806662 -0.230373366991732 -0.140047457462561
0.193903217051236 0.177768436809724 -0.197984016803462
0.070727280142624 0.043031338920086 -0.045857748098690 -
0.050109924001695 -0.020425572319505 0.132028698813317
0.026008308514166 0.087667786211664 0.015560641028290 -
0.075207398920555 -0.055065956594002 0.125789656810085
-0.169029190193360 0.055096351031629 0.197390048715848
0.009791669324485 -0.048168870705726 -0.162429674692663
-0.106609294757620 -0.071913614460922 0.082678429459722
0.103101499465413 0.049557962354660 -0.223831243007837
0.106060050789005 -0.076758446917267 -0.130805258270847
0.045214410203335 0.071071045200805 0.046222442718969
0.093134809331123 -0.021350514171814 -0.095641288119474 -
0.001082421548158 0.029175377290496 0.089968170593367
-0.152227463060215 0.217895124410079 0.244991645091168 -
0.141466467041346 -0.170115688645732 0.040691406503792
-0.179397676904817 0.141749349215187 0.242505974867190 -
0.064762797110997 -0.113937228934775 -0.079380665825574
0.063144962760447 -0.128229131712850 -0.108671270936407
0.104970977693918 0.107929829005911 -0.068537894130631
0.087645456896733 -0.108639624374033 -0.125934932278416
0.080013613594518 0.094270228314570 -0.014380481730488
-0.008500789084204 0.196856649142897 0.091614824634961 -
0.168832383885727 -0.144016502975402 0.202298845667227
-0.100011373074783 0.235724277236567 0.202079613407467 -
0.175313440757470 -0.178200279390053 0.126403412816066
-0.025517465637877 -0.078904128329645 0.003724748442582
0.089449887898146 0.062317935718414 -0.129361285460971
0.015550504895494 -0.108720945129567 -0.053501753415028
0.102090312791687 0.088677708477593 -0.106307547607905
0.141470754246707 0.035882885191712 -0.124427419213626 -
0.075141953512983 -0.013304157734193 0.217750058487535
0.059596927271626 0.147419465139481 0.004173582646856 -
0.147155518197301 -0.101478336454925 0.235697342107845

-0.088528219154791 0.041412378387912 0.112994177867487
0.003688429287030 -0.029459688204286 -0.076172107428979
-0.067802199947487 -0.016725268195133 0.061167791930265
0.045533596315000 0.015101981259139 -0.104121919148689
-0.000881045829582 -0.201888424758196 -0.254125499843651
0.106087208244065 0.151290426869834 0.030365868979789
0.089273359414680 -0.243145243973727 -0.202548800840364
0.009673662547237 0.068291126145311 0.142793743952084
0.042779412862328 0.071306312671120 -0.007967190821185 -
0.075451175834660 -0.091237869793328 0.034822502677610
0.003211220419637 0.106683223560100 0.046202761375486 -
0.087292122363214 -0.072733646634784 -0.018592697000610
-0.139036213073629 -0.001182138913407 0.144359828925734
0.053487686692997 -0.002798515243653 -0.189708131057709
-0.063450978762803 -0.129192421933109 0.017188021491176
0.142058740016265 0.097266277415044 -0.234565496757577
0.101622960244213 -0.048907073835952 -0.115247946291840
0.019827565545675 0.050288064536231 0.070926699626461
0.078958883759112 0.009310117769411 -0.068863990622897 -
0.022975661602013 0.004642969182039 0.106231634369325
-0.165562005444270 0.193310441433610 0.248649612784529 -
0.112738231739599 -0.149803840537111 -0.003916849414051
-0.175411342126565 0.097100225690635 0.221203897693140 -
0.022336998668274 -0.078864221182309 -0.126800570557977
0.077415994706534 -0.124484916621117 -0.121385979502946
0.095989317255073 0.104479134340850 -0.044853308131449
0.096035315991907 -0.097874227074778 -0.129027214387147
0.066002608191945 0.084577104406442 0.009053706835531
-0.052244578832310 0.232199310879938 0.149413327282662 -
0.187603779960941 -0.172149715924005 0.188431385568051
-0.135719456270841 0.237263186644437 0.234734456048379 -
0.163821016577374 -0.182778600298646 0.084558581349933
-0.004783570961897 -0.097445698217658 -0.027511690608151
0.099832123047066 0.079036267622587 -0.121999383348440
0.036538091566111 -0.117090660536111 -0.077650906542703
0.102633974501924 0.095705772548769 -0.090447132024345
0.108877890543171 0.077666287306436 -0.075541582096642 -
0.102867194607733 -0.046458755129591 0.224292591780767

Columns 37 through 42

```
  0.214080726410500  -0.161981511674428  -0.173250787008775
 0.098073026818320   0.218760130963152  -0.020310451770861
-0.022471217555557   0.105832650303530   0.080873729047846  -
 0.133304136572511  -0.127298584695078   0.100698664282856
-0.066431101224213   0.101832396218134   0.091218713832999  -
 0.096771958571741  -0.124991252866572   0.062728445103013
 -0.076365209277621  -0.115056887702879  -0.054629726296734
 0.241831137036597   0.155260571179466  -0.191344544080014
  0.047210637996604  -0.179472982498136  -0.134320017341592
 0.251335689098130   0.241411704114164  -0.169700650827986
 0.088280684984880   0.031070741116024  -0.002661698111269  -
 0.100490188441330  -0.028604157825817   0.101299987165575
 0.037098729570691   0.068257208126919   0.036350551652753  -
 0.120695809819798  -0.079195476775948   0.104718661934727
 -0.223386132746258   0.056803983462027   0.106131066084300
 0.083119961997287  -0.073188857605109  -0.107333251042814
 -0.158035360529704  -0.041857362174979   0.020004751993391
 0.190119409199504   0.059157606839592  -0.171500064755352
  0.135090917022448  -0.061115818025340  -0.078870091831597
 0.008394833613688   0.092520649883564   0.032314560289413
 0.119622633171040  -0.017140247033315  -0.044691057243904  -
 0.046746146551724   0.035640661588802   0.069706035352661
-0.187721407372355   0.178201848143828   0.176867476543986  -
 0.131497193904975  -0.231695581857739   0.057517808180214
-0.237316211510770   0.124080650122018   0.155564943803940  -
 0.009204000075949  -0.160304069002326  -0.043260832391649
  0.072287040498893  -0.101782996324152  -0.087758336810366
 0.119305388572423   0.146472941156450  -0.064384561993915
  0.103588239494883  -0.085425795559244  -0.085480365614137
 0.067125771765516   0.122327531021087  -0.019012469227885
-0.003805856563202   0.167735612376974   0.115159812331348  -
 0.251269872156558  -0.214962441537096   0.188098309292625
-0.121125683991763   0.191065320598374   0.164845778499382  -
 0.199626949476633  -0.246500488025166   0.123031578315256
 -0.046907401559587  -0.053771977504472  -0.019152095272275
 0.133354372471944   0.081722159795607  -0.100087614198939
```

0.008891405643297 -0.080332071383830 -0.054082997437053
0.131639636128919 0.115978595381393 -0.087472665897616
0.182194361279657 0.022902549480580 -0.038457473792818 -
0.164610148943346 -0.023756415926616 0.166489161346587
0.088428114604495 0.113243082063954 0.050086565111097 -
0.235586156186553 -0.143285663756310 0.197173110717624
-0.120698499419776 0.037847225482022 0.064837051971750
0.045112265020898 -0.039763594393196 -0.052751075227037
-0.090175198741741 -0.007333582927807 0.024944282131012
0.091324132113308 0.019410987714557 -0.079892506421689
0.214572297658220 -0.134140249292668 -0.152718103367017
0.052761254128925 0.181902517028457 0.012159998882505
0.219867515575489 -0.052557384778305 -0.099806214255064 -
0.078194823563653 0.075741224142168 0.110982538802088
-0.100134271060794 0.105931996719843 0.104638701882205 -
0.078561305758803 -0.129410721276491 0.042717030738370
-0.116179888050489 0.076491299791532 0.089911733184343 -
0.020865606686060 -0.092344562432025 -0.003722628737838
0.092547156653331 -0.189123683562089 -0.154326873892781
0.231880403301242 0.253440963698588 -0.146955524899498
0.184813949796255 -0.175798853689079 -0.173495620067609
0.143084403008194 0.237804400164337 -0.059567041313822
0.010346808738224 0.089848567070081 0.060544755312760 -
0.132015807371156 -0.106045241074992 0.106926446669592
-0.043969252476235 0.099560499013847 0.082486847085917 -
0.109516007152434 -0.120778882625241 0.077939929086782
-0.132662621155732 -0.072260455137826 -0.009184907219094
0.219025950863264 0.099552409777063 -0.188350805199490
-0.013924835486147 -0.147988937002494 -0.094811070288477
0.247952985281220 0.199471286818495 -0.181603239560654
0.106844425023093 0.006832754612882 -0.023005385968128 -
0.078938851662591 0.000807080271773 0.089741172769079
0.063868488567483 0.048082961914152 0.016586954767627 -
0.110418670164616 -0.052625703232642 0.102629696574555
-0.231323891909186 0.098066126899702 0.135363806105210
0.027738121563717 -0.124779092648408 -0.068935435510205
-0.188896803236200 -0.002871487422044 0.054299439067922
0.151330975512228 0.007074545848124 -0.151070931233343

-0.017898716879209 -0.078094757893844 -0.086344026806651
0.039681167215313   0.112980185666377   0.006977311136729
0.038041714958652 -0.087356569613505 -0.068562632657301 -
0.018569262882579   0.063188754985322   0.049258341981293
0.149529109825049   0.059497347359187 -0.002897811404177 -
0.196898601548065 -0.246349474503283   0.100242740674903
0.039610771157698   0.147008716399447   0.088669659046572 -
0.249605373772384 -0.206844222263247   0.004521337029509
-0.110917354642293   0.016906847552999   0.047141463009733
0.069516614540656 -0.012535629295423 -0.075711427369474
-0.073769037374000 -0.026398107101651   0.006987685477853
0.108895650196737   0.044874295145978 -0.089783376807282
0.235069943486968 -0.108633663646466 -0.142837742626595 -
0.000257059650567   0.149930246362640   0.057563707951803
0.208517641016720 -0.013828327156900 -0.071003403228683 -
0.129663771754962   0.023214870840409   0.145246480931411
-0.112346545979090   0.095407621963931   0.101346822468001 -
0.050509908095058 -0.114408262343153   0.020216953582024
-0.118300350344237   0.059476572389296   0.078539427297788
0.007205120160680 -0.069604326185264 -0.025236470059810
0.125682352376970 -0.182511453669619 -0.160723799481538
0.197716419625569   0.246192918572564 -0.113390683315432

Columns 43 through 48

-0.071466119872939 -0.120580047871592   0.037612781425883
0.139971804216792   0.085580489062259 -0.241159460927570
0.104584714794462 -0.048907944454934 -0.122621419759559
0.017328798247776   0.047023449273991   0.077160545717944
0.077639941459575   0.006390516834758 -0.074748628917862 -
0.024335197435017   0.006302324092066   0.105014454457738
-0.170359346492276   0.187440804454601   0.253389402563637 -
0.103231431554742 -0.139017728994537 -0.015821350997357
-0.179248880338734   0.092905561296020   0.230460907704641 -
0.015846646021949 -0.073273157990038 -0.136993586074801
0.078136577668555 -0.120055861105304 -0.119711022879042
0.091639268190015   0.095941884295345 -0.041335475084103

0.093245972816279 -0.089246198861782 -0.125566466348826
0.058108416528777 0.076036564539690 0.015109032273044
-0.052674957036272 0.222644129055268 0.140439604640348 -
0.181040278081216 -0.158671769033414 0.185130162626428
-0.131462726793278 0.226062175060249 0.226357213983704 -
0.154921142409095 -0.165486092915656 0.082494831310542
-0.002658620137502 -0.099909935563098 -0.026613861050141
0.104211333613404 0.078949860912121 -0.127033669394346
0.038281555337310 -0.118012465324245 -0.077458096101715
0.101931670730010 0.092679454773331 -0.091656140165096
0.105588141974408 0.082965646198555 -0.077228618237139 -
0.108561477004711 -0.050290076314112 0.230925514476932
0.016760168688536 0.186335966312687 0.054542796449043 -
0.171851852956911 -0.127498534715537 0.233643165788130
-0.082594119226694 0.007793546354312 0.097272346703003
0.033646514972399 -0.003229747796024 -0.107563131032499
-0.045667775405059 -0.044606697453231 0.036517155060923
0.068447290983187 0.035803361212981 -0.119432756885924
0.190449902126668 -0.126482101635327 -0.241164503412674
0.052026801170626 0.104965741040733 0.098627126116981
0.154136903918746 -0.006247728113726 -0.160447275785223 -
0.046342501119620 0.015307774074961 0.192383093206930
-0.089606099899147 0.109773491043120 0.141323531581934 -
0.055675826826633 -0.075929713774372 0.000672585856952
-0.090521923507691 0.064046491792666 0.124841466242994 -
0.015080501935039 -0.044089430506954 -0.052149693462589
0.121050133282141 -0.230406826356847 -0.208018419030931
0.171778627953245 0.174978576386055 -0.111960799987467
0.176453957224225 -0.192296159507491 -0.250737640273644
0.116328931300381 0.150811275036334 0.004897033555457
-0.023833483845044 0.123641921128200 0.076418482303829 -
0.091964749419093 -0.082881681303431 0.104631409907747
-0.059168243847492 0.122849684112047 0.112575753030192 -
0.079445739418441 -0.085538021374457 0.057561793136630
-0.039034840900802 -0.143552245126247 -0.004059411084242
0.146956503727629 0.102478433608994 -0.223157081696074
0.059305023094743 -0.218063802590315 -0.133003695280646
0.179602799385734 0.159915804693277 -0.182195488296187

0.069140718809646 0.042208942756249 -0.048057374422416 -
0.050644452302206 -0.022503363111762 0.129492972888985
0.024166975073677 0.085373862224395 0.011649435449415 -
0.075982164581313 -0.053871834210331 0.124826993682623
-0.167981287413560 0.047852932388262 0.199604750494580
0.022192406578792 -0.039069341113177 -0.172981281744365
-0.104728962051917 -0.072174251320647 0.088788171930172
0.108519371931754 0.049179120302283 -0.227722009377385
0.104063363561754 -0.073226969710462 -0.130168871319876
0.040446605642109 0.063636584214878 0.045445976726271
0.087183521150117 -0.019140715352613 -0.093226287855711 -
0.004083472259359 0.024740712940550 0.088074448682747
-0.153644281214370 0.221632820928818 0.247229689858682 -
0.141418461165627 -0.161782708279068 0.047782977560965
-0.177367288145648 0.140826478163355 0.243440585631636 -
0.057839074881532 -0.105971024592199 -0.077075209612060
0.062467476843336 -0.123915131764851 -0.103854249376310
0.102143461767508 0.098698657854051 -0.068207112977148
0.086228416843942 -0.106302960254191 -0.122914259739388
0.075445895111014 0.086273939310532 -0.015621263087822
-0.010260903757956 0.201383971850551 0.089297300746508 -
0.175421636058427 -0.139749166433756 0.214430102564443
-0.102777011754620 0.231378574092197 0.197190682117487 -
0.168811611235333 -0.166859400381101 0.126897353424257
-0.026342826507222 -0.077144781387599 0.005869787831381
0.089454438753107 0.059584785473071 -0.129912742526269
0.016656777840980 -0.107141012114070 -0.050849369180782
0.099944747042759 0.082595757565406 -0.108462219409795
0.139430496023799 0.031743339061880 -0.128451123077947 -
0.073364381524561 -0.010460556089562 0.214139825015527
0.063139996715355 0.148914515635920 -0.007091451096071 -
0.153268295237124 -0.098933635366133 0.249938227730138
-0.086251584762543 0.035591410606052 0.110177787242859
0.008647152496947 -0.023998967652481 -0.079447688041562
-0.070875519256036 -0.018248134221512 0.067236759467820
0.049847597289390 0.016152306367955 -0.112438961334532
-0.000883737220359 -0.188774645765229 -0.243038703584710
0.095003739384949 0.134200265528726 0.034834748492211

```
0.091648389229085  -0.236032274533269  -0.202256953500037  -
0.002151799786228   0.055949788140611   0.155433916515867
0.045622331801399   0.066473744564138  -0.018989483017562  -
0.073033248452167  -0.082890786106016   0.037276803845797
0.004321736500023   0.101428902596247   0.039186812664093  -
0.083649864229032  -0.065842690406400  -0.020836544178489
 -0.142963051183362   0.003270874327477   0.158067721195288
0.053165778263915  -0.006977883279554  -0.193287839835327
```

Appendix III Radio Frequency

Radio Frequency (RF) is the oscillation rate. Its range is from 3 kHz to 300 GHz (Beasley and Miller, 2008). In synchrotron facilities, the electrical field generated by high RF exists in the linear accelerator, Booster Ring (BR) and Storage Ring (SR) to accelerate the electrons.

In CLS, the oscillations of the electric field occur at frequency of 500 MHz. This number is determined by the length of the section being accelerated, compared to the wavelength of the electron.

Appendix IV Bode Plot and Residual Analysis

IV.1 Bode Plot

In classic control theory, the Bode plot is a group of diagrams of magnitude and phase versus frequency to evaluate the frequency function of the system. It was devised by Hendrik Wade Bode in the 1930s.

If the transfer function of the system is like Equation A.1, the magnitude of it is shown as follows:

$$M = 20log|G(j\omega)| \tag{A.1}$$

The phase is shown as follows:

$$\Phi_G = -tan^{-1}\frac{\omega}{\omega_c} \tag{A.2}$$

where ω and ω_c are the input and cutoff angular frequencies, respectively.

IV.2 Residual Analysis

The residual analysis is a method for model validation.

Assume there is a model:

$$y(t) = G(z)u(t) + H(z)e(t) \tag{A.3}$$

where $y(t)$ is the output signal; $u(t)$ is the input signal; $G(z)$ is the transfer function of the system; $H(z)$ is the transfer function to describe the disturbance; $e(t)$ is the noise of the system.

The noise $e(t)$ is part of the output, but it can't reproduce. In Mathematics, it is named "left-over", the residuals are its Latin name. If the residuals of the model are independent of the input, that means the model is good otherwise not good..

Residuals analysis is the way to test the independence between input and output residuals by computing the cross-correlation function. If the correlation function lies between the confidence lines for positive lags, this suggests the model is good. The function in MATLAB for computing the residual analysis is "*resid*".

Appendix V Correlation and Spectral Analysis

V.1 Correlation Analysis

In statistics, Correlation analysis refers to the process of understanding relationship among variables. There are coefficients to measure the degree of a correlation. The most common one is the Pearson correlation coefficient. It can be obtained by their standard deviation. The formula is shown in A.4.

$$\rho_{X,Y} = corr(X,Y) = \frac{cov(X,Y)}{\sigma_X \sigma_Y} = \frac{\mathbb{E}[(X-\mu_X)(Y-\mu_Y]}{\sigma_X \sigma_Y} \tag{A.4}$$

where σ_X and σ_Y are standard deviations, and μ_X and μ_Y are expected values.

When there are a series of measurements of input and output signals written as u_i and y_i, the correlation coefficient can be shown in Equation A.5.

$$r_{uy} = \frac{\sum_{i=1}^{n}(u_i - \bar{u})(y_i - \bar{y})}{(n-1)\sigma_u \sigma_y} \tag{A.5}$$

where σ_X and σ_Y are standard deviations, and $\bar{u}$ and $\bar{y}$ are the means of the measurement.

V.2 Spectral Analysis

In signal processing, spectral analysis is for estimating the spectral density of the samples of signal. The main method for spectral analysis is Discrete Fourier Transformation (DFT).
The transfer function of the input and output signal can be denoted by DFT:

$$G\left(e^{i\omega t}\right) = \frac{Y(e^{i\omega t})}{U(e^{i\omega t})} \tag{A.6}$$

After Fourier representation the time series signals, they are expressed in a standard way which can be compared with different time series. And the result is the spectrum of the signals.

In Matlab, these two kinds of analysis can be obtained by command. Autocorrelation and Power Spectrum of Noise Matlab Scripts are as follows:

```
[cory, lags]=xcorr(noise,48,'unbiased');
% cory is the autocorrelation function;lags is the length of the
autocorrelation fuction %
f=fft(cory);
m=abs(f);
F=100;
f1=(0:leng(m)-1)F/length(m);
% power density of noise %
plot(f1,m);
grid on;
```

Appendix VI Noise

In signal processing theory, there are various noises types such as pink, blue, black and white.

Pink Noise is also called flicker noise. Its power density is inversely proportional to the frequency with a 3dB/octave decreasing. The power density of Blue noise is proportional to the frequency with 3dB/octave increasing. The power density of Brown noise is inversely proportional to the frequency square with a 6dB/octave decreasing. The power density of purple noise is proportional to the frequency square with a 6dB/octave increasing (Tuzlukov, 2002).

White noise is a fundamental concept for the modeling of disturbances such as senior noise and environmental disturbances. In signal processing, white noise is defined that it is a random signal with a constant power spectral density (Figure A.1). That means white noise has equal power within any fixed frequency.

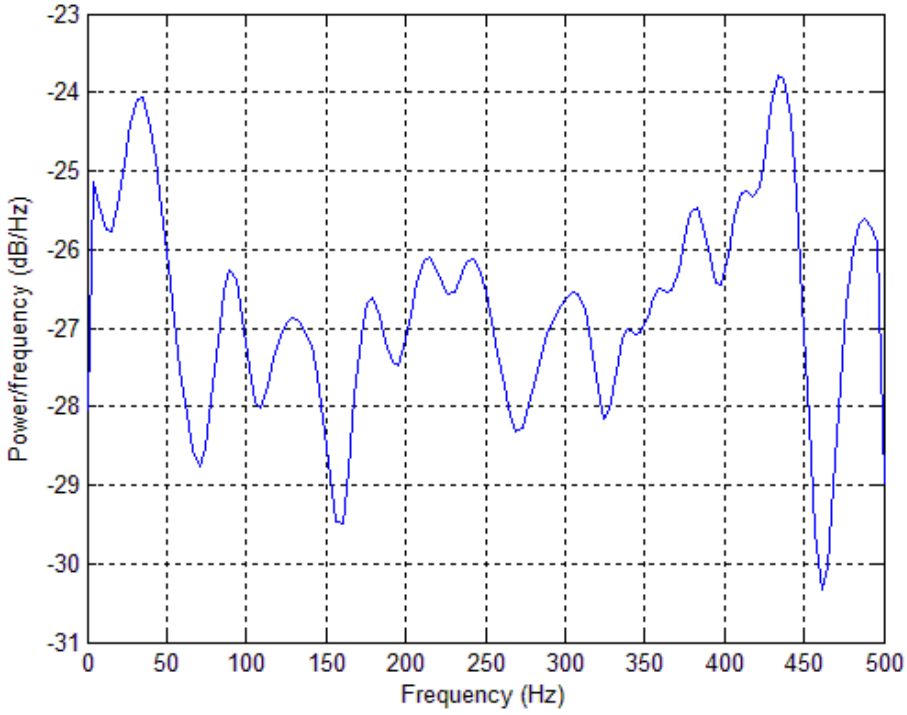

Figure A.1 Power spectral analysis of a random white noise

Its statistical properties shown by Equation A.7 and A.8 are its expected value equals zero, and its autocorrelation is Driac Delta function (Appendix IX).

$$\mu_n = \mathbb{E}\{n(t)\} = 0 \tag{A.7}$$

$$r_{nn} = \mathbb{E}\{n(t)n(t-\tau)\} = \delta(t) \tag{A.8}$$

When the amplitude of the white noise is normally distribution (Gaussian distribution, see Appendix X), it can be called Gaussian White noise. In signal processing, this kind of noise is a very common noise to apply in the system simulation as disturbance. It is shown in Figure A.2.

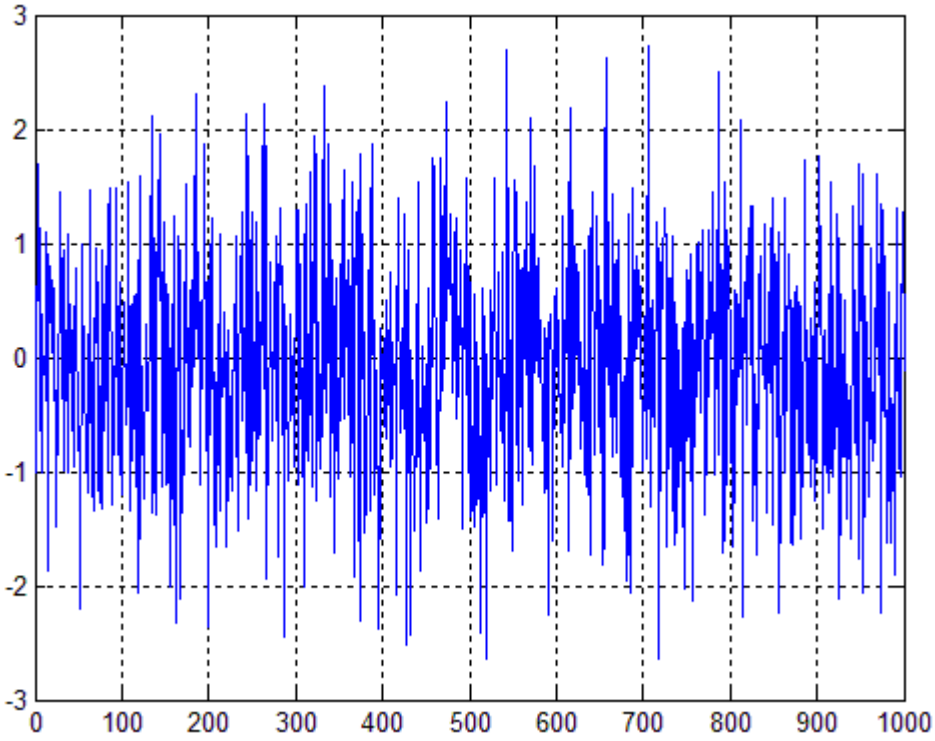

Figure A.2 Gaussian white noise with $\mu = 0$ (mean), $\sigma = 1$ (standard deviation), $p = 1dBW$ (power) random generated by Matlab

Appendix VII PID Controller

The Proportional-Integral-Derivative (PID) control is one of the earlier control strategies (Johnson, 2005). The good features of PID control are simplicity, robustness and wide applicability. Therefore, it is applied widely in industrial control. From its born, there are so many active research topics on it.

A typical structure of a PID control system is illustrated by:

$$u(t) = K_p[e(t) + \frac{1}{T_i}\int_0^t e(\tau)d\tau + T_d\frac{de(t)}{dt}] \tag{A.9}$$

where $u(t)$ is the input signal of the plant model; the error $e(t)$ is defined as $e(t) = r(t) - y(t)$, and the $r(t)$ is the reference input signal.

The block diagram of PID controller is shown in Figure A.3.

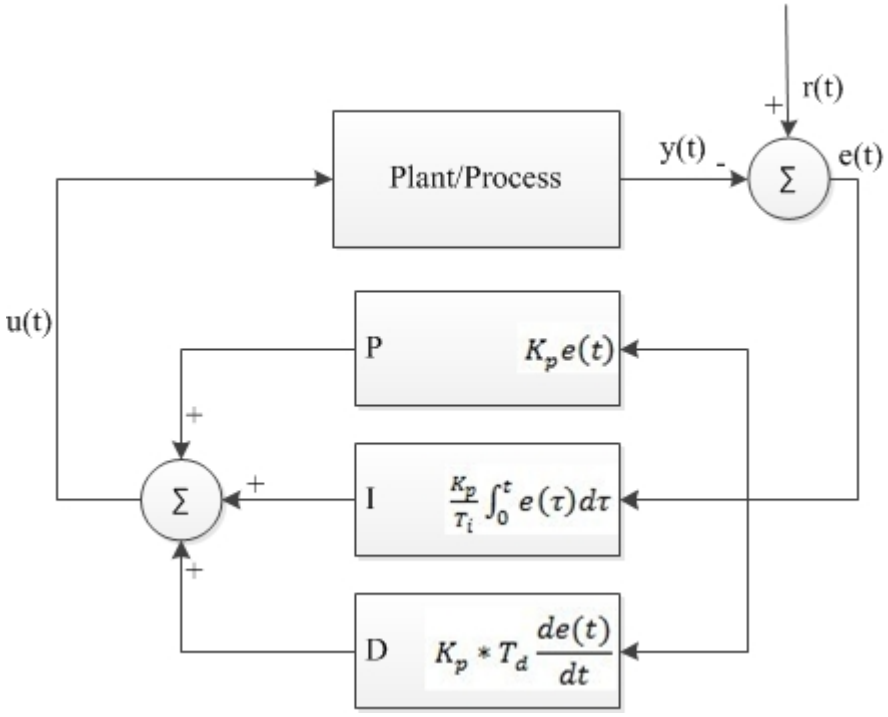

Figure A.3 Block diagram for PID algorithm

The transfer function of the PID controller can be obtained by Laplace Transformation to the Equation.

$$U(s) = K_P(1 + \frac{1}{T_i s} + T_d s) \tag{A.10}$$

When it is used in the control system, we just need to tune the parameters K_P, T_i and T_d.

From 1940s up to now, there are many various tuning methods to have been proposed. They can make the control system gaining much better and more acceptable responses based on the desirable objectives, e.g., percent of overshoot, setting time, rising time, steady-state error, integral of absolute value of the error (IAE) and etc.

Appendix VIII PID Controller Tuning Methods

VIII.1 Ziegler-Nichols Method

Ziegler-Nichols method is very useful PID controller tuning method, which was proposed by John G. Ziegler and Nathaniel B. Nichols (1942).

The key rules of this method are as follows:

(1) Assuming the integrator time T_i and the derivative time T_d to 0;

(2) Varying the proportional gain K_p from 0 to ultimate gain K_u which is the output value when the loop is stable.

(3) Obtaining the period T_u which is the time of the frequency at the stability limit.

(4) Calculating P, I and D gains by T_u and K_u as Table A.1.

Table A.1 Ziegler- Nichols Method

Control Type	K_p	T_i	T_d
P	$K_u/2$	-	-
PI	$K_u/2.2$	$1.2K_p/T_u$	-
PID	$0.6K_u$	$2K_p/T_u$	$K_p * K_p/8$

The Matlab scripts of Ziegler-Nichol Methods are as follows (Xue et al., 2007):

```
function [Gc,H]=printpid(Kp,Ti,Td,N,key)
  switch key
  case 1, Gc=Kp;
  case 2, Gc=tf(Kp*[Ti,1],[Ti,0]); H=1;
  case 3, nn=[Kp*Ti*Td*(N+1)/N,Kp*(Ti+Td/N),Kp];
          dd=Ti*[Td/N,1,0]; Gc=tf(nn,dd); H=1;
  case 4, d0=sqrt(Ti*(Ti-4*Td)); Ti0=Ti; Kp=0.5*(Ti+d0)*Kp/Ti;
          Ti=0.5*(Ti+d0); Td=Ti0-Ti; Gc=tf(Kp*[Ti,1],[Ti,0]);
          nH=[(1+Kp/N)*Ti*Td, Kp*(Ti+Td/N), Kp];
          H=tf(nH,Kp*conv([Ti,1],[Td/N,1]));
  case 5, Gc=tf(Kp*[Td*(N+1)/N,1],[Td/N,1]); H=1;
end
Ti=[]; Td=[]; H=1;
if length(vars)==4,
   K=vars(1); L=vars(2); T=vars(3); N=vars(4); a=K*L/T;
```

```
if key==1, Kp=1/a;
   elseif key==2, Kp=0.9/a; Ti=3.33*L;
   elseif key==3 || key==4, Kp=1.2/a; Ti=2*L; Td=L/2;
end
elseif length(vars)==3,
       K=vars(1); Tc=vars(2); N=vars(3);
if key==1, Kp=0.5*K;
   elseif key==2, Kp=0.4*K; Ti=0.8*Tc;
   elseif key==3 || key==4, Kp=0.6*K; Ti=0.5*Tc; Td=0.12*Tc;
end
   elseif length(vars)==5,
          K=vars(1); Tc=vars(2); rb=vars(3); N=vars(5);
          pb=pi*vars(4)/180; Kp=K*rb*cos(pb);
if key==2, Ti=-Tc/(2*pi*tan(pb));
elseif key==3||key==4, Ti=Tc*(1+sin(pb))/(pi*cos(pb)); Td=Ti/4;
end

end
[Gc,H]=printpid(Kp,Ti,Td,N,key);
```

VIII.2 Optimum Error Criteria Method

Optimum error criteria method was proposed by Zhuang and Atherton (1993). There are three cases in this method: integral squared error (ISE), integral squared time weighted error (ISTE) and integral squared time-squared weighted error (IST^{2}E) (Tan et al., 2006).

The general form of the optimum error criteria method is shown in Equation A.11.

$$E_i(\theta) = \int_0^\infty [t^i * e(t)]^2 \, dt \tag{A.11}$$

where $e(t)$ is the error of input signal and setpoint.

Therefore, the three case of this method can be present by following equations, respectively:

$$E_{ISE}(\theta) = \int_0^\infty [e(t)]^2 \, dt \tag{A.12}$$

$$E_{ISTE}(\theta) = \int_0^\infty [t * e(t)]^2 \, dt \tag{A.13}$$

$$E_{\mathrm{IST2E}}(\theta) = \int_0^{\infty} [t^2 * e(t)]^2 \, dt \tag{A.14}$$

The Matlab scripts of optimum error criteria Method are as follows (Xue et al., 2007):

```
function [Gc,H]=printpid(Kp,Ti,Td,N,key)
  switch key
  case 1, Gc=Kp;
  case 2, Gc=tf(Kp*[Ti,1],[Ti,0]); H=1;
  case 3, nn=[Kp*Ti*Td*(N+1)/N,Kp*(Ti+Td/N),Kp];
          dd=Ti*[Td/N,1,0]; Gc=tf(nn,dd); H=1;
  case 4, d0=sqrt(Ti*(Ti-4*Td)); Ti0=Ti; Kp=0.5*(Ti+d0)*Kp/Ti;
          Ti=0.5*(Ti+d0); Td=Ti0-Ti; Gc=tf(Kp*[Ti,1],[Ti,0]);
          nH=[(1+Kp/N)*Ti*Td, Kp*(Ti+Td/N), Kp];
          H=tf(nH,Kp*conv([Ti,1],[Td/N,1]));
  case 5, Gc=tf(Kp*[Td*(N+1)/N,1],[Td/N,1]); H=1;
end

k=vars(1); L=vars(2); T=vars(3); N=vars(4); Td=[];
if length(vars)==5, iC=vars(5);
    switch key
           case 1
                A=[1.048,1.042,0.968,1.154,1.142,1.061;
0.897,0.897,0.904,0.567,0.579,0.583;
                  1.195,0.987,0.977,1.047,0.919,0.892;
0.368,0.238,0.253,0.220,0.172,0.165;
                  0.489,0.385,0.316,0.490,0.384,0.315;
0.888,0.906,0.892,0.708,0.839,0.832];
           case 2
                A=[1.473,1.468,1.531,1.524,1.515,1.592;
0.970,0.970,0.960,0.735,0.730,0.705;
                  1.115,0.942,0.971,1.130,0.957,0.957;
0.753,0.725,0.746,0.641,0.598,0.597;
                  0.550,0.443,0.413,0.552,0.444,0.414;
0.948,0.939,0.933,0.851,0.847,0.850];
    end
ii=0;
if (L/T>1) ii=3;
end;
tt=L/T;
a1=A(1,ii+iC);
b1=-A(2,ii+iC);
a2=A(3,ii+iC);
b1=-A(4,ii+iC);
Kp=a1/k*tt^b1;
Ti=T/(a2+b2*tt);

if key==1| key==2
    a3=A(5,ii+iC);
    b2=A(6,ii+iC);
    Td=a3*T*tt^b3;
end
else,
```

```
    Kc=vars(5);Tc=vars(6);k=vars(7);
    switch key
        case 1, Kp=0.509*Kc; Td=0.125*Tc; Ti=0.051*(3.302*k+1)*Tc;
        case 2, Kp=(4.437*k-1.587)/(8.024*k-1.435)*Kc;
Ti=0.037*(5.89*k+1)*Tc; Td=0.112*Tc;
    end
end
[Gc,H]=printpid(Kp,Ti,Td);
```

Appendix IX Driac Delta Function

Driac Delta Function (δ function) is a very useful function in mathematics (Driac, 1958). It is defined as:

$$\delta(x) = \begin{cases} +\infty, & x = 0 \\ 0, & x \neq 0 \end{cases} \tag{A.15}$$

with

$$\int_{-\infty}^{+\infty} \delta(x)dx = 1 \tag{A.16}$$

Strictly speaking, δ function is just said to be a distribution, not a function because of its too singular (Vladimirov, 1971). It is just a kind of generalized idea function.

Appendix X Normal Distribution

In probability theory, the normal distribution shown by Figure A.4 is fundamental continuous probability distribution. It is defined by the equation as follows:

$$f(x) = \frac{1}{\sigma\sqrt{2\pi}} e^{-\frac{(x-\mu)^2}{2\sigma^2}} \tag{A.17}$$

where μ : Mean of the distribution;

σ: Standard deviation.

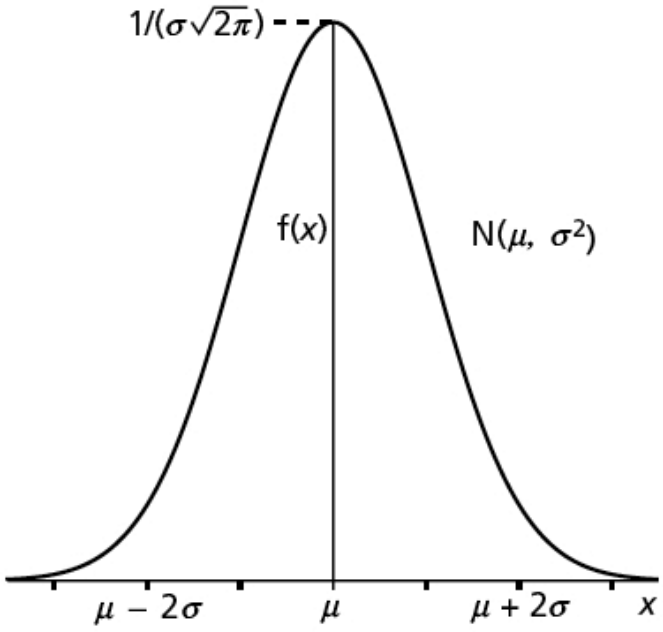

Figure A.4 Function plot of normal distribution (http://content.answcdn.com/main/content/img/oxford/Oxford_Statistics/0199541454.normal-distribution.7.jpg)

The normal distribution is also called Gaussian distribution. It is extremely important in statistics and often used for real-valued random variables in the science study. One reason for its popularity is the central limit theorem, which states that, given certain conditions, the mean of a sufficiently large number of independent random variables, each with a well-defined mean and

variance, will be approximately normally distributed (Rice, 1995). Therefore, when the physical quantities are expected to be the sum of many independent variables, their distribution is very close to normal. Another reason is when the variables are normally distributed, many methods can be derived, e.g., the least square and propagation uncertainty.